2013-01-01

An Evaluation Of The Cerro Process As An Efficient Ro Concentrate Management System

Guillermo Guadalupe Delgado
University of Texas at El Paso, ggdelgado@miners.utep.edu

AN EVALUATION OF THE CERRO PROCESS AS AN EFFICIENT RO CONCENTRATE MANGEMENT SYSTEM

GUILLERMO GUADALUPE DELGADO

Department of Civil Engineering

APPROVED:

Anthony Tarquin, Ph.D., Chair

Thomas Davis, Ph.D.

Doug Rittmann, Ph.D.

Shane Walker, Ph.D.

Jorge Gardea-Torresdey, Ph.D.

Benjamin C. Flores, Ph.D.
Dean of the Graduate School

Dedication

This dissertation is lovingly dedicated to my parents, Laurencio & Lucrecia. Their sacrifice and love have sustained me throughout my life.

AN EVALUATION OF THE CERRO PROCESS AS AN EFFICIENT RO CONCENTRATE MANAGEMENT SYSTEM

by

GUILLERMO GUADALUPE DELGADO, MSEnE

DISSERTATION

Presented to the Faculty of the Graduate School of

The University of Texas at El Paso

in Partial Fulfillment

of the Requirements

for the Degree of

DOCTOR OF PHILOSOPHY

Department of Civil Engineering

THE UNIVERSITY OF TEXAS AT EL PASO

December 2013

Acknowledgements

I am most grateful to the members of my committee, Dr. Davis, Dr. Rittmann, Dr. Walker, and Dr. Gardea for their time, and expertise throughout this project.

I am most grateful to Dr. Tarquin; his mentoring for all this years has been the best education.

I would personally like to thank the entire CIDS staff; especially to Isaac Campos, Luisin Conchin, Jessito, and Ana Isis Hernandez, one of the most intelligent person I have ever met.

I would like to thank my best friend, Neo Ortega. His unconditional support will be always remembered. Farewell my friend.

I need to thank my parents, my family, and my wife. Without them, my life would be so much different, and I am grateful for that.

To all of you, Thanks!

Abstract

The Concentrate Enhanced Recovery Reverse Osmosis (CERRO) Process is a new method to treat RO concentrate and brackish water with high concentrations of silica and calcium sulfate. Prior investigations have shown that the CERRO process can treat this kind of water without fouling or scaling the membranes, but the main factors that allow the system to operate in such conditions were not studied. The research presented here is an evaluation of the CERRO process as an efficient RO concentrate management system. The parameters of operation of the system were evaluated and improved. The precipitation of calcium sulfate was identified as the main limitation of the system, and the most important operational factors were detected. It was found that the constant decay in the crossflow velocity reduces the concentration polarization at the membrane surface and the capacity of the system to be periodically cleaned were the most important operational factors that allow the process to operate without fouling or scaling the RO membranes. This study will be a very important asset for future projects in the further improvement of the process.

Table of Contents

List of Tables

List of Figures

Chapter 1: Introduction

This chapter discusses the limitations of desalination systems and the CERRO process capabilities to overcome these limitations. Additionally, this chapter describes the objectives of the research conducted and the experimental tasks performed in this study.

1.1. Problem Statement

It is necessary to find new sources of freshwater. Traditional sources of supply (e.g. rivers, lakes, aquifers) are increasingly expensive, unavailable, or controversial. It is at this point where desalination technologies offer the potential to substantially reduce water scarcity by converting the almost inexhaustible supply of seawater and vast quantities of brackish groundwater into new sources of freshwater. Thermal and membrane desalination are the most common technologies used worldwide. However, membrane desalination is the most common technology that it is used in the United States (Committee on Advancing Desalination Technology and National Research Council 2008), and Reverse Osmosis (RO) desalination is the most common desalination system used of all membrane desalination systems. Advances in reverse osmosis (RO) technology over the past three decades have led to a significant reduction in the production cost of water desalination. In other words, capital and treatment cost have become a secondary limitation for the implementation of RO systems around the United States. Brackish water desalination, however, is often challenging because of the high costs associated with residual RO concentrate management, especially at inland locations. It is at this point where the implementation of new technologies is necessary to reduce the volume of the RO concentrate produced during the desalination process and minimize the cost of concentrate disposal.

Until today, there are only a few methods for concentrate disposal and fewer methods capable to treat the concentrate and reduce its volume (Mickley 2009). The most common limitation of RO desalination systems is produced by the presence of sparingly soluble salts (i.e. $CaSO_4$, $CaCO_3$) and fouling agents like silica (SiO_2) in the water. For example, The Kay Bailey Hutchison (KBH) desalination plant, located in El Paso, Texas has a limited recovery of 80% due to the high concentrations of silica present in the concentrate (>120 mg/L) (Delgado 2009) . When these constituents are present in the water, limited recovery rates are expected due to possible supersaturation of the dissolved ions in the water which will produce precipitation inside the system.

In the past years, many studies have been done to reduce the impact of these scaling and fouling agents in RO systems (Hater et al. 2011; Zhang et al. 2011; Fan et al. 2010; Lyster et al. 2010). However, the treatment of RO concentrate requires a change in the paradigm in which desalination systems are currently operated; more specifically, RO desalination systems. In the past few years, there has been an increment in the investigation of new methods capable to reduce the volume of the concentrate produced during the desalination process and to treat water with high concentrations of sparingly soluble salts. The Brackish Groundwater National Desalination Research Facility (BGNDRF) is a federal facility that promotes advanced water treatment research and technology development for the desalination of brackish water that is rich in calcium sulfate ($CaSO_4$). Similarly, the Center for Inland Desalination Systems (CIDS), located at The University of Texas at El Paso, is a center studying desalination-related issues such as mining the concentrated brine produced during the desalination process. These two organizations are examples of the effort taken to improve desalination systems for future

applications around the United States. This project was one of the multiple desalination projects developed in CIDS as part of its agenda to improve the performance of desalination processes.

1.2. Concentrate Enhanced Recovery Reverse Osmosis (CERRO©) Process

In 2010, an article was published (Tarquin et al. 2010) showing the results of a desalination process called Seawater Reverse Osmosis (SWRO) Batch processing. In this article, it is mentioned that the process was capable of treating RO concentrate without apparent scaling or fouling of the membranes due to silica polymerization or $CaSO_4$ precipitation. The system consisted of one or more seawater RO membrane vessels connected in parallel in a batch mode. Even though batch processing is a common practice in bench scale systems for evaluation of RO membranes (Hater et al. 2011; Sahachaiyunta et al. 2002), this project was one of the first to develop a pilot RO process to treat RO concentrate with saturated silica in a batch mode. The feed water used to test the process in this project was KBH concentrate with a silica concentration of 130 mg/L and a total dissolved solids (TDS) concentration of 10,720 mg/L. The KBH desalination plant is limited in the recovery of its process (75%-82%) due to the high concentration of silica. However, Tarquin et al showed that high recoveries, between 70% and 90% of the KBH concentrate, could be achieved in a batch mode operation. Additionally, Tarquin et al showed that the final concentrate had a silica concentration above 800 mg/L without apparent signs of membrane fouling. Until today, this has been one of the highest concentrations of silica achieved by a pilot RO system without fouling the membranes. After a detailed evaluation of the parameters of design of the SWRO system, it was concluded that the conditions in which the system was operated had the characteristics of a novel process. For that reason, on August 6, 2010, a patent application was submitted (UTEP Provisional patent

application number 61/233,761) and the name of the process was changed to "Concentrate Enhanced Recovery Reverse Osmosis Process" or CERRO process.

As mentioned before, the CERRO process has shown excellent results treating RO concentrate with high concentrations of silica and $CaSO_4$ (Tarquin et al. 2010; Tarquin 2008). However, it has never been clearly established why the CERRO process presents such resistance to scaling and fouling. The parameters to design a system, based in the CERRO process, change the configuration in which SWRO membranes are operated, but it does not change the composition of such membranes. In other words, the CERRO process utilizes SWRO components that have been tested in continuous flow (Kumar et al. 2006); however, the CERRO process presents different results despite the fact that it operates with SWRO membranes (Tarquin et al. 2010; Tarquin 2008). These results led to the theory that SWRO membranes will present a different performance depending on the conditions in which they are operated. The most common operation of RO and SWRO membranes is in a continuous flow design. This design has shown a very low resistance to silica supersaturation even with the use of antiscalants (Hater et al. 2011; Zhang et al. 2011; Sahachaiyunta et al. 2002). As an example, the KBH desalination plant reports a silica concentration of 130 mg/L in its concentrate (Tarquin 2008; Delgado 2009). At higher concentrations, the silica starts to polymerize, producing fouling of the membranes. It is at this point where the CERRO process has shown that high recoveries can be achieved if the parameters of operation in the RO system are changed. However, it is not known which parameters of operation allow the membranes to resist supersaturation conditions. This project presents a detailed analysis of the CERRO process. This project was an evaluation of the parameters of operation of the CERRO process and the identification of those parameters

that allowed the system to work under supersaturation conditions without fouling or scaling the SWRO membranes.

1.3. Objectives

1.3.1. Evaluation of the Parameters of Operation of the CERRO Process

The CERRO process represents a paradigm shift in the operation of RO and SWRO desalination processes. The conventional design of RO and SWRO desalination systems is in a steady-state continuous flow configuration. This type of design has proven to be very useful to operate in conditions of low saturation concentrations. Pretreatment of the feed water with antiscalants and acids has improved the performance of continuous flow systems, increasing the recovery (Fan et al. 2010; Klepetsanis and Koutsoukos 1998; Zhang et al. 2011). However, these systems are still very susceptible to scaling or fouling problems if supersaturation is reached during the treatment. Conversely, the CERRO process has shown an excellent resistance to these problems. In order to identify the difference in the performance of the system, it was necessary to identify the parameters that have been changed between the CERRO process and conventional systems. For instance, conventional systems are steady-state continuous flow systems. On the other hand, the CERRO process is a non-steady-state batch system. In this project, the performance of the system was studied while the operating parameters were changed. The impact on the performance of the system by these changes was evaluated. At the end of the project, the most important parameters that allowed the CERRO process to operate in conditions of supersaturation were identified. It was found that the residence time of the system and the capacity to clean the membranes rapidly after each batch are key factors in the performance of the CERRO process. One of the main objectives of this project was to reach a better

understanding of how the modification of the process can achieve different results, even though the same components are used.

1.3.2. Improvement of the CERRO Process

The CERRO process is in an early stage of development. Despite the excellent results achieved by the system, the energy consumption and cost of operation of the process are high (Tarquin et al. 2010). The optimization of the process is necessary to improve the performance, increase recovery, and reduce the cost of operation. The solution to this problem was a complicated task for several reasons:

- There was a limited amount of data for evaluation.
- The system is a non-steady-state system in a batch configuration. There are no prior research projects to establish a baseline of operation.

At the end of the project, the energy consumption had been reduced significantly without the use of energy recovery devices. It was found that the treatment time of the process directly affected the operating cost and the energy consumed by the system.

1.4. Significance of the Study

This project was a detailed evaluation of the CERRO process. The findings in this project have opened the possibility to increase the recovery of desalination systems by reducing the volume of concentrated brine produced during the process. Additionally, the results showed that the design of desalination systems is not limited to a continuous flow configuration. This research showed that changing the configuration in which the SWRO membranes are operated affects the performance of the process; and more importantly, the risk of fouling or scaling the membranes is reduced. The CERRO process has the potential to become a standard practice for

desalination. This project will be an important asset for the future development and improvement of the CERRO process.

1.5. Research Tasks

The experimental protocol in this project was carried out with the use of CERRO pilot units. Several batches were run under different conditions (i.e. different pH, water chemistry, acid dosage, and others). Water samples were taken and analyzed in situ or in the water and waste water laboratory located at UTEP (see appendix A). The impact of the parameters of operation in the performance of the system was evaluated by determination of the final recovery, energy consumption, and the state of the SWRO membrane elements at the end of the experiments. There were three different sources for the feed water in this project: KBH concentrate, Alamogordo brackish water, and Alto, New Mexico brackish water. In some experiments, the ionic composition of the KBH concentrate was changed by the addition of brine solutions with different types of salts (e.g. $CaCl_2$, NaCl, Na_2SO_4) to simulate a different source of water. One batch with permeate water as a feed was included after every batch. This batch was made to evaluate the permeability of the SWRO membranes after each test. The batch was run at 300 psi and the permeate flow was measured. The change in the permeate flow was considered as an indicator that the membrane was getting fouled or scaled.

Chapter 2: Literature Review

2.1. Desalination Systems and Concentrate Management

Desalination, using various forms of membrane treatment technologies to provide potable and higher-quality reuse water, has increased steadily in the United States. A byproduct of these technologies is a process stream containing elevated total dissolved solids. That stream is known as concentrate. Of the estimated 320 U.S. municipal desalination facilities, 96% are inland brackish water plants and only 4% seawater plants (Mickley and Jordahl 2013). Figure 2.1 shows the distribution of the desalination systems used in municipal plants in the United States (modified from Mickley 2013).

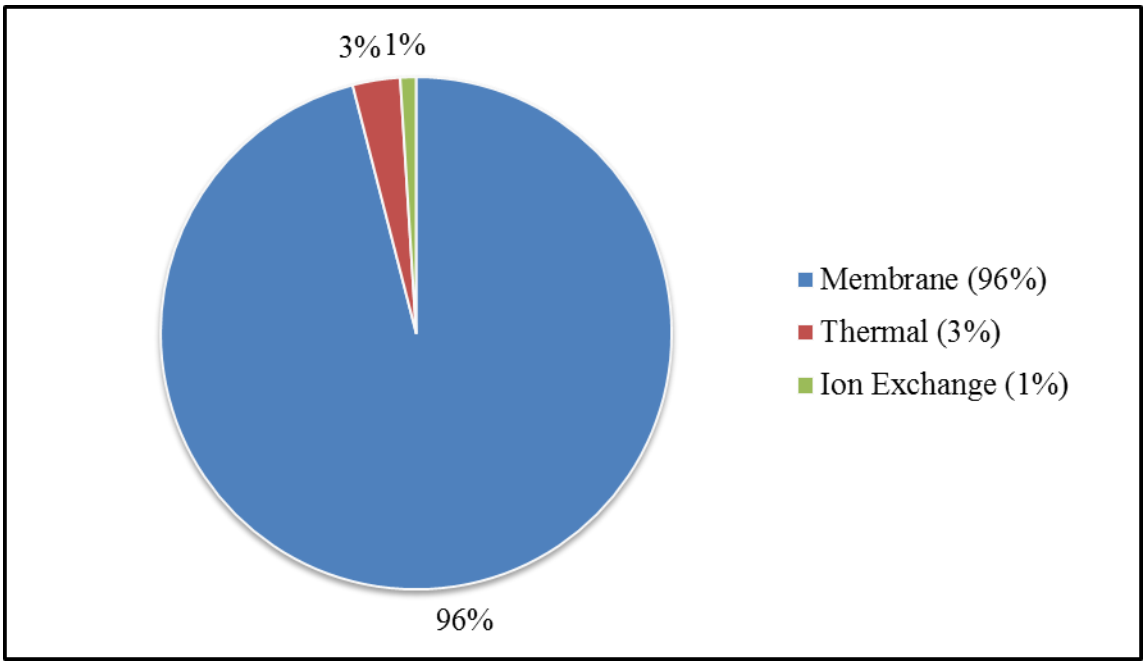

Figure 2.1: Distribution of Desalination Systems Used in the U.S. (Mod. From Mickley 2013)

As mentioned before, all desalination systems produce a stream of concentrated brine that needs to be sustainably managed. Until today, there are only a few methods for disposal of this concentrate and even fewer capable to treat and reduce the volume of concentrate.

Mickley and Jordahl (2013) describe five conventional methods for the disposal of the concentrate produced during desalination processes.

- **Surface Water Discharge**
  - Direct ocean outfall
  - Shore outfall
  - Co-located outfall
  - Discharge to river, canal, lake
- **Disposal to sewers**
  - Sewer line
  - Direct line to waste water treatment plants
  - Brine line
- **Subsurface Injection**
  - Deep well injection
  - Shallow well
- **Evaporation Pond**
  - Conventional evaporation pond
  - Enhanced Evaporation pond
- **Land Application**
  - Percolation pond/rapid infiltration basin
  - Irrigation

Mickley and Jordahl (2013) made a detailed description of these methods and the conditions in which they can be used for disposal of the concentrate. In the same way, they explain the limitations of these methods of disposal. For example, evaporation ponds require large extensions of terrain and are limited to areas with certain weather conditions (e.g. yearly rainfall and solar radiation). Similarly, subsurface injection can only be used in areas that have the proper geological conditions. Figure 2.2 shows the distribution of the concentrate disposal methods used in municipal desalination plants in the U.S. (modified from (Mickley 2009)

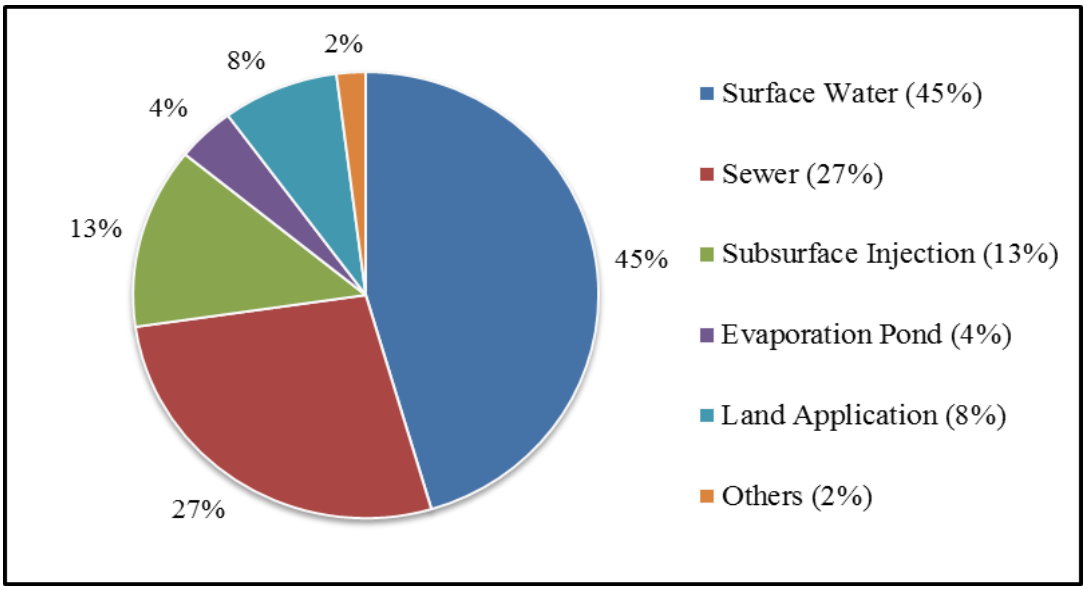

Figure 2.2: Distribution of Concentrate Disposal Methods in the U.S.

Different reports (Mickley 2009; Mickley and Jordahl 2013) have mentioned that the management of the concentrate has become problematic for three main reasons:

- The production of fresh water by means of desalination has increased considerably in the past decade. For that reason, the production of concentrate has increased, making its management more difficult. This happens because some of the conventional methods of disposal are limited in the volume of concentrate they can dispose (i.e. evaporation ponds).

- The current regulations for disposal, particularly for discharges affecting receiving waters, are becoming more restrictive as salinity and contaminant levels in both surface water and groundwater continue to increase.
- Treatment cost of desalination has decreased considerably because of more efficient and less expensive, membranes among other factors. Concentrate management costs, however, have not decreased. Capital cost has not decreased (with the exception of evaporation ponds) and operating costs have increased because of more detailed monitoring requirements. As a result, concentrate management costs have become an increasing percentage of total desalination plant costs.

These tendencies indicate that desalination processes will be the solution for the shortage of freshwater in some places in the U.S. (and the world). However, it is necessary to improve these processes in order to reach a sustainable and feasible production of freshwater by desalting brackish and seawater. It is in the reduction of the concentrate volume produced by conventional desalination systems where one solution to this problem could be found. However, the solution to this problem is not an easy task. This is due to high costs associated with the treatment of the concentrate. Since conventional methods are not capable of treating the concentrate further, new processes have to be designed. Some of these processes are cost-prohibitive due to their high capital cost and/or high operating cost. However, there are a growing number of locations, particularly in the southwest, where the use of conventional methods of disposal are not possible or feasible and alternative options are needed.

As was mentioned before, there are only a few processes capable of treating concentrated brine produced in desalination systems. Mickley and Jordahl (2013) made a detailed analysis of the current methods available to treat water with high TDS concentrations and/or concentrate. Some of these methods are discussed below.

2.2. High-Recovery Processing

High-Recovery (HR) processing is defined as processing feed water to attain recoveries of 90% or higher. The technical challenge of achieving HR depends on feed water quality, primarily the presence of sparingly soluble salts and silica. There are instances where high recovery levels can be achieved in a one-step membrane process. More typically, however, brackish feed water recoveries above 90% will require further treatment of the concentrate. When the feed water contains relatively high concentrations of sparingly soluble salts and/or silica (the case of the KBH desalting plant), solubility limits are reached and precipitation is likely to occur. Sparingly soluble salts from groundwater of typical concern include

- $CaCO_3$ (Calcium Carbonate)
- $BaCO_3$ (Barium Carbonate)
- $MgCO_3$ (Magnesium Carbonate)
- $CaSO_4$ (Calcium Sulfate)
- $BaSO_4$ (Barium Sulfate)
- SiO_2 (Silica)
- $Mg(OH)_2$ (Magnesium Hydroxide)

Brackish water RO and Electrodialysis Reversal (EDR) typically use antiscalants and dispersants to allow greater recovery of the feed. Most antiscalants interfere in the kinetics of precipitation of the salt. However, the use of antiscalants is not enough to reach high recoveries. Further treatment of the concentrate is required.

The HR processing utilizes three approaches to address this precipitation/scaling potential for secondary treatment of the concentrate.

2.2.1. Precipitates Are Allowed to Form within the Desalination Equipment

In these processes, volume reduction takes place after the point where precipitation of some species occurs. The precipitates are kept from scaling membranes by

a) Precipitation on a circulating slurry such as the SPARRO process (Juby and Schutte 2000).
b) High velocities and shear rates such as VSEP (Delgado 2009).
c) Proprietary surfaces that inhibit attachment under flow conditions such as ALTELARAIN (Altela Inc. 2013).

2.2.2. Unique Processing Sequences Allow High Recovery by other Means

Some approaches use unusual sequences of treatment steps to achieve high recovery. For example, ARROW uses chemical precipitation following two membrane steps and, in some cases, ion-exchange softening as an integral step. Other examples of processes that use this approach of treatment are ZDD, which uses a unique form of ED called Electrodialysis Metathesis (Davis and Rayman 2008), and the HERO process which uses ion exchange and operates at high pH values (Aquatech Intl. 2011).

2.2.3. Precipitating Species Are Removed Before the Desalination Steps

This is the most common approach to high recovery. In this approach, chemical treatment steps before the desalination process are used in order to reduce concentrations of species that might otherwise precipitate upon concentration of the solution. There are many versions of this approach with different groups giving their own name to essentially similar processing schemes. Some examples are:

- Chemically-Enhanced Seeded Precipitation CESP (Rahardianto et al. 2010)
- Accelerated Chemical Demineralization ACD (Cohen 2008)
- High Performance Reverse Osmosis HiPRO (Keyplan 2010)
- Intermediate Chemical Demineralization ICD (Gabelich et al. 2007)

All the studies mentioned before have confirmed that, for large volumes of concentrate, high recovery is not a technical problem, but a technology constrained by cost. The current investigations are mainly focused in the optimization of these processes. The most important objectives of these projects are the reduction of energy requirements as well as the reduction of operation and capital cost.

2.3. Limitations of Desalination Systems

The presence of sparingly soluble salts is one of the most important limitations in membrane and thermal desalination. Carbonate and sulfate minerals (e.g. $CaCO_3$, $CaSO_4$) precipitation is a common problem in desalination processes. However, sulfate minerals solubility limits are not affected by pH changes, but temperature affects them slightly. This particular characteristic represents a problem for desalination systems. If high recoveries are needed, the $CaSO_4$ has to be removed from the water. This action requires the addition of one or

more processes to the desalination system, which often renders it cost-prohibitive. In the section below, the problem of $CaSO_4$ precipitation is discussed thoroughly.

2.3.1. Limitations due to $CaSO_4$ Precipitation

The precipitation of $CaSO_4$ from aqueous solutions onto surfaces occurs when an electrolyte solution containing calcium and sulfate ions is supersaturated. This precipitation can occur if ions are added to the solution or if water is extracted from the solution (the case of desalination). The crystal form of $CaSO_4$ precipitation in aqueous solutions depends mostly on the temperature of the solution (Prisciandaro et al. 2003). At low temperatures, gypsum ($CaSO_4*2H_2O$) will be formed. For that reason, gypsum is the most common sulfate mineral that precipitates in membrane desalination. The solubility of $CaSO_4$ in water can be calculated using equation 2.1 (Uchymiak et al. 2008).

$$SI = \frac{\{Ca^{+2}\} * \{SO_4^{-2}\}}{K_{sp}}$$

Equation 2.1

Where:

SI = Saturation index of $CaSO_4$

$\{Ca^{+2}\}$ = Activity corrected concentration of Calcium

$\{SO_4^{-2}\}$ = Activity corrected concentration of Sulfate

K_{sp} = Constant solubility product of $CaSO_4$

If the saturation index (SI) value is less than one, it means that the solution is undersaturated with $CaSO_4$. If the SI is equal to one, it means that the $CaSO_4$ is in equilibrium; and if the SI is greater than one, it means that the solution is supersaturated with $CaSO_4$. The

normal concentration of the ions has to be corrected by calculating the activity coefficients of the ions. This means that the solubility of $CaSO_4$ is greatly affected by the chemical composition of the water.

When the SI value is positive, precipitation of $CaSO_4$ is likely to occur. When this precipitation happens inside the membrane desalination system, crystals of gypsum get attached to the surface of the membrane, creating an impermeable layer that dramatically reduces the production of fresh water. The kinetics of gypsum precipitation have been studied broadly (Gilron and Hasson 1987; Sheikholeslami and Ong 2003; Fan et al. 2010; He et al. 2009). These studies have shown that some organic compounds (e.g. organophosphonates, polyacrylic acids) have the property to reduce the impact of gypsum (and other minerals) crystallization in desalination systems. These compounds are called antiscalants, and their use has become a common standard in desalination systems. It has been shown that antiscalants interfere in the kinetics of precipitation; however, they do not affect the solubility of gypsum. Additionally, at high SI values, the antiscalants performance starts to decay. For that reason, the risk of scaling the membranes still remains. Figure 2.3 shows the effects of different antiscalants in a RO unit with gypsum saturated feed water (Shih et al. 2005).

Figure 2.3 is a good example of how the antiscalants affect the kinetics of gypsum precipitation, but do not improve its solubility limit. Additionally, it has been shown that high concentrations of antiscalants are ineffective and, at some point, cost-prohibitive. Until now, the antiscalants interaction with the kinetics of gypsum has not been completely understood. This happens because most of the commercially available antiscalants are patented products and the companies do not release the exact chemical composition of the antiscalants for its study (Delgado and Tarquin 2012).

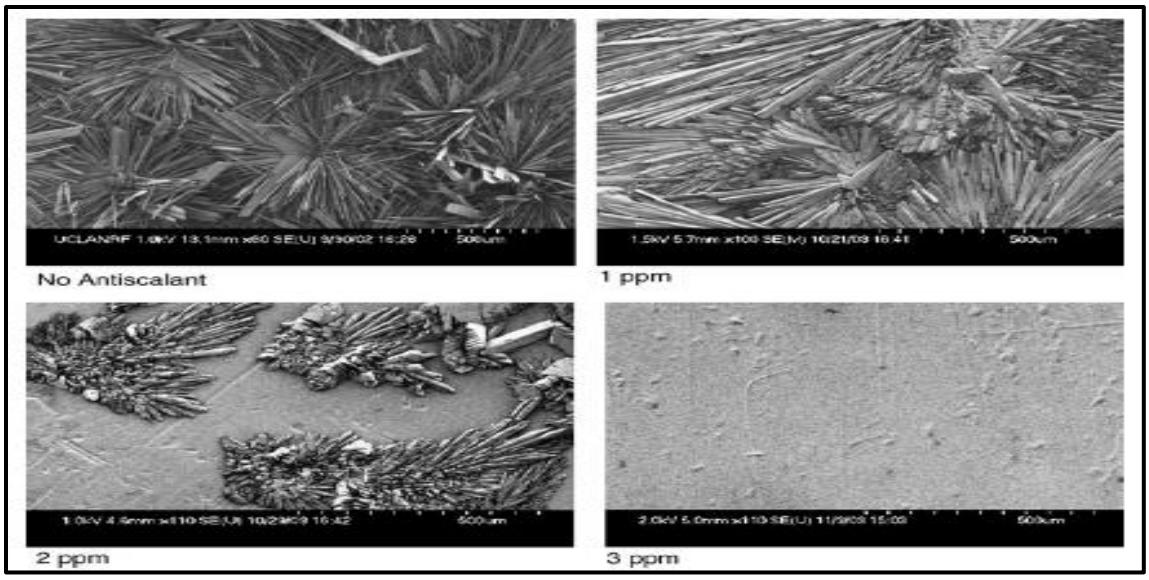

Figure 2.3: Effect of Antiscalant on Crystal Accumulation and Morphology (Shih et al. 2005)

Analyzing the kinetics of gypsum precipitation has not been an easy task. Different studies have shown that supersaturation can be reached for a brief period of time before precipitation occurs (Sheikholeslami and Ong 2003; Shih et al. 2004). This phenomenon is commonly called induction time. Different researchers have calculated that the induction time of gypsum presents a logarithmic rate of decay that is a function of the SI of the solution among other factors (Alimi et al. 2003; Prisciandaro et al. 2003). Additionally, these studies have shown that the kinetics of precipitation present an exponential rate of crystal nucleation. This particular characteristic has been used in some processes as an advantage to improve the recovery of the system (e.g. SPARRO process). However, this same characteristic is the most problematic issue in conventional membrane desalination. The incrustation of one single crystal of gypsum in the membrane will lead to an exponential accumulation of crystals at the beginning with a stable accumulation afterwards. Figure 2.4 shows the evolution of the surface number density (SND) of gypsum crystals at different SI's (Uchymiak et al. 2008).

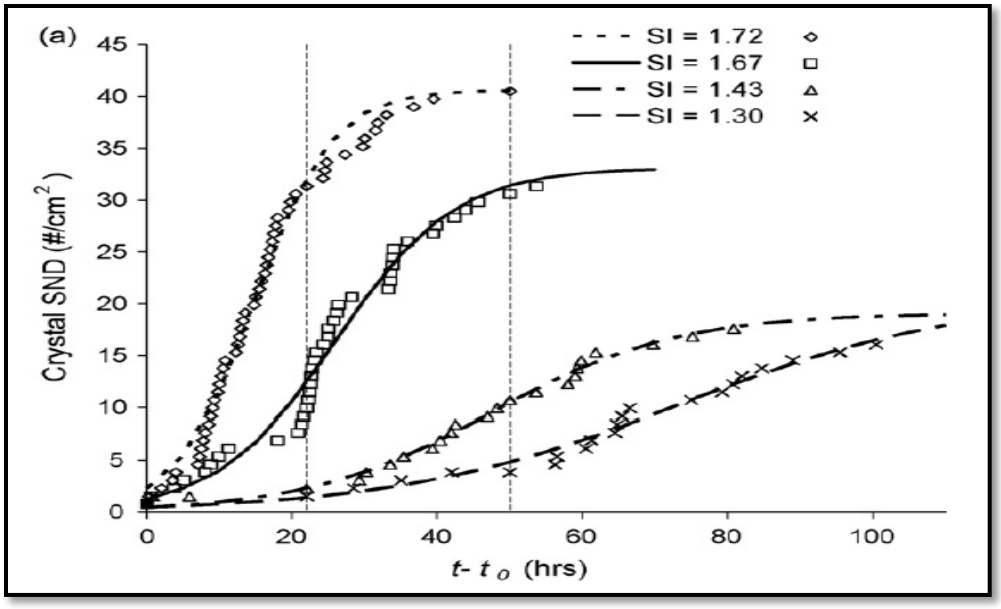

Figure 2.4: Evolution of SND of Gypsum at Different SI's (Uchymiak et al. 2008).

Figure 2.4 shows the number of gypsum crystals formed per square centimeter of membrane as a function of time. Additionally, it shows that crystal nucleation formation is affected by the gypsum SI. In the same way, it can be seen that there is an exponential accumulation of gypsum crystals on the surface of the membrane, with a stable accumulation after some time. This is probably due to the reduction in the membrane area and the increment of the cross flow velocity in the system due to a localized decline of the flux.

It is important to notice that the time units are presented in hours. For a batch treatment system such as the CERRO process, this is a key factor that affects the performance of the process. This particular characteristic was evaluated in further sections of this document.

As a conclusion of this topic, it is important to notice that all the studies presented before have been done under steady-state conditions. In other words, all the parameters that are a function of other parameters did not change as a function of time. Non-steady state conditions have not been thoroughly studied.

2.3.2. Limitations due to Silica Polymerization

Similar to gypsum precipitation, silica (SiO_2) polymerization represents a major limitation for desalination processes. Multiple studies have shown that low concentrations of silica will foul RO membranes in relatively short periods of time (Hater et al. 2011; Koo et al. 2001). The kinetics of silica polymerization are governed by three stages where the nucleation period of a silica nanoparticles is followed by particle growth and particle aggregation. The initial step of silica polymerization occurs via coalescence of monosilicic acid molecules and the expulsion of water (Tobler 2008):

$$H_4SiO_4 + H_4SiO_4 \leftrightarrow (OH)_3Si - O - Si(OH)_3 + H_2O \quad \text{Equation 2.1}$$

Further polymerization leads to the formation of trimers, tetramers, etc. to cyclic oligomers and eventually three-dimensional internally condensed nanospherical polymers. During the second stage, this nucleus grows by further deposit of monomers to trimers of larger oligomers. The last stage is known as coarsening or Ostwald ripening where larger particles grow at the expense of smaller ones (Tobler 2008). Figure 2.5 shows an illustration of the polymerization process of monomeric silica (Parker 2005).

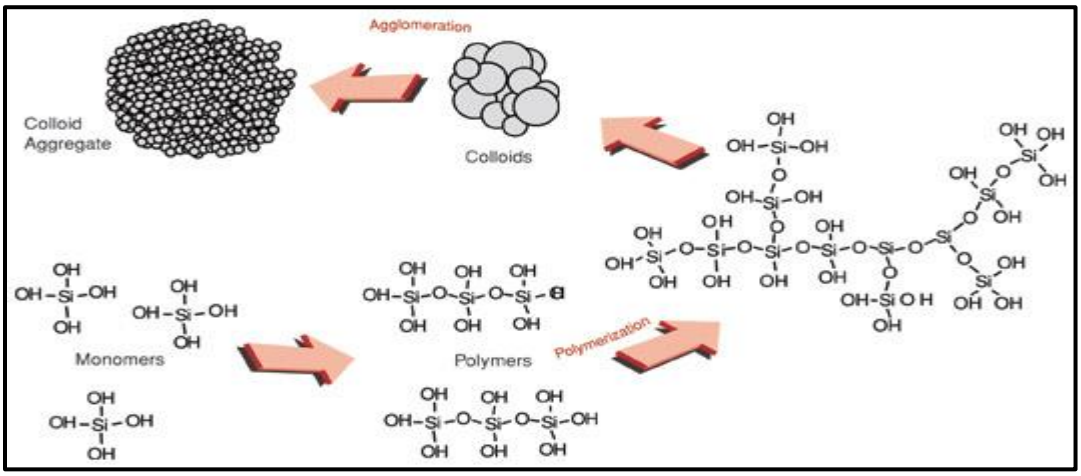

Figure 2.5: Silica Polymerization Process (Parker 2005)

Compared with other components present in brackish water (e.g. Cl^-, Na^+, Ca^{+2}, SO_4^{-2}), silica is always present in low concentrations (20-70 mg/L). However, silica has a very low solubility (less than 150 mg/L) at natural pH values. For that reason, the treatment of water with high concentrations of silica is often problematic. Additionally, silica polymers have the property to react with polyvalent metals (e.g. Ca^{+2}, Mg^{+2}) producing silicates (Tobler 2008). All these properties make silica a recurrent limitation for membrane and thermal desalination processes (Lisitsin et al. 2005). The most common approach to solve the problem of high concentrations of silica is the use of antiscalants. There is a large number of commercially available antiscalants for silica, and they have been studied thoroughly (Hater et al. 2011; Koo et al. 2001; Sahachaiyunta et al. 2002). As most antiscalants, silica antiscalants interfere in the kinetics of silica polymerization, but do not affect the solubility of monomeric silica. It was proposed that silica antiscalants get attached by electrostatic attraction of negatively charged silica monomers to positively charge groups of the antiscalant. Additionally, it was found that antiscalants modify the geometric structure of silica particles, but do not increase the solubility of silica in the water (Zhang et al. 2011). Figure 2.6 shows the polymerization of silica as a function of time and the retardation effects by the addition of different dosages of antiscalants (Zhang et al. 2011).

Figure 2.6 shows the rate of silica polymerization by measuring the decay in the concentration of soluble silica or monomeric silica. It can be seen that the time units are given in hours. It is important to mention because for a conventional RO system, 20 hours of treatment before a cleaning procedure is fairly short. However, the graph shows that, even for the control without antiscalant, the polymerization of silica takes several hours. It was determined in this

research that this particular characteristic can be used in order to achieve high recoveries without fouling the RO membranes.

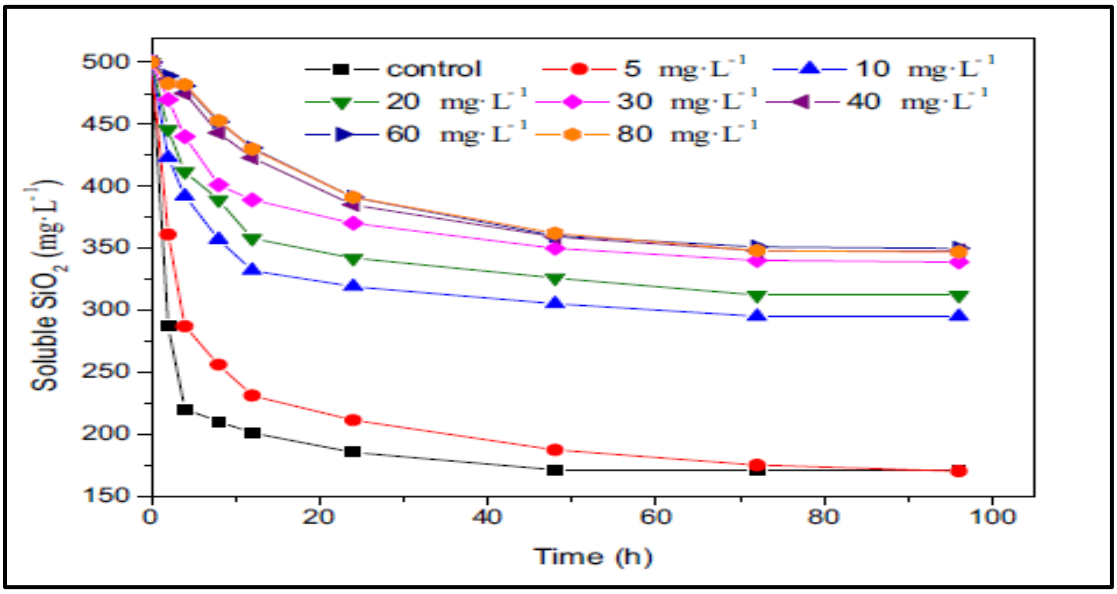

Figure 2.6: Silica Polymerization at Different Antiscalant Concentrations (Zhang et al. 2011)

According to the findings in this section, the precipitation of sparingly soluble salts and silica polymerization are two common problems in desalination systems. It has been found that the use of antiscalants is a good approach to improve the recovery of conventional desalination systems. However, there is a parameter in the studies that has not been thoroughly studied in the impact of the processes. The induction time of precipitation is a factor present in the limitations previously described, precipitation and polymerization. It is understandable that, in a conventional desalination system, the induction time is not an important factor; or at least one that cannot be controlled. This happens because conventional systems are designed to operate for several days (sometimes months) without any type of cleaning procedures. This design can lead to a steady formation of crystals or polymers in the surface of the membrane. On the other hand, the CERRO process is designed in a batch mode. The treatment time can be fixed to be lower than the induction time of precipitation or polymerization. In the next sections of this

document, it is shown that high recoveries can be achieved in short periods of time thereby avoiding fouling or scaling problems.

Chapter 3: Concentrate Enhanced Recovery Reverse Osmosis

The CERRO process started as a pilot scale system designed to test the effects of treating KBH concentrate with SWRO membranes. Initially, the system was designed to test the limitations of SWRO membranes to treat the concentrate produced by the KBH desalination plant. With an average silica concentration of 130 mg/L, the expectations of reaching high recoveries were low. However, the system showed that recoveries between 85 and 90% were achievable (Tarquin et al. 2010; Tarquin 2008). In previous publications, the treatment unit was identified as a SWRO batch system. Later, the name was changed to Concentrate Enhanced Recovery Reverse Osmosis (CERRO) process and, on August 6, 2010, a patent application was submitted (UTEP Provisional patent application number 61/233,761). Multiple tests have been done testing the CERRO process capabilities for treating RO concentrate and brackish water. Three different pilot units have been designed using the principle of the CERRO process to treat water in a batch configuration. All units showed an exceptional resistance to silica and calcium sulfate scaling. However, the tests performed in these studies did not identify the parameters of operation that allowed the units to present such resistance. In order to understand this behavior, it is necessary to identify the parameters of operation of the CERRO process. The parameters of design of the system are shown below.

3.1. Parameters of Design of the CERRO Process

The CERRO process is designed to operate in a batch configuration. Batch processing is commonly used for bench-scale units for experimental purposes (Uchymiak et al. 2008; Shih et al. 2005). The batch configuration is often used as part of an experiment until a predetermined recovery is reached; then, the system is switched to a continuous flow configuration to simulate

the conditions in which conventional desalination systems operate (Kumar et al. 2006; Lisitsin et al. 2005; Hater et al. 2011). However, how a batch configuration may affect the performance of a desalination system has not been studied. The CERRO process utilizes membrane elements designed to operate in continuous flow, but these elements presented a different performance when operated in the conditions of batch processing.

3.1.1. CERRO Unit with Single-Membrane Element (CERRO SME)

The first pilot unit based on the CERRO process was a single-membrane element batch system with a capacity of 30 gallons per batch. The specifications of the SWRO membrane are shown in Table 3.1.

Table 3-1: SWRO Membrane Specifications

Parameter	Specifications
Membrane Dimensions	21" x 2.4"
Membrane Type	Polyamide Thin-Film Composite
Maximum Operating Temperature	113°F (45°C)
Maximum Operating Pressure	1,000 psi (69 bar)
Maximum Pressure Drop	15 psig (1.0 bar)
pH Range, Continuous Operation	2 - 11
pH Range, Short-Term Cleaning	1 - 13
Maximum Feed Silt Density Index	SDI 5
Membrane Area	13 ft^2

The unit operates with a high pressure positive displacement pump with a capacity of 2.4 gallons per minute (9.0 L/min). The operating pressure of the system varies from 300 psi to 800 psi depending on the quality of the feed water. The pump has a pressure limit of 1000 psi.

The feed water is typically pretreated with acid solutions to remove the alkalinity present in the water. Antiscalants for sulfates are added to the water to avoid calcium sulfate

precipitation during the treatment time. The acid and antiscalants have to be added manually by the operator.

After the water is pretreated, the system starts passing water through the SWRO membrane element. The membrane element produces one stream of permeate and one stream of concentrate. The concentrate is recirculated to the feed tank where it will be treated again. This has to be done because SWRO membranes have low recovery rates (~10%). The system is stopped after the final recovery is reached. Figure 3.1 shows a schematic of the CERRO process.

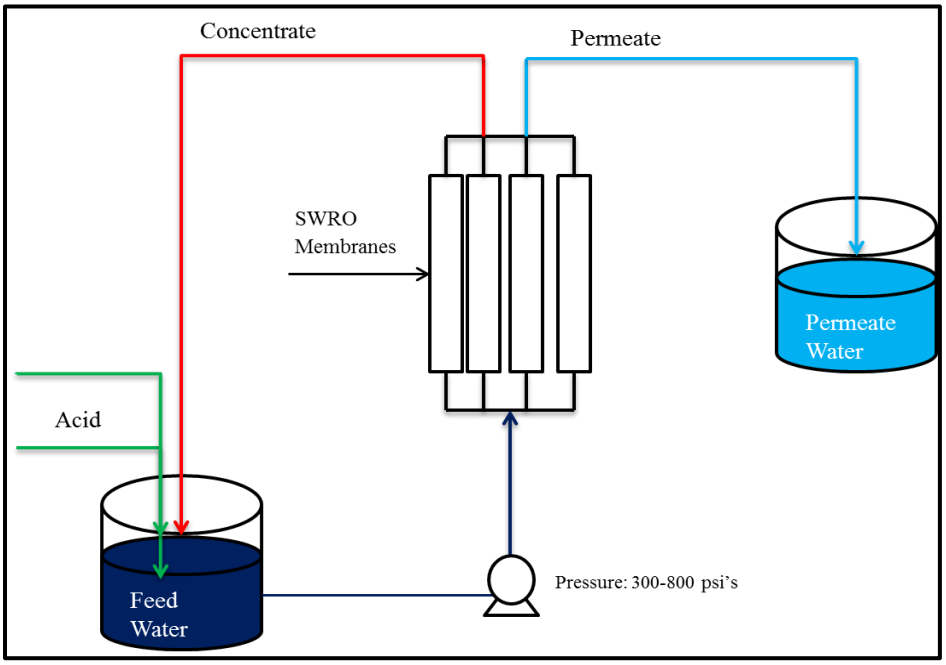

Figure 3.1: Schematic of the CERRO Process

3.1.2. CERRO Unit with Two-Membrane Elements (CERRO TME)

The second pilot unit was developed by Industrial Water Services (IWS) under the supervision of Professor Anthony Tarquin. This unit was an improvement of the single-membrane element unit previously described. This unit contained two SWRO membrane elements (21"x2.5") connected in parallel and the volume capacity was increased to 50 gallons

per batch. It operated with a high pressure positive displacement pump with the same operating conditions as the single-membrane element. Another improvement of the unit was the addition of electronic dosing controllers for the acid and the antiscalants. This unit was tested at the BGNDRF in 2011 for the desalination of brackish water with high concentrations of gypsum. After several tests, the system presented no evidence of gypsum scaling when the brackish water reached supersaturation; and, in some cases, precipitation. However, the recovery of the system was limited due to precipitation of calcium sulfate. During this project, it was found that the chemistry of the water and the addition of antiscalants played a very important role in the treatment of this kind of water.

3.1.3. CERRO Unit with Multiple-Membrane Elements (CERRO MME)

This unit was designed by IWS under the supervision of Professor Anthony Tarquin. In this unit, four SWRO membrane elements were connected in parallel and the volume capacity was increased to 300 gallons per batch. This unit was designed to be fully automated and run multiple of batches.

The system had four GE-Osmonics desalination membranes (40” x 4”) in a parallel single stage configuration. The unit contained a plastic permeate collection tank and a 300-gallon cone-bottom plastic tank on a metal stand. The high pressure positive displacement feed pump could discharge 32 gpm (121 L/min) at 1200 psi and produce up to 6 gpm (22.7 L/min) of permeate at the normal operating pressure of 700 psi. The system included numerous sensors for measuring pH, permeate and concentrate flow rates, pressures, temperatures, and conductivities. The readings awere data-logged at one minute intervals and stored on a computer that was accessible at all times via the internet. Figure 3.2 shows an image of the CERRO unit with multiple-membrane elements (Tarquin et al. 2010).

Figure 3.2: Fully Automated CERRO Unit (Tarquin et al. 2010)

3.2. Comparison between the CERRO Process and Conventional RO Processes

As mentioned before, the CERRO process utilizes SWRO membrane elements that are commercially available, but it operates them in a different configuration than conventional desalination systems. The conditions of operation of conventional desalination systems are set in a continuous flow system. The concentrating factor inside the membrane elements is relatively the same as a function of time. In the CERRO process, the concentrating factor increases over time as the feed water gets more concentrated. It was found that this particular characteristic allows the CERRO process to operate in conditions of supersaturation for a brief period of time. Another important characteristic of the CERRO process is that it can be cleaned frequently to minimize the incrustation of crystals on the surface of the membranes. Table 3.2 shows the differences between the CERRO process and conventional continuous flow systems.

Table 3-2: Different Characteristics between Conventional Systems and the CERRO Process

General Characteristics	Conventional RO System	CERRO Process
Process Configuration	Continuous Flow	Batch
Recovery Approach	Membrane elements connected in series, and multiple stages connected in series	Recirculation of the concentrate to the feed tank
Crossflow Velocity	Decreases along the membranes	Increases along the membranes
Residence Time	<5 minutes	20 - 120 minutes
Treatment Time	30 - 90 days	20 - 120 minutes
Concentrating Factor	Increases over distance, it is not a function of time. Remains constant along the membrane elements	Increases over time along the membrane elements
Membrane Flushing	30 - 90 days	Could be done after every batch
Membrane Cleaning	Several Months	Could be done after every batch

It was found that these differences in the operation of RO membranes affected their performance. The results obtained in this project have shown that batch processing can reduce the risk of scaling or fouling of membranes. The experimental approach taken in this project, the results obtained during experimentation, and the final conclusions are shown in the next sections of this document.

Chapter 4: Identification of Important Parameters of Operation and Improvement of the CERRO Process

Different parameters of operation of the CERRO process were identified. The objective of this study was to identify which parameters of operation had the higher impact on the performance of the CERRO process. After the parameters were identified, the improvement of the process was done by modifying the parameters to reduce the operating cost and/or improve the recovery of the system. The parameters of operation that were studied in this project are shown in Table 4.1.

Table 4-1: Parameters of Operation in the CERRO Process

Parameter of Operation	Observed Impact in the Process
Treatment Time	Could be lower than precipitation time of salts
Crossflow Velocity	Increases over time reducing the concentration polarization layer
Acid Dosage	Removes alkalinity present in the water
Antiscalant Dosage	Increases induction time of calcium sulfate
Temperature	Impacts the permeate production, may affect the membrane
Pressure	Increases permeate production, but impacts operation cost
Membrane Flushing	Removes the final concentrate from the membranes
Water Chemistry	Increases the solubility of some salts, affects recovery due to precipitation

The water chemistry is included as a parameter of operation even though it is not. It was found that that the water chemistry plays an important role for recovery in the CERRO process in the same way as in any desalination system.

4.1. Parameters of Operation: Treatment Time

The evaluation of this parameter was done using the CERRO unit with a single-membrane element (see section 3.1.1). The analysis of previous data showed that the CERRO unit passed the feed water through the SWRO membrane element several times before reaching the final recovery. This happened because the low recovery of the SWRO membrane forced the high pressure pump to cycle the feed water many times during the batch. It was calculated that the CERRO SME unit had an average of 9.0 cycles per batch. This means that one batch of 20 gallons in the CERRO unit will require pumping 190 gallons of feed water. This information is supported by Table 4.2 which shows the number of cycles of different batches run using the CERRO SME unit.

Table 4-2: Number of Cycles of Different Runs

Batch (Date)	Treatment Time (minutes)	Batch Volume (Gallons)	Final Recovery	Number of cycles
6/14/2011	85	20	92%	10.20
12/21/2010	55	15	91%	8.80
12/17/2010	45	15	88%	7.20
10/22/2010	95	30	88%	7.60
10/8/2010	95	30	88%	7.60
10/1/2010	120	30	90%	9.60
6/23/2010	140	30	87%	11.20
6/16/2010	115	30	85%	9.20

The number of cycles was calculated by multiplying the flow (2.4 gpm) of the positive displacement pump by the duration of the batch. That value was then divided by the batch volume. It can be seen that the number of cycles is proportional to the duration time and the volume of the batch. Other factor that affected the number of cycles was the salinity of the water.

4.1.1. Improvement of the Treatment Time

The treatment time of operation is one of the most important factors of the CERRO process. The excessive number of cycles is the reason that the system has an elevated operating cost (Tarquin et al. 2010). Additionally, the treatment time is directly related to the silica polymerization and, in some part, calcium sulfate precipitation.

The approach taken to reduce the treatment time in the system was by the addition of two more SWRO membrane elements. This was done in order to increase the membrane area and the permeate flux. The feed flow could not be changed due to the type of pump used in the system. The primary concern associated with adding more membranes was the possibility of fouling or scaling the membranes; more precisely, the last membrane element. The new membranes had the capacity to operate in series or parallel and to be connected to the SME already installed in the unit. Several experiments were done using two or three membrane elements, resulting in a reduction of the treatment time of the unit. A performance test of the unit with permeate water as a feed showed that the membranes kept the same flux after the experiments. Table 4.3 shows the results of different experiments using the new set of membranes.

Table 4-3: CERRO SME Results with New Membrane Elements

Batch (Date)	No. of Membrane Elements	Membrane Configuration	Treatment Time (minutes)	Batch Volume (Gallons)	Final Recovery	Number of cycles
12/14/2012	2	Parallel	12.5	10	86%	3.00
12/14/2012	2	Series	20	20	81%	2.40
12/18/2012	2	Parallel	25	20	76%	3.00
12/18/2012	2	Parallel	25	20	81%	3.00
12/18/2012	3	Series	15	20	75%	1.80
12/18/2012	3	Series	15	20	75%	1.80
12/20/2012	3	Series	15	20	76%	1.80
12/20/2012	3	Series	19	20	76%	2.28

After each experiment, the membrane elements were flushed with permeate water from the KBH plant. Then, the unit was run with permeate water as a feed at 300 psi. This method was developed as a method for easily determining if the membrane was fouling. After each experiment, the permeate flow rate of the unit remained constant and no signs of scaling or fouling were detected.

4.1.1.1. Energy Reduction and Cost Analysis

The reduction in the treatment time helped to reduce the operating cost of the system. It was calculated that the power consumption of the CERRO SME unit decreased 73% on average by reducing the treatment time. This reduction was determined by calculating the power requirements of the unit. It was found the CERRO SME unit required an average of 60 kWh per 1000 gallons before the addition of more membrane elements. This amount of power would have an average cost of $4.84 per 1000 gallons. With additional membrane elements, the power required was reduced to 16.6 kWh per 1000 gallons. It was calculated that this amount of power would have an average cost of $1.29 per 1000 gallons. These calculations were based in the assumption that,

a) The operating pressure remained constant at 700 psi,
b) The power cost was $0.08 per kWh, and
c) The pump efficiency was 75%.

Table 4.4 shows the calculations for the energy cost in the CERRO SME unit before the addition of the new set of membrane elements based on the treatment time.

Table 4-4: Energy Cost of the CERRO SME Unit

Batch (Date)	Treatment Time (Hours)	Batch Volume (Gallons)	Final Recovery	Number of cycles	Power (kWh)	Power (kWh/kgal)	Cost ($/kgal)
6/14/2011	1.42	20	92%	10.63	1.38	69.10	$5.53
12/21/2010	0.92	15	91%	9.17	0.89	59.61	$4.77
12/17/2010	0.75	15	88%	7.50	0.73	48.77	$3.90
10/22/2010	1.58	30	88%	7.92	1.54	51.48	$4.12
10/8/2010	1.58	30	88%	7.92	1.54	51.48	$4.12
10/1/2010	2.00	30	90%	10.00	1.95	65.03	$5.20
6/23/2010	2.33	30	87%	11.67	2.28	75.87	$6.07
6/16/2010	1.92	30	85%	9.58	1.87	62.32	$4.99
						Average	$4.84

Table 4.5 shows the energy cost calculations of the CERRO SME unit with the new set of membranes. There is a small difference in the treatment time for different batches with the same volume. This is due to a change in the salinity of the KBH concentrate during the time of the tests. The KBH plant utilizes feed wells with different salinities at different times.

Table 4-5: Energy Cost after the Addition of New Membrane Elements

Batch (Date)	Treatment Time (Hours)	Batch Volume (Gallons)	Final Recovery	Number of cycles	Power (kWh)	Power (kWh/kgal)	Cost ($/kgal)
12/14/2012	0.21	10	86%	3.125	0.20	20.32	$1.63
12/14/2012	0.33	20	81%	2.5	0.33	16.26	$1.30
12/18/2012	0.42	20	76%	3.125	0.41	20.32	$1.63
12/18/2012	0.42	20	81%	3.125	0.41	20.32	$1.63
12/18/2012	0.25	20	75%	1.875	0.24	12.19	$0.98
12/18/2012	0.25	20	75%	1.875	0.24	12.19	$0.98
12/20/2013	0.25	20	76%	1.875	0.24	12.19	$0.98
12/20/2013	0.32	20	76%	2.375	0.31	15.45	$1.24
						Average	$1.29

Another factor that affects the treatment time is the final recovery. In the experiments made using the new membranes, relatively low recovery rates were achieved (75%-80%). There are two factors that need to be approached in future projects: the identification of the optimal recovery of the unit, and the possibility to design the system to operate in one cycle per batch.

4.1.1.2. Cost Analysis

A cost analysis of the process was made to find the permeate production of the process the will produce a revenue. The data used for these calculations was the same reported by Tarquin et al in 2010 and modified with the information obtained from the new experiments. Table 4-6 shows the data used for the cost analysis.

Table 4-6: Parameters used for the Cost Analysis

Parameter	Units	Value
Initial RO Concentrate volume	gpd	100,000
Interest Rate	%	5
Evaporation rate	inch/year	90
Excavation	$\$/yd^3$	3
Excavation amortization time	years	20
Equipment life	years	20
Water selling Price	$/kgal	2
SWRO membrane life	years	3
Power cost	$/kWh	0.08
Pump and motor efficiency	%	75
RO membrane cost	$\$/ft^2$	2
SWRO Flux	gpd/ft^2	27
SWRO operating pressure, psi	psi	700
antiscalant cost	$/9 lb gal	11
H_2SO_4	$/gal	2.53
H_2SO_4 Feed rate	mL/gal	0.5
Evaporation pond depth	ft	3
CERRO Power Requirements	kWh/kgal	16.16
Antiscalant Dosage	mL/gal	0.02

The cost analysis of the CERRO process was performed for a treatment of 100,000 gallons per day at different recoveries. The method of disposal of the concentrate was assumed to be by evaporation pond. Most of the parameters in Table 4-6 were taken from Tarquin et al (2010) with the exception of SWRO flux, acid feed rate, and the CERRO power requirements. These values were obtained from the new set of experiments.

4.1.1.3. Evaporation Pond Analysis

The area required to contained the concentrate produced by the CERRO process was obtained by dividing the volume of concentrate produced per day by the evaporation rate in El Paso (90 in/year) (Texas ET Network, 2013). Then, the volume of the pond was calculated by multiplying the pond area by the depth of the pond (3 feet) and the result was reported in cubic yards. Table 4-7 shows the volume of the pond at different recoveries. It can be seen that the volume required, and thus the excavation cost, decreases at higher recoveries since there is less volume of concentrate for disposal.

Table 4-7: Pond Volume and Annual Cost

Recovery	Evaporation Pond volume (yd^3/year)	Excavation cost ($/year)
0%	6,018	$1,449
10%	5,416	$1,304
20%	4,814	$1,159
30%	4,213	$1,014
40%	3,611	$869
50%	3,009	$724
60%	2,407	$579
70%	1,805	$435
80%	1,204	$290
90%	602	$145
100%	00	$00

4.1.1.4. Membrane Area Analysis

The membrane area required to treat 100,000 gallons per day was calculated by dividing the permeate production by the operational flux of the process. The operational flux in the CERRO process changes continuously over time. For that reason, a safety value of 27 gpd/ft^2 (average of fluxes) was used for these calculations. Table 4-8 shows the membrane area required at different recoveries and the annual cost. It can be seen that the membrane area required for treatment increases as the recovery increases due to an increment in the production of permeate.

Table 4-8: Meambrane Area and Membrane Annual Cost

Recovery	Membrane Area (ft^2)	Membrane Cost ($/year)
0%	0	$00
10%	370	$272
20%	741	$544
30%	1111	$816
40%	1481	$1,088
50%	1852	$1,360
60%	2222	$1,632
70%	2593	$1,904
80%	2963	$2,176
90%	3333	$2,448
100%	3704	$2,720

4.1.1.5. Power Requirement Analysis

The requirement cost was made using the values obtained in section 4.1.1.1. With an average of 2.5 cycles per batch with the new set of membranes, it was estimated that the CERRO process requires 16.6 kWh per every thousands gallons of permeate. Based in the information reported by Tarquin et al (2010), the kWh cost in El Paso, Texas is $0.08. With this information,

the energy consumption and its cost was calculated in a yearly basis. Table 4-9 shows the results of the energy consumption and the annual cost for permeate production.

Table 4-9: Annual Energy Requirements and Cost

Recovery	Power Requirement (kWh/year)	Power Cost ($/year)
0%	0	$00
10%	162	$4,719
20%	323	$9,437
30%	485	$14,156
40%	646	$18,875
50%	808	$23,594
60%	970	$28,312
70%	1131	$33,031
80%	1293	$37,750
90%	1454	$42,468
100%	1616	$47,187

4.1.1.6. Acid and Antiscalant Calculations

The cost of acid and antiscalant for the CERRO process was calculated by multiplying the dosage of each of these compounds by the 100,000 gallons per day of feed water that will be treated. These two parameters are the only ones that remained constant despite the recovery because they are in function of the volume of feed and not permeate or concentrate. The cost of acid and antiscalants was obtained from the values reported by Tarquin et al (2010). According to the results, it was found that the annual cost of the addition of H_2SO_4 will be $12,200 based in a dosage of 0.5 mL of acid per gallon of feed water. In the same way, it was found that the annual cost of antiscalant dosage will be $2,122 based in a dosage of 5 ppmv.

4.1.1.7. Total Cost, Revenue, and Net Revenue

The total cost of the process was estimated by adding the disposal, membrane, energy, antiscalant, and acid costs obtained during the analysis. The revenue of the process was estimated by multiplying the permeate flow by the selling price of water in El Paso. Tarquin et al (2010) used a value of $2.00 per 1000 gallons of water. The net revenue was calculated by resting the total cost from the revenue. Table 4-10 shows the results of the total cost, revenue, and net revenue analysis for the CERRO process.

Table 4-10: Total Cost, Revenue, and Net Revenue

Recovery	Total cost ($/year)	Revenue ($/year)	Net revenue ($/year)
0%	$15,769	$0,000	-$15,769
10%	$20,615	$7,300	-$13,315
20%	$25,461	$14,600	-$10,861
30%	$30,307	$21,900	-$8,407
40%	$35,152	$29,200	-$5,952
50%	$39,998	$36,500	-$3,498
60%	$44,844	$43,800	-$1,044
70%	$49,690	$51,100	$1,410
80%	$54,536	$58,400	$3,864
90%	$59,382	$65,700	$6,318
100%	$64,228	$73,000	$8,772

According to the calculations, it was found that the break-even point occurred at about 65% recovery. At a lower recovery rate, the annual cost is higher than the revenue rendering the process cost prohibitive. Figure 4.1 shows the trend of the total cost, revenue and net revenue at different recoveries.

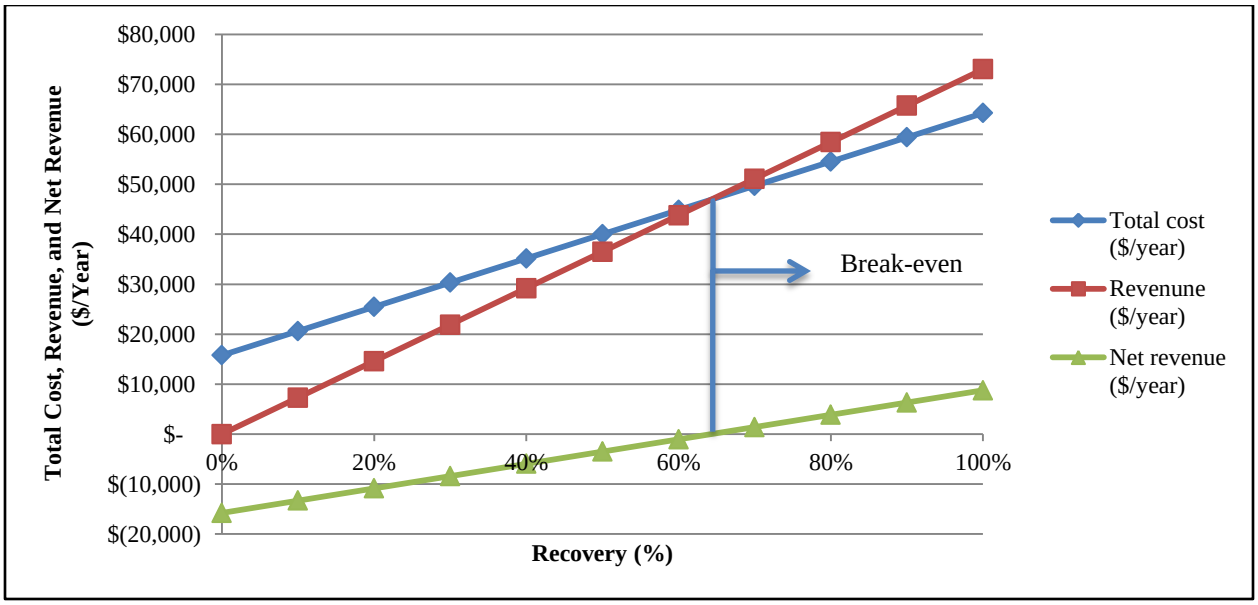

Figure 4.1: Trends for Total Cost, Revenue, and Net Revenue

This analysis was made with the information available until today. There are other costs associated with the process that were not included in the analysis. Costs like personnel, installation, maintenance, design, and others were not included due to a lack of accurate information to include them into the analysis. It will be necessary for future projects to include more parameters for a more detailed projection of the cost associated with the CERRO process.

4.1.1.8. Operation in One Cycle per Batch

The reduction in the number of cycles improved the cost effectiveness of the system greatly. It is necessary to study the possibility of reducing the number of cycles to one per batch; yet, it is difficult to predict the performance of the membrane elements under such conditions. It is unknown if the membranes will or will not be scaled, and if it is cost effective. This project has resulted in significant improvements to the CERRO process, but the system can be further optimized.

4.2. Parameters of Operation: Crossflow Velocity

One of the theories about the ability of the CERRO process to operate with high concentrations of silica and calcium sulfate without scaling the membranes was related to the impact of the crossflow velocity on the membrane surface. In conventional RO systems, the crossflow velocity decreases as the feed water reaches the last membrane elements. The reduction in the crossflow velocity increases the concentration polarization. This can lead to an excessive concentration of ions, causing the formation of crystals on the membrane surface. Figure 4.1 shows a diagram of the crossflow velocity inside the membrane element (Kim 2012).

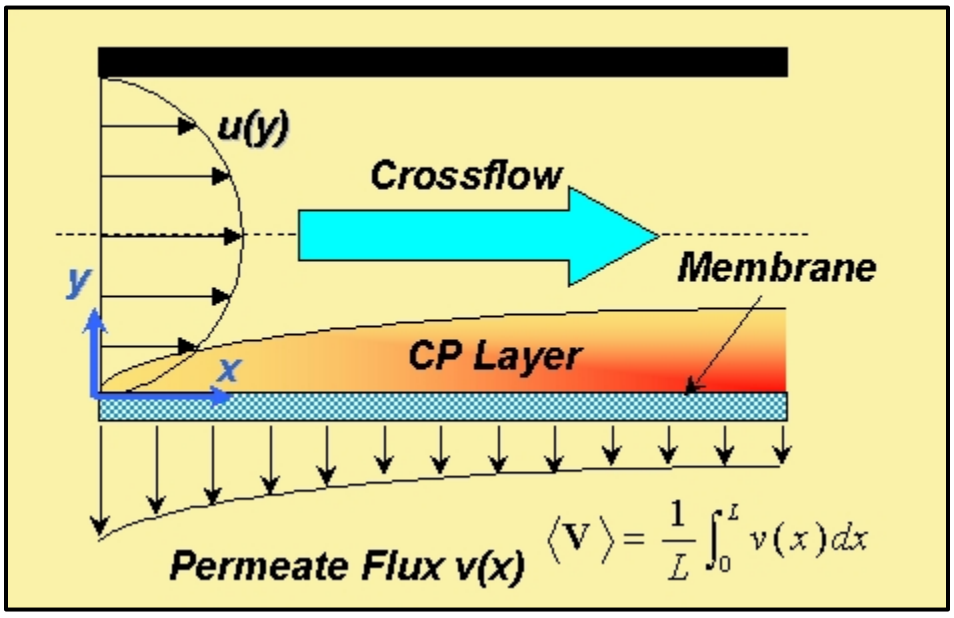

Figure 4.2: Crossflow Velocity Profile (Kim 2012)

The crossflow velocity in the CERRO process increases as the recovery of the system increases. This happens because the system is operated at constant pressure. As the osmotic pressure of the feed water increases, the permeate flux decreases, but the feed flow remains constant. This effect produces a continuous increase in the concentrate flow as a function of time. Figure 4.2 shows the permeate and concentrate flows of one test made using the CERRO SME unit.

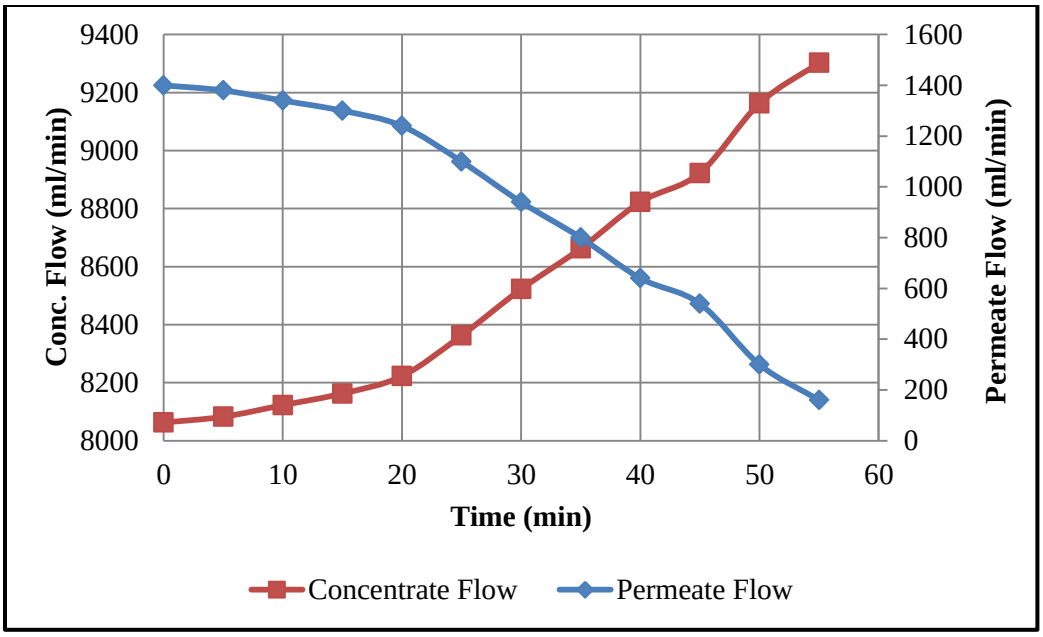

Figure 4.3: Permeate vs. Concentrate Flow

It was believed that the continuous increase in the crossflow velocity kept a very thin concentration polarization layer, thereby preventing the crystal formation on the membrane surface.

4.2.1. Analysis of the Crossflow Velocity

According to DOW answer center (DOW INC. 2012), the crossflow velocity (v) can be calculated by taking the feed flow rate (Q_{feed}) divided by the cross sectional area (A_{cs}) of the feed channel spacer.

$$v = \frac{Q_{feed}}{A_{cs}} \qquad \text{Eq 4.1}$$

The cross sectional area (A_{cs}) can be calculated by multiplying the height of the spacer (h) by the wide of the membrane element (w).

$$A_{cs} = h * w \qquad \text{Eq. 4.2}$$

The cross flow velocity was calculated for one experiment made in December 12, 2010. The batch was performed using the CERRO unit with a single seawater reverse osmosis membrane element. The dimensions of the membrane element were 0.07cm in height and 53.34 cm wide. These dimensions gave a cross sectional area of 3.73 cm^2. Figure 4.4 shows the change in the crossflow velocity during the time of the batch.

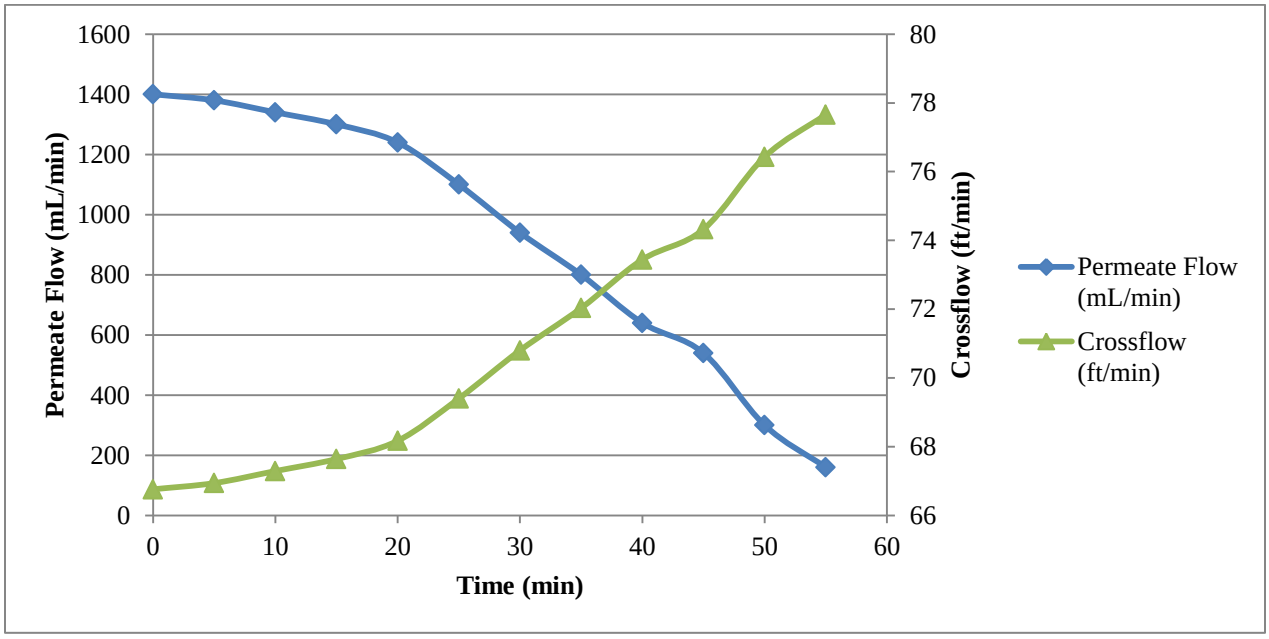

Figure 4.4: Crossflow Velocity over Time

Figure 4.4 shows that there is an increment in the crossflow velocity of about 16% over time during the batch due to the decay in the permeate flow. The decay in the permeate production happened because the batch was run at a constant pressure. As the osmotic pressure of the concentrate was increasing, less water was forced to pass through the membrane resulting in a higher crossflow velocity and a lower permeate flux.

4.2.2. Permeate Flux and Concentration Polarization

The analysis of the crossflow velocity changes in the CERRO process yield to the conclusion that the permeate flux changes had to be evaluated in order to find the concentration polarization factor in the membrane surface. According to the literature (Harsa 2005), the permeate flux (J_W) can be calculated using equation 4.3.

$$J_W = K_W(\Delta P - \Delta\pi) \quad \text{Eq 4.3}$$

Where K_W is the mass transfer coefficient of water or membrane permeability coefficient, ΔP is the difference between the feed pressure and the permeate pressure, and $\Delta\pi$ is the difference between the osmotic pressure of the feed and the osmotic pressure of the permeate. The problem with equation 4.3 is that K_W is a property of the membrane element that is not available. However, the permeate flux can be calculated experimentally by dividing the permeate flow by the active area of the membrane.

$$J_W = \frac{Q_{perm}}{Area} \quad \text{Eq 4.4}$$

The flux analysis was made using the same information used in the crossflow analysis section. According to the manufacturer (DOW Inc.), the seawater RO membranes of 2.5" by 21" have an active membrane are of 13 ft^2, and the recommended flux for this type of membranes is 13 gal/ft^2-day (DOW INC. 2012). Figure 4.5 shows the results of the permeate flux calculations during the batch. It can be seen that the flux in the CERRO process is higher during most of the batch than the recommended flux given by the manufacturer. The problem with having a high flux is that the concentration polarization in the surface of the membranes is high and there is a latent risk of fouling the membranes due to precipitation and or polymerization of some minerals.

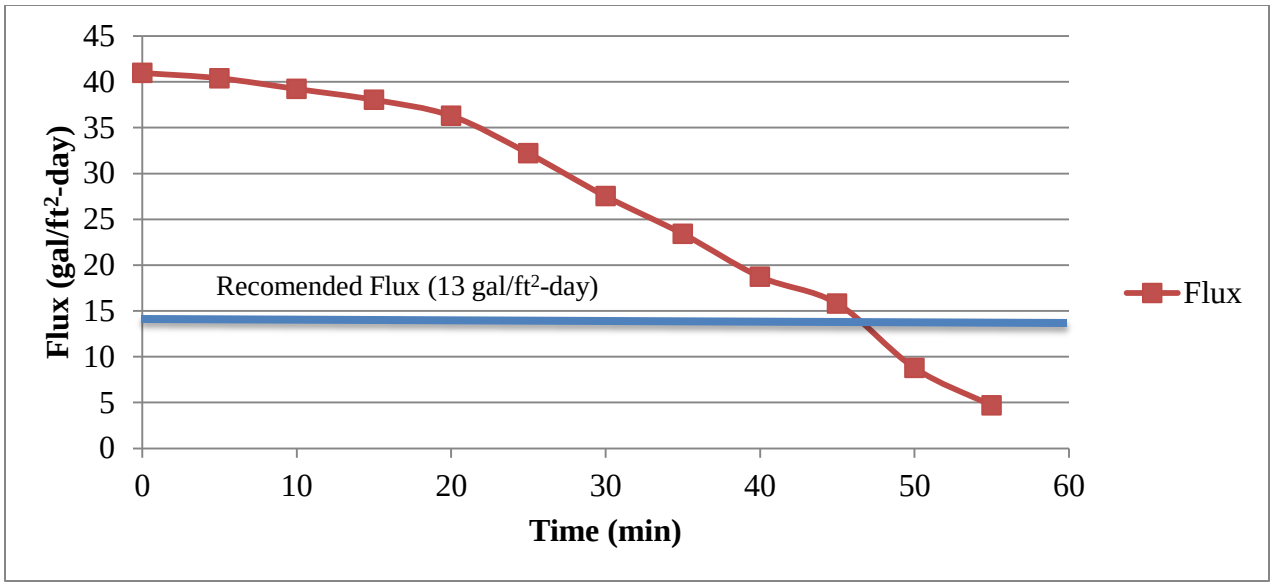

Figure 4.5: Flux Change over Time

The concentration polarization factor (β) can be calculated using equation 4.4 (Harsa 2005).

$$\beta = e^{J_w/K_{CP}} \quad \text{Eq 4.4}$$

Where K_{CP} is known as the concentration polarization mass transfer coefficient (Harsa 2005) and can be calculated using equation 4.5.

$$K_{CP} = 0.023 \frac{D_L}{d_H} (Re)^{0.83} (Sc)^{0.33} \quad \text{Eq 4.5}$$

Where:

D_L = Diffusion coefficient for solute in water

d_H = Hydraulic diameter of the feed channel

Re = Reynolds number

Sc = Schmidt Number

Schmidt Number was calculated using equation 4.6.

$$Sc = \frac{\mu}{\rho * D_L} \quad \text{Eq 4.6}$$

Where μ is the dynamic viscosity of the water, and ρ is the density of the water. The density and viscosity of the water were calculated using the spread sheet developed by the Karlsruhe Institute of Technology (Karlsruhe Institute of Technology 2009) which calculates the viscosity and density of the water as a function of salinity and temperature.

Reynolds number was calculated using equation 4.7.

$$Re = \frac{\rho v d_H}{\mu} \quad \text{Eq 4.7}$$

It is necessary to mention that the diffusion coefficient (D_L) is different for each solute present in the water. For that reason, the concentration polarization factor is different for each ion present in the water. In this analysis, the concentration polarization was calculated only for the Na^+, Ca^{+2}, Cl^-, and SO_4^{-2} ions. The diffusion coefficients for these ions were obtained from the Handbook of Chemistry and Physics (Weast 2005) Table 4-11 shows the diffusion coefficients of the ions mentioned before.

Table 4-11: Diffusion Coefficients Used for Calculations

ION	**Na^+**	**Ca^{+2}**	**$SO4^{-2}$**	**Cl^-**
D_L (m^2/s)	1.33E-09	7.92E-10	1.07E-09	2.032E-09

Figure 4.6 shows the results obtained for the concentration polarization of Sodium during the batch. It can be seen that the concentration polarization at the beginning of the batch is 1.76.

This means that the concentration of Sodium at the membrane surface is 1.76 times greater than the feed concentration. However, the concentration polarization decays over time to 1.06. This means that the concentration of sodium in the membrane surface is almost the same as the feed concentration. Thanks to the decay in the permeate flux, and the increment in the crossflow velocity, the concentration polarization drops at the end of the batch.

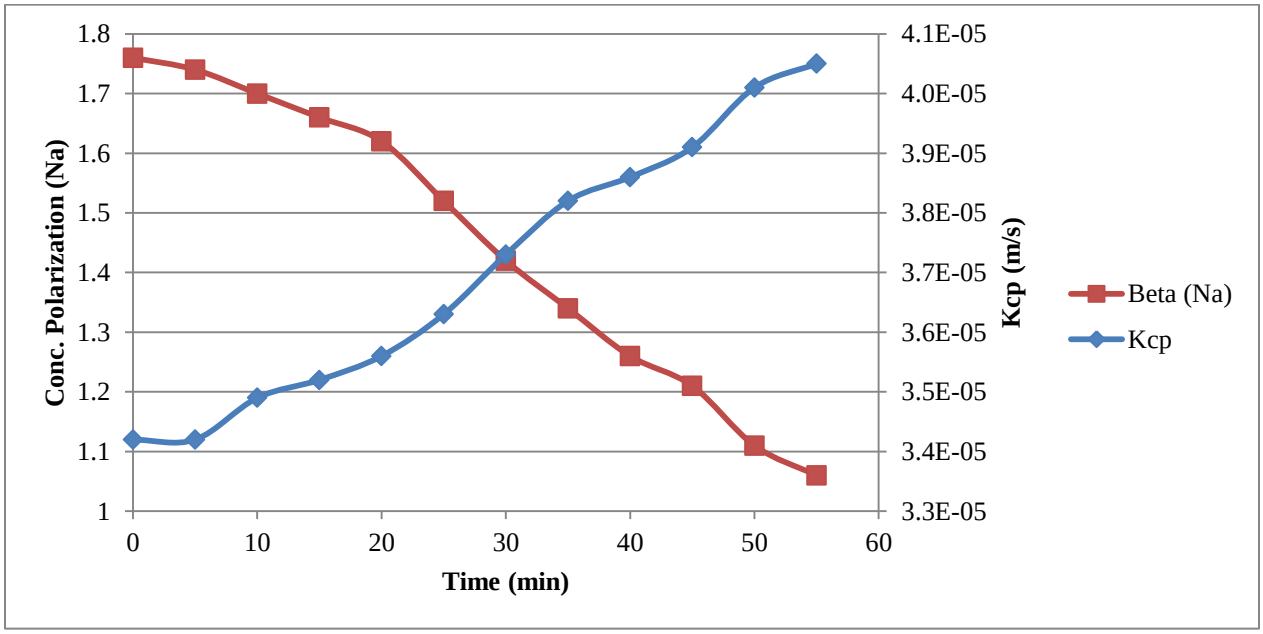

Figure 4.6: Concentration Polarization and Mass Transfer Coefficient

The same calculations were made for calcium, chloride, and sulfates ions in the same batch. Figure 4.7 shows the change of the concentration polarization of these ions at the surface of the membrane. The ions used for this analysis showed the same trend: A high concentration polarization factor at the beginning of the batch with a steady decline due to a flux decline in the system. It can be seen that calcium and sulfate ions have a higher concentration polarization factor than sodium and chloride. This happens because calcium and sulfate ions have lower diffusion coefficients than sodium or chloride ions.

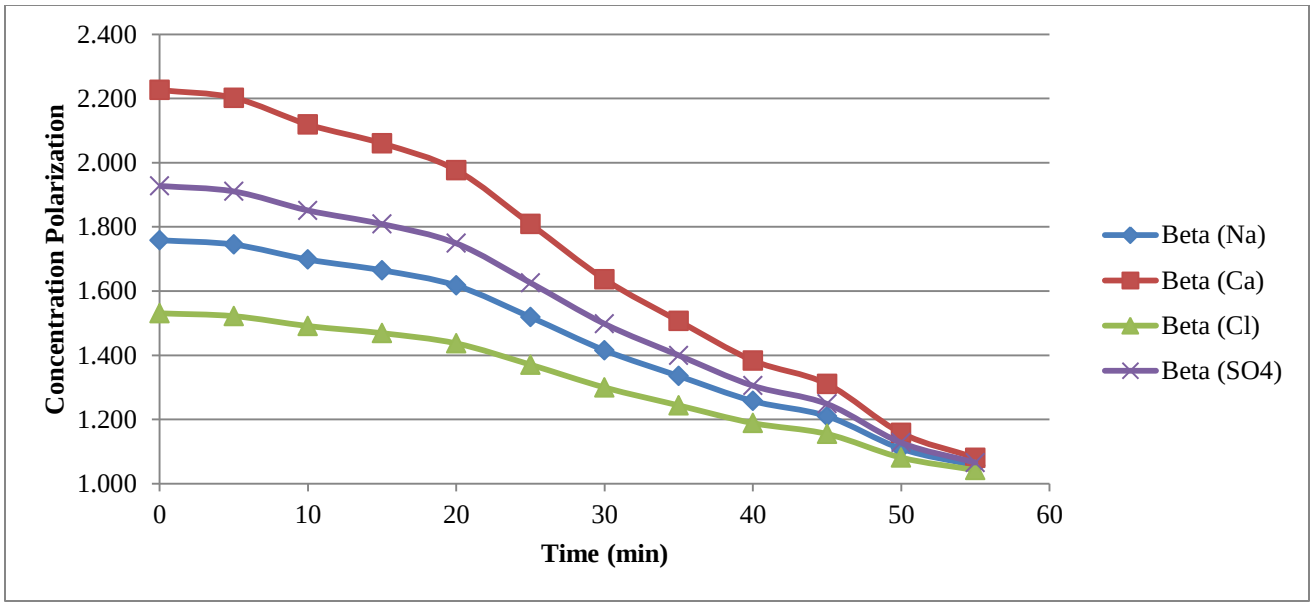

Figure 4.7: Concentration Polarization of Different Ions

This analysis was repeated for two more experiments made in the CERRO unit to demonstrate the repeatability of the experiments. Figure 4.8 shows the average of three experiments made in the CERRO unit. The error was calculated using equation 4.8.

$$Error = \frac{\sigma}{\sqrt{n}} \qquad \text{Eq 4.8}$$

Where σ is the standard deviation of the data points and n is the number of data points (3). The analysis of these experiments showed a very similar trend. The highest error (5%) is localized at the end of the batch, but with a very low error at the beginning (2.6%). These results show that the CERRO process experiments have a very good reproducibility. Two of the three experiments were performed in June, 2010. The Third experiment was made in December 2010. It can be seen that after six months of operation, the CERRO process still has a very similar performance.

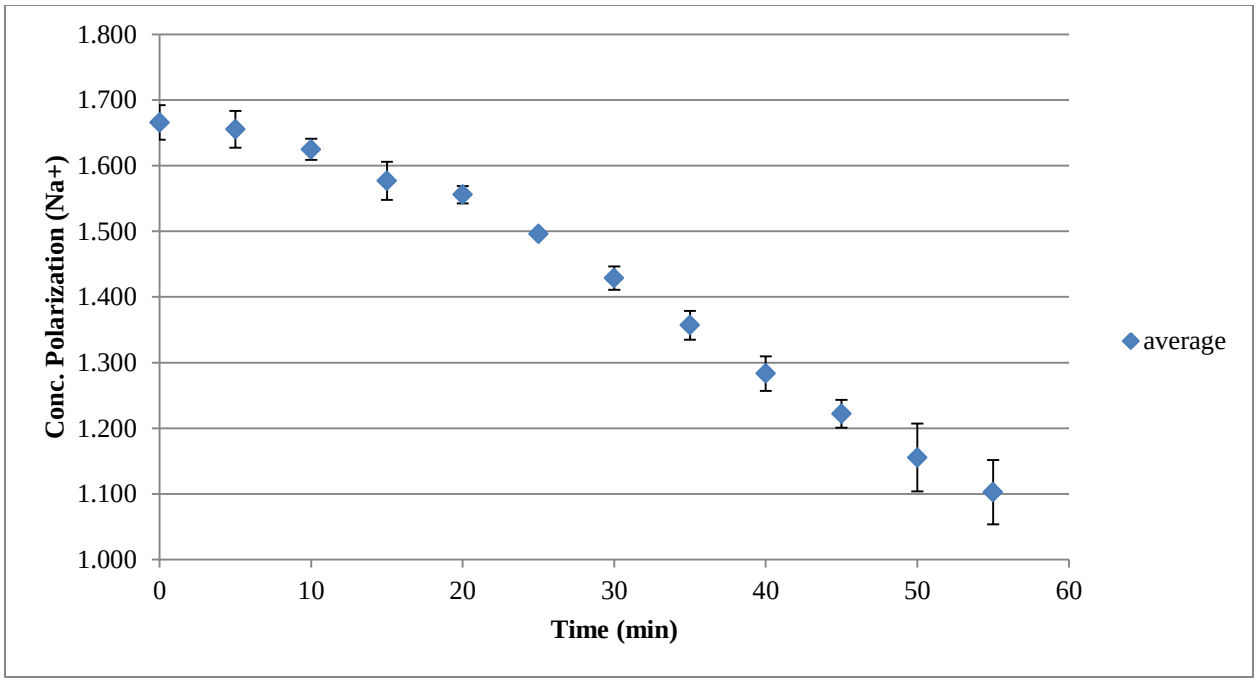

Figure 4.8: Concentration Polarization of Sodium of Three Batches

4.2.3. Concentration Polarization at Low Crossflow Velocities

Several experiments were performed using the CERRO SME unit were the crossflow was reduced by using a bypass valve prior to the membrane elements. The objective of these experiments was to observe the impact of a significant change in the crossflow in the process. Table 4-12 shows the crossflow and flux of one batch were the feed flow was cut by a 60% by opening the bypass valve. The results showed a reduction of 63% in the crossflow velocity inside the membrane element compared with the experiment shown in section 4.2.1, but showed the same increment over time (17%) than the experiment without the bypass valve. On the other hand, the permeate flux remained relatively the same and about 2.5 times higher than the recommended flux of operation (13 gal/ft^2-day). According to the results, it seems that the operation in a batch mode allows the membrane elements to operate at higher fluxes without the risk of fouling or scaling de membranes.

Table 4-12: Crossflow and Flux Results with Low Feed Flow

Time (min)	Permeate Flow (ml/min)	Concentrate Flow (ml/min)	Crossflow (ft/min)	Flux (gal/ft^2-day)
0	1200	2,400	21.083	35.118
5	1,170	2340	20.556	34.240
10	1,230	2220	19.502	35.996
15	1,110	2,640	23.191	32.485
20	1,035	2,700	23.718	30.290
25	975	2,730	23.982	28.534
30	780	2,800	24.597	22.827

After the crossflow and flux were obtained, the concentration polarization factor was calculated for this batch at different times. Figure 4.9 shows the concentration polarization factor (β) of different ions present in the feed at different times.

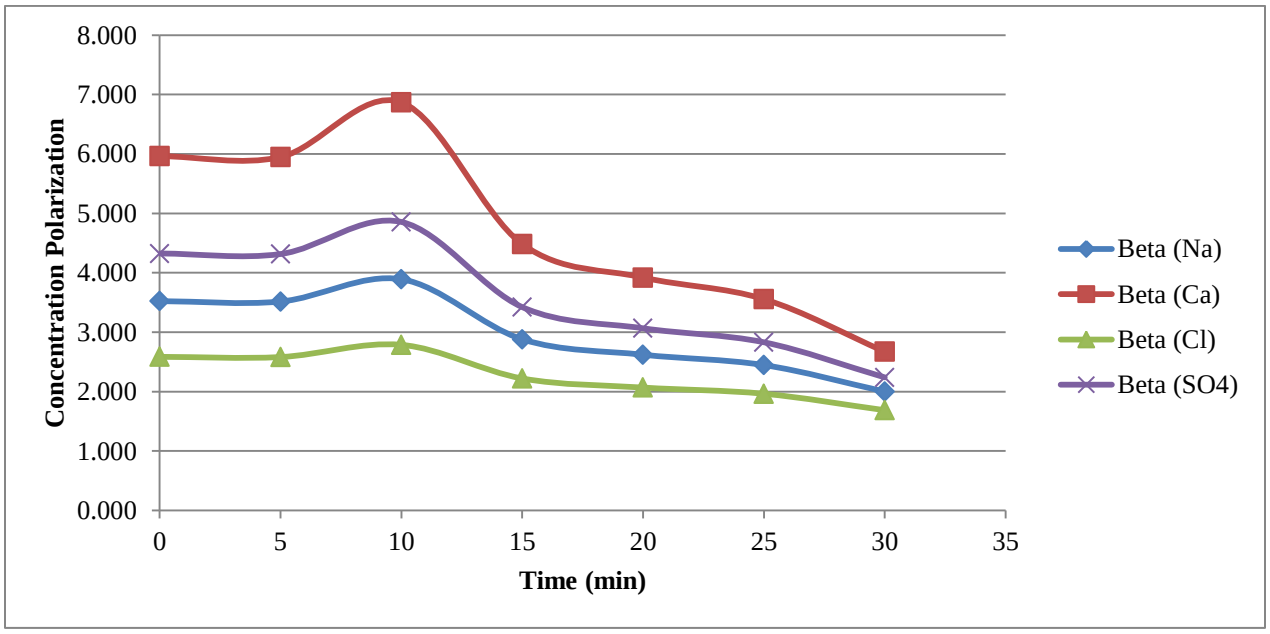

Figure 4.9: Concentration Polarization with Low Crossflow

According to the data, the concentration polarization started about three times higher than the experiment shown in section 4.2.1, but the batch time was 25 minutes lower. This experiment shows a similar decline in the concentration polarization as the batch shown in

section 4.2.1. These results showed that the increase of the crossflow in a batch process reduces the accumulation of ions in the membrane surface, thus reducing the risk of fouling the membranes and, if the treatment time is short, the precipitation of salts inside the membranes can be avoided.

4.2.4. Concentration Polarization in a Continuous Flow Mode

One experiment was performed using the CERRO SME unit simulating the conditions of continuous flow operation. This experiment was made by opening the bypass valve was opened to a point where the concentrate flow was lower than the permeate flow. The concentrate flow was not returned into the feed tank, but instead, the feed tank was continuously filled with KBH concentrate. Table 4-13 show the results obtained from this experiment.

Table 4-13: Results of the Continuous Flow Experiment

Time (min)	Perm Q (ml/min)	Conc Q (ml/min)	Crossflow (ft/min)	Flux (gal/ft2-day)	Conc Cond (uS/cm)	Feed Cond (uS/cm)	Rec (%)
10	410	120	1.054	12.0	59,200	19,140	68
15	410	120	1.054	12.0	65,000	19,140	71
20	410	120	1.054	12.0	73,500	19,140	74
25	410	120	1.054	12.0	66,400	19,140	71
30	410	120	1.054	12.0	66,900	19,140	71
35	410	120	1.054	12.0	69,300	19,140	72
40	410	120	1.054	12.0	59,000	19,140	68

For this experiment, the crossflow velocity was reduced a 98% in comparison to the experiment presented in section 4.2.1. With this information, the concentration polarization at the membrane surface was calculated. Figure 4.10 shows the concentration polarization of different ions during the time of the experiment.

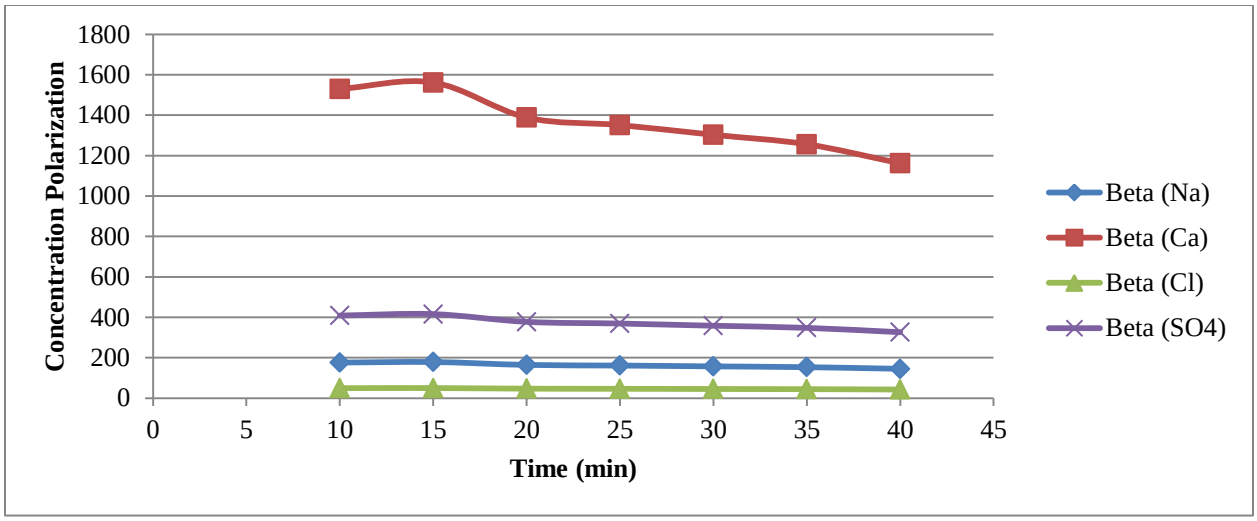

Figure 4.10: Concentration Polarization in Continuous Flow Operation

The concentration polarization during this experiment was extremely high. At the end of the run, it was detected that the permeability of the membrane decayed a 27%. The membrane was rinsed with permeate for several minutes, then, it was cleaned with $CaSO_4$ and silica cleaning solution from King Lee Technologies at a low pH. The permeability of the membrane remained 27% below its original condition. This test showed that the KBH concentrate cannot be treated with a conventional RO system. The continuous operation of a RO process will lead to an irreversible fouling of the membranes.

4.2.5. Flux Normalization and Mass Transfer Coefficient

The CERRO process is not a steady state system. This means that the parameters of operation are constantly changing with the exception of the operating pressure. The constant change in temperature, crossflow, flux, osmotic pressure, and feed quality makes the normalization of the information necessary to obtain more descriptive results. According to the literature (Harsa 2005; DOW INC. 2012), the normalization of the flux can be made by multiplying the flux measured during operation by temperature and pressure correction factors (Equation 4.9).

$$J_{Norm} = J_{w,A} \frac{TCF_{ST}}{TCF_A} \frac{PCF_{ST}}{PCF_A} \quad \text{Eq 4.9}$$

TCF_{ST} and PFC_{ST} are the temperature and pressure correction factors at standard conditions. TCF_A and PCF_A are the temperature and pressure correction factors of the condition A. $J_{w,A}$ is the permeate flux measured at condition A.

ASTM international, in its section "Standard Practice for Standardizing Reverse Osmosis Performance Data" (ASTM International 2013) recommends to calculate the TCF using Equation 4.10.

$$TCF_A = 1.03^{(T_A - 25)} \quad \text{Eq 4.10}$$

According to AST international, this simplified equation can be used if the manufacturer does not provide the equation used during the standardization process. DOW Inc. recommends to calculate the temperature correction factor using Equation 4.11a or 4.11b depending on the temperature of operation (DOW INC. 2012).

$$TCF_A = e^{[2640\left(\frac{1}{298} - \frac{1}{273+T_A}\right)]}; for\ T \geq 25\ C \quad \text{Eq 4.11a}$$

$$TCF_A = e^{[3020\left(\frac{1}{298} - \frac{1}{273+T_A}\right)]}; for\ T \leq 25\ C \quad \text{Eq 4.11b}$$

The pressure correction factor is calculated by balancing the operating pressure with the losses during operation and the osmotic pressure of the feed-concentrate stream and the osmotic pressure of the permeate. ASTM international, DOW Inc., and Harsa recommend to use Equation 4.12 to calculate the pressure correction factor.

$$PCF_A = P_{Feed} - \frac{h_L}{2} - P_{perm} - \pi_{Feed} + \pi_{perm} \quad \text{Eq 4.12}$$

P_{feed} is the pressure in the feed channel, h_L is the pressure drop along the feed channel, P_{perm} is the permeate pressure, π_{Feed} is the osmotic pressure of the feed and π_{perm} is the osmotic pressure of the permeate. DOW Inc. recommends to calculate the osmotic pressure of the solution using Equation 4.13.

$$\pi = 1.12 * (273 + T) * \sum m_j \quad \text{Eq 4.13}$$

Where m_j is defined as the molality of the compound j. For that reason, the molality of the feed and permeate has to be calculated. Molality is defined as the concentration of a solute j in moles per liter (M_j) divided by the density of the solvent (water).

$$m_j = \frac{M_j}{\rho_W} \quad \text{Eq. 4.14}$$

For desalination systems, the change in the density due to salinity and temperature has to be taken into account. The spread sheet developed by the Karlsruhe Institute of Technology (Karlsruhe Institute of Technology 2009) was used for density and viscosity calculations. This spread sheet calculates the viscosity and density of water based in the salinity and temperature of the water.

4.2.5.1. Flux Normalization Results

The experiment shown in section 4.2.1 was used for the analysis of flux normalization. The batch took a time of 55 minutes to achieve 75% recovery. The feed water was KBH concentrate with a TDS of 15,217 mg/L. Figure 4.11 shows concentration of the most abundant ions present in the concentrate at different times.

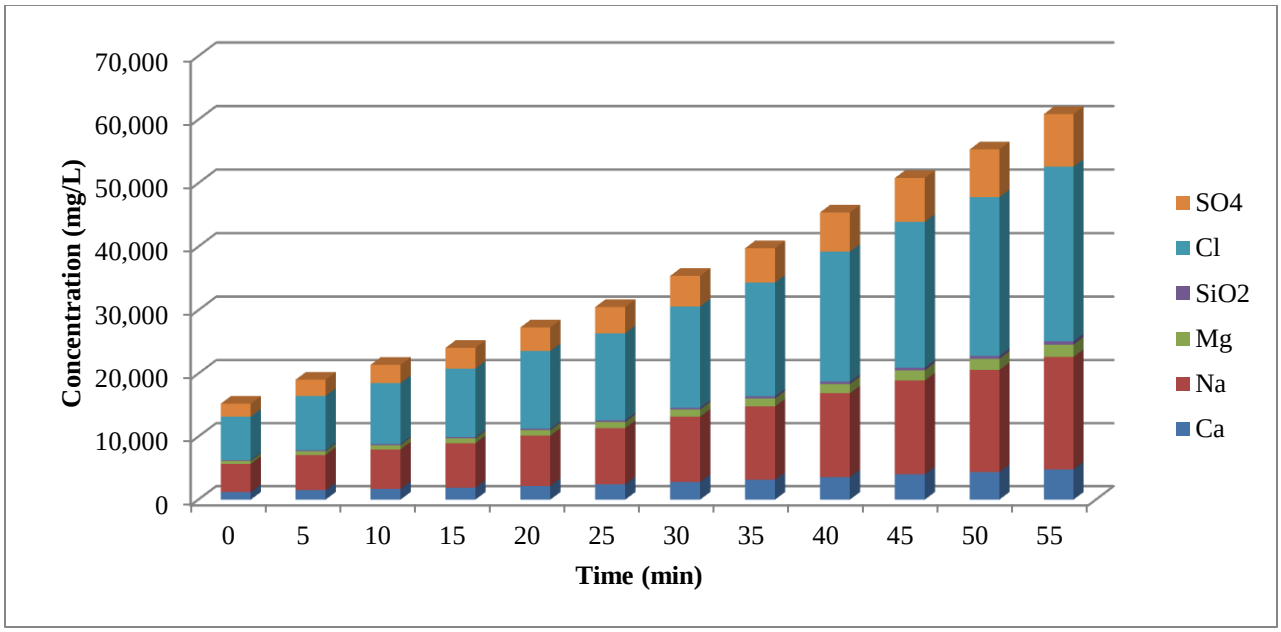

Figure 4.11: CERRO Concentrate Ion Composition at Different Times

With the information shown in Figure 4.11, the osmotic pressure of concentrate solution was calculated using Equation 4.13. It is important to mention that, according to DOW Inc., this equation does not yield accurate results for TDS concentrations above 42,000 mg/L. For that reason, the values obtained after minute 40 of the batch were discarded for the analysis. Table 4.12 shows the TFC and PFC at different times during the batch.

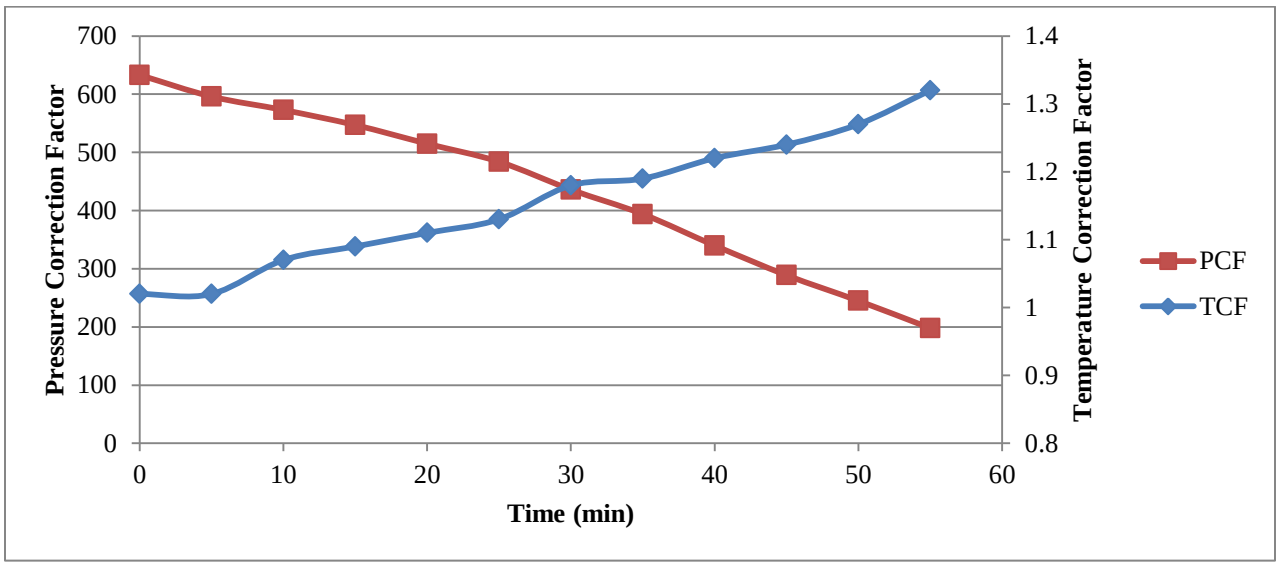

Figure 4.12: TCF and PCF over Time

Figure 4.12 shows that the TCF increases over time due to an increase in the temperature. The PCF decreases over time because as the feed gets more concentrated, the osmotic pressure gets closer to the pressure of operation.

The standard conditions of operations were obtained from DOW Inc. (DOW INC. 2012). Table 4-14 shows the standard operation conditions and the PCF_s and TCF_s.

Table 4-14: Standard Conditions of Operation

Element SW30-2521		
Parameter	**Unit**	**Value**
Temperature	C	25
Pressure	psi	800
TDS	mg/L as NaCl	32,000
Recovery	%	4
PCF	psi	409
TCF	N/A	1

With the values shown above, the flux was normalized using Equation 4.9. Figure 4.13 shows the measured flux of the experiment and the normalized flux.

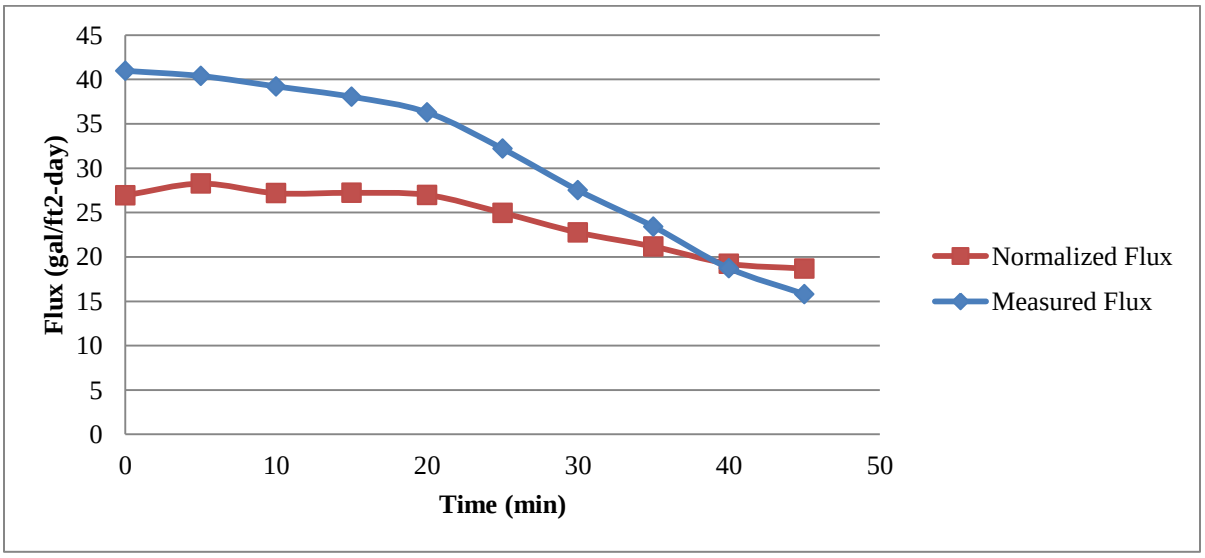

Figure 4.13: Normalized and Measured Flux over Time

Four experiments using the CERRO SME unit were used for the analysis of flux normalization. Two experiments were performed in December 2010 and two in June 2011. These experiments were selected because there is a time lapse of about six months in which the system was operated periodically. These calculations were made in order to determine if the membrane was showing flux decay over time due to fouling. The flux was normalized for the four experiments at different times. Figure 4.14 shows the average of the normalized flux at different times. The error was calculated using Equation 4.8.

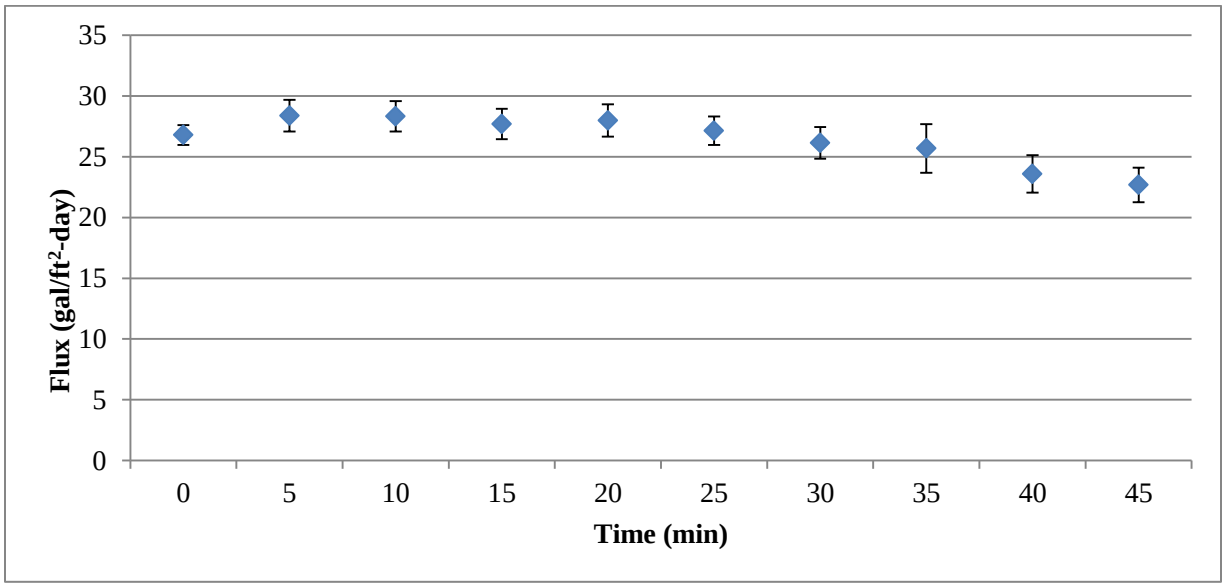

Figure 4.14: Average Flux of Four Experiments

Figure 4.9 shows that there is no significant change in the permeability of the SWRO membrane.

4.2.5.2. Mass Transfer Coefficient (Kw)

The mass transfer coefficient or membrane permeability (K_w) was calculated using Equation 4.3. This calculation was made to compare the results obtained above with the data obtained during experimentation. Equation 4.3 was modified to solve for K_w giving equation 4.14.

$$K_w = \frac{JW}{(\Delta P - \Delta \pi)} \qquad \text{Eq 4.14}$$

K_w was calculated for the four experiments mentioned above. The average of the results was taken and the error was calculated using Equation 4.8. Table 4-15 shows the K_w for the four experiments and the experimental error.

Table 4-15: Membrane Permeability Coefficient of Different Batches

Experiment	Kw (gal/ft^2-day-psi)	Statistical Error (%)
12-21-2010	5.64	3.5
12-17-2010	6.10	5.2
6-16-2011	6.31	3.2
6-14-2011	5.78	4.2
Average	5.96	3.53

It was established that the membrane permeability was 5.96 gal/ft^2-day-psi. This value was used to estimate the permeate flow of a batch with the conditions of the experiment used in section 4.2.1 and the calculated permeate flow was compared with the measured permeate flow in the experiment. Figure 4.15 shows the measured permeate flow and the calculated permeate flow using the K_w of the membrane. The permeate flux was calculated using equation 4.3 and the permeate flow was calculated by multiplying the flux by the active area of the membrane (13 ft^2). It can be seen that the calculated and the measured permeate flow are very close to the same behavior with a small difference at the beginning of the batch. It is interesting in the results that the calculated flow showed a linear decay with a coefficient of determination of 0.9918. The good correlation between the permeate flow calculated with the K_w obtained from the experimental data and the measured permeate flow yields to the conclusion that information is relievable and accurate.

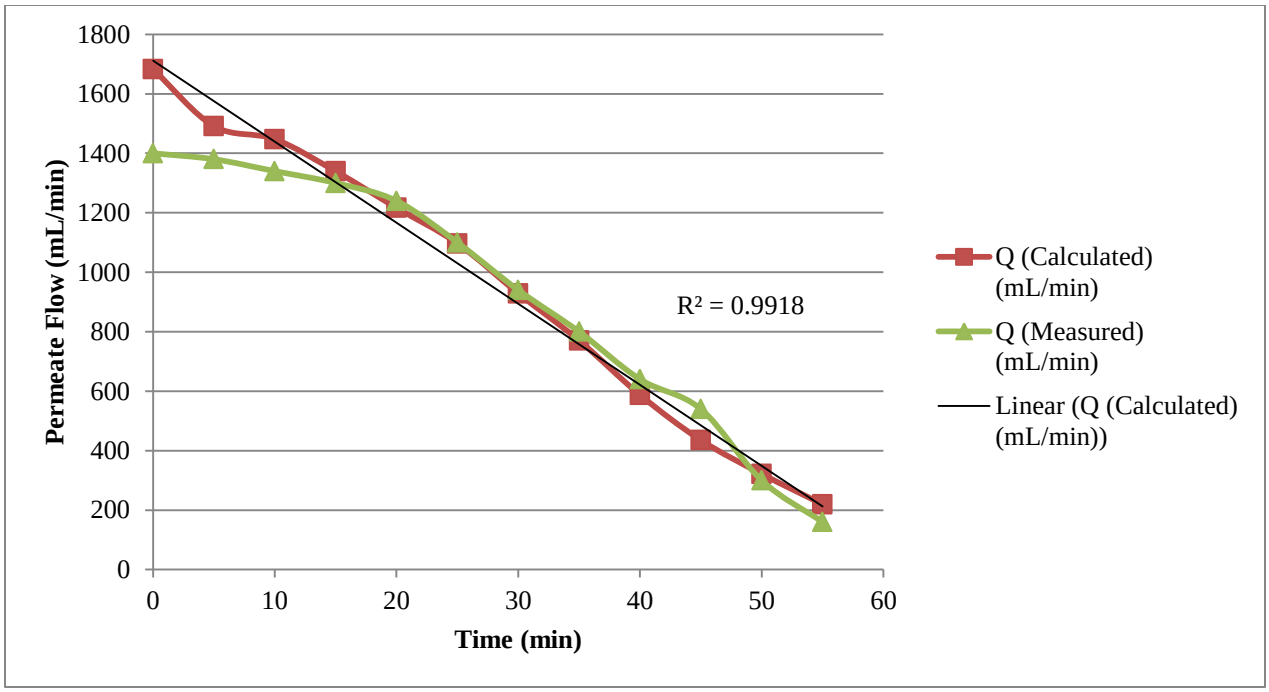

Figure 4.15: Permeate Flows (Calculated and Measured)

4.3. Parameters of Operation: Acid Dosage

The addition of acid to the feed water in the CERRO process was part of the standard operation presented by Tarquin et al in 2010. At that time, it was considered that the high concentration of alkalinity in the water was likely to cause calcium carbonate precipitation on the membrane surface. Calcium carbonate precipitation is considered the most important scaling factor in membrane desalination (Mickley and Jordahl 2013).

4.3.1. Reduction of the Acid Dosage

The addition of acid as pretreatment in desalination systems is a common practice, and sulfuric acid is commonly used due to its low cost. However, low cost or not, it stills represent an increase in the operation cost of desalination processes. After evaluating the parameters of operation in the CERRO process, particularly the treatment time, the idea that calcium carbonate

can reach supersaturation in the system without scaling the SWRO membranes came as a hypothesis. Calcium carbonate precipitation, or precipitation of calcium sulfate or silica, has an induction time. It was thought that a treatment time shorter than the induction time of calcium carbonate could reduce the amount of acid needed in the system. For that reason, several experiments were done wherein the amount of sulfuric acid was cut by 50% of the original dose. Originally, Tarquin et al reported the addition of sulfuric acid to get the pH of the feed below 4.5. At that pH, all the alkalinity present in the water is in the carbonic acid form. Under this parameter, the KBH plant requires an average dosage of 1 mL of sulfuric acid per gallon of KBH concentrate to remove the alkalinity. The amount of acid was cut to 0.5 ml per gallon of KBH concentrate and several batches were run under these conditions. Table 4-16 shows the results of the test using 50% of the acid dosage.

Table 4-16: Results from Different Tests with 50% Less H_2SO_4

Batch (Date)	Permeate Flow (ml/min)	Concentrate Flow (ml/min)	Bypass Flow (ml/min)	Permeate Production after the Test (ml/min)
4/25/2013	1240	3180	4200	840
4/25/2013	1300	3120	4500	870
4/25/2013	1300	3000	4500	880

These results showed that the amount of acid needed for pretreatment of the water can be at least 50% less than the reported by Tarquin et al in 2010. The reduction of the acid dosage in the CERRO process affects the operation cost as well. According to the results reported by Tarquin et al, the acid dosage will cost $0.63 per 1000 gallons to treat water with the same alkalinity as the KBH concentrate (400 mg/L as $CaCO_3$). Based in the same calculations, the

acid dosage cost was reduced to $0.33 per 1000 gallons. Figure 4.16 shows the difference in the cost of the acid dosage before and after this analysis.

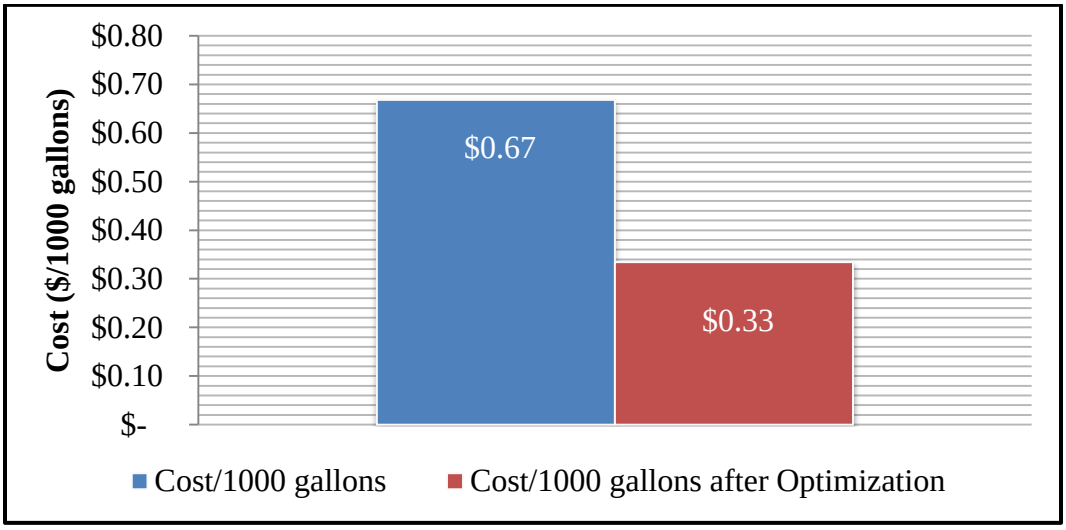

Figure 4.16: Acid Dosage Cost

4.4. Parameters of Operation: Antiscalant Dosage

The addition of antiscalants is a common practice in desalination processes. Thermal desalination and membrane desalination often use antiscalants in their processes (Fan et al. 2010). Antiscalants are often used to avoid the precipitation of sparingly soluble salts (see section 2.2) inside the desalination system. Previous studies have shown that antiscalants affect the induction time of sparingly soluble salts, but do not improve the solubility of the salts (Lyster et al. 2010; Shih et al. 2005; Prisciandaro et al. 2003). The performance of different types of antiscalants specific for calcium sulfate and the dosage were evaluated to perform an analysis of the importance of antiscalants in the CERRO process. A total of 7 antiscalants from three different companies and different dosages were studied. The results and findings are shown below.

4.4.1. Experimental Procedure

In 2010, the CERRO TME unit was tested in the BGNDRF located in Alamogordo, New Mexico. The brackish water that was used as feed for the unit contained high concentrations of Ca^{+2} and SO_4^{-2} ions. Figure 4.17 shows the water chemistry of the brackish water used for this study.

Preliminary tests using the CERRO TME unit showed that the recovery of the system was limited by calcium sulfate precipitation at 68% recovery. An evaluation of the type and dosage of antiscalant was done to improve the recovery of the system.

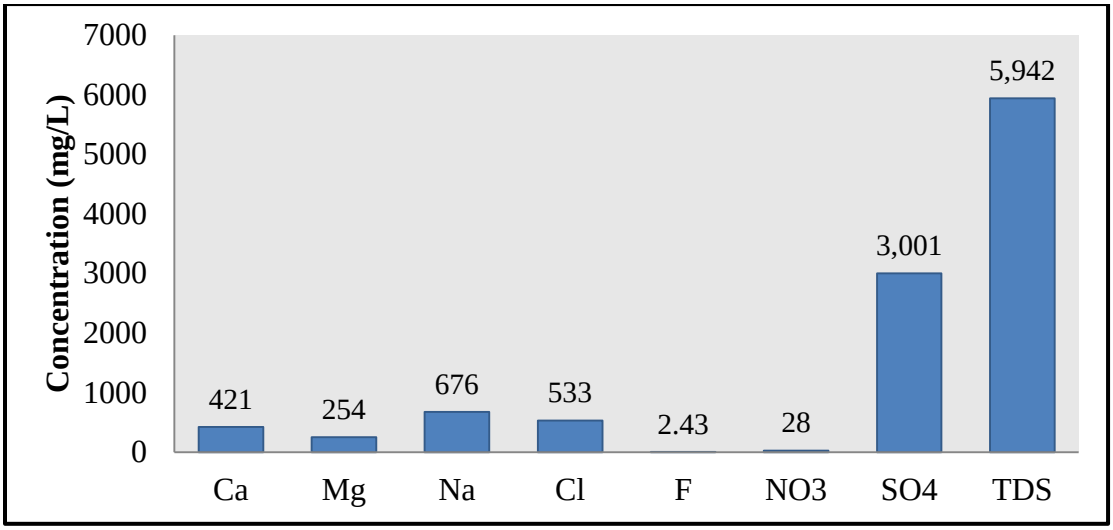

Figure 4.17: Chemical Composition of Alamogordo Brackish Water

Bench-scale experiments were performed to evaluate the effectiveness of the antiscalants keeping the calcium sulfate under supersaturation. The experimental procedure was made as follows:

- Brackish water from Alamogordo, New Mexico was used in all experiments
- A 1 molar standard solution of $CaCl_2$ was prepared in the laboratory.
- A 1 molar standard solution of Na_2SO_4 was prepared in the laboratory.

- A volume of 500 mL of brackish water was poured into a beaker. The water was mixed with a magnetic mixer from this point until the end of the experiment.
- One type of antiscalant and dosage were added to the brackish water. The dosage was based in a volume to volume ratio and the units are given in parts per million by volume (ppmv).
- Using a pipette, a certain volume of $CaCl_2$ was added to the brackish water. The amount of $CaCl_2$ varied depending on the supersaturation concentration desired for that particular test.
- Using a pipette, a certain volume of Na_2SO_4 was added to the brackish water under the same conditions as the $CaCl_2$.
- The turbidity of the water (see appendix A-7) was monitored as a function of time to identify the induction time of calcium sulfate.
- The same experiment was performed with different brands of antiscalants and different dosages.
- It was considered that the antiscalants effectiveness stopped when the turbidity reached a value of 5 NTU.
- A control solution with no antiscalants was used in all experiments.

4.4.2. Tests Results

The tests performed in the lab showed that different antiscalants performed differently under supersaturation conditions of calcium sulfate. One experiment conducted with a 0.03 molar concentration of calcium sulfate and an antiscalant concentration of 0.8 ppmv showed a similar performance between all the antiscalants. Figure 4.18 shows the results obtained in this experiment.

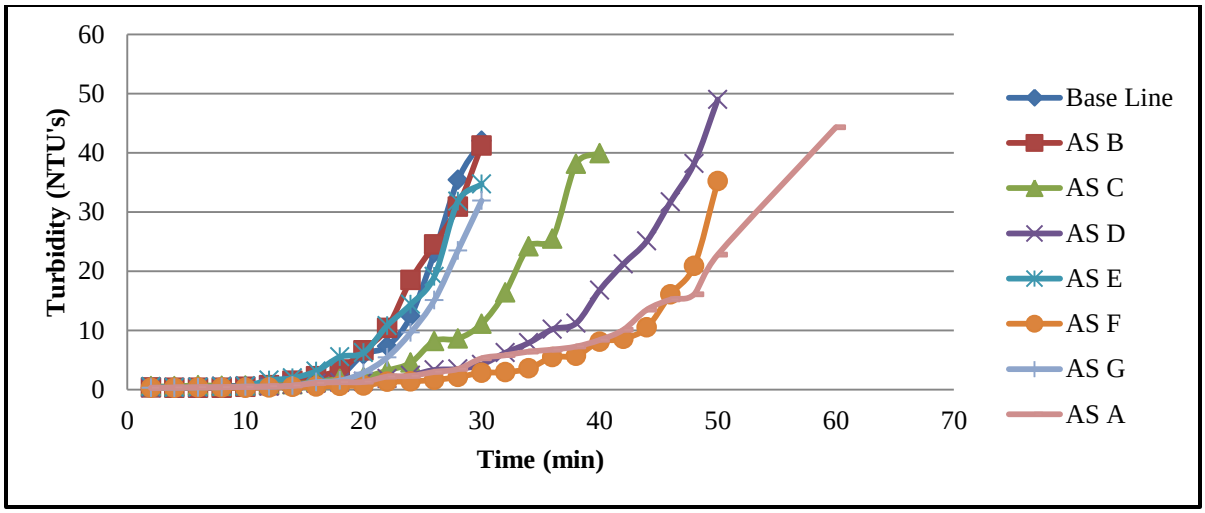

Figure 4.18: Antiscalant Performance at 0.03 M and 0.8 ppmv

During this experiment, the induction time for the precipitation of calcium sulfate was determined to be between 12 and 14 minutes for the control solution with no antiscalants. This is consistent with the induction time reported in previous research which was 763 seconds (12.7 min) (Shih et al. 2004).

More experimentation showed that at higher calcium sulfate concentrations, most of the antiscalants were less effective. Additionally, higher concentrations of the same antiscalants did not improve their performance. Figure 4.19 shows the results of a test conducted with a calcium sulfate concentration of 0.04 M and 2 ppmv of antiscalants.

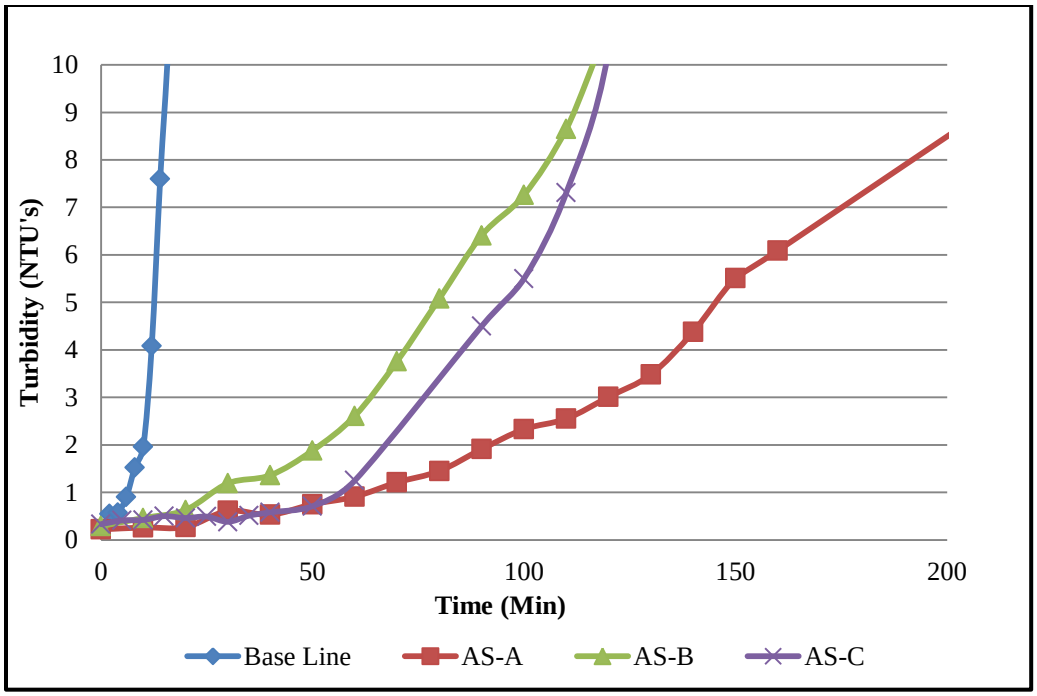

Figure 4.19: Antiscalants Performance at 0.04 M and 2 ppmv

After the initial experimentation with different antiscalants was finished, additional experiments were performed with different dosages of the same antiscalant. For these experiments, the antiscalant that showed the best performance was selected.

The results indicated that the dosage of the antiscalant is an important factor in its performance. The results of a test made using a calcium sulfate concentration of 0.05 M and different dosages of antiscalant (from 1 to 6 ppmv) showed that the induction time can be increased to 600 minutes (100 times the baseline). Figure 4.20 shows the results of this experiment.

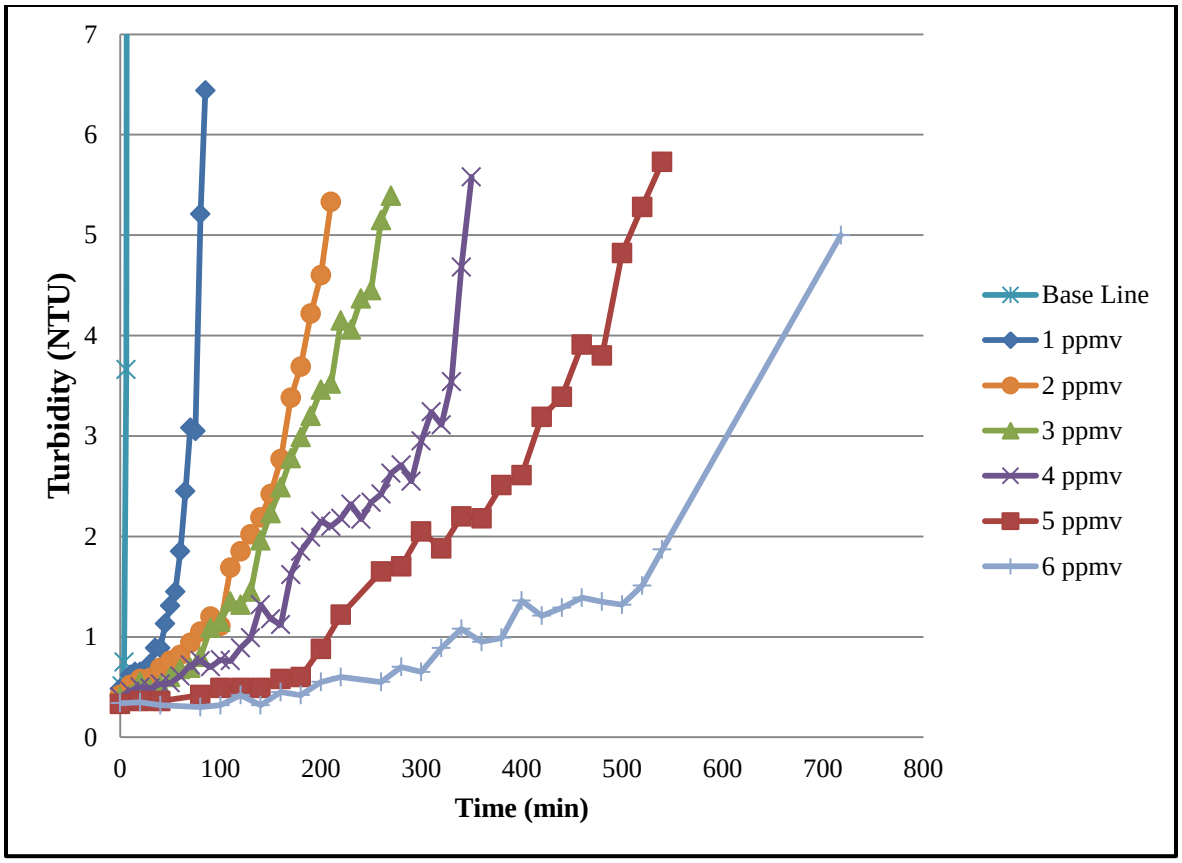

Figure 4.20: Antiscalants performance at 0.05 M and different Dosages

During this project, it was determined that the antiscalants are concentrated at the same rate as the ions in the feed water. The concentration of the ions and antiscalants at a specified recovery in the CERRO unit can be calculated using equation 4.14.

$$C_{Rec} = \frac{C_0}{(1 - Rec)}$$

.Eq 4.14

Where:

C_{Rec} = Concentration at a determine recovery

C_0 = Initial Concentration

Rec = Recovery of the system

Based on equation 4.1, the concentration of the antiscalant in the CERRO unit at a specified recovery with different initial concentrations was calculated. Figure 4.21 shows the concentration of the antiscalant at different recovery rates.

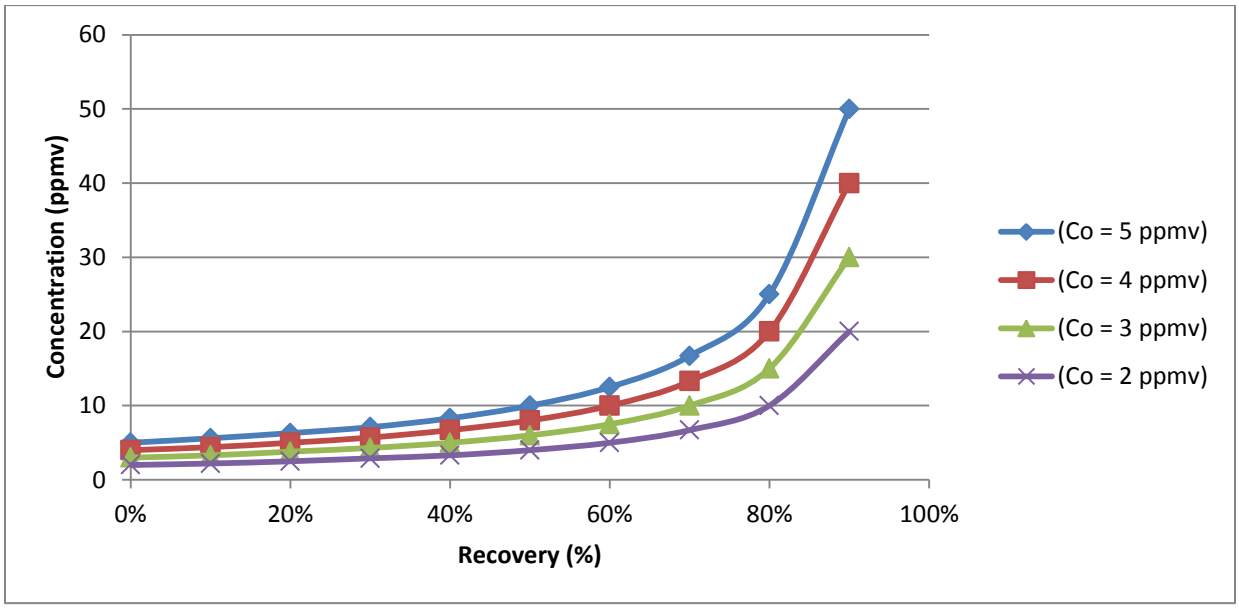

Figure 4.21: Antiscalant Concentration at Different Recoveries

This calculation showed that the amount of antiscalant increases as the system reaches higher recoveries.

One experiment was done to determine the performance of the antiscalant at high dosages (above 5 ppmv). Figure 4.22 shows the results of the experiment.

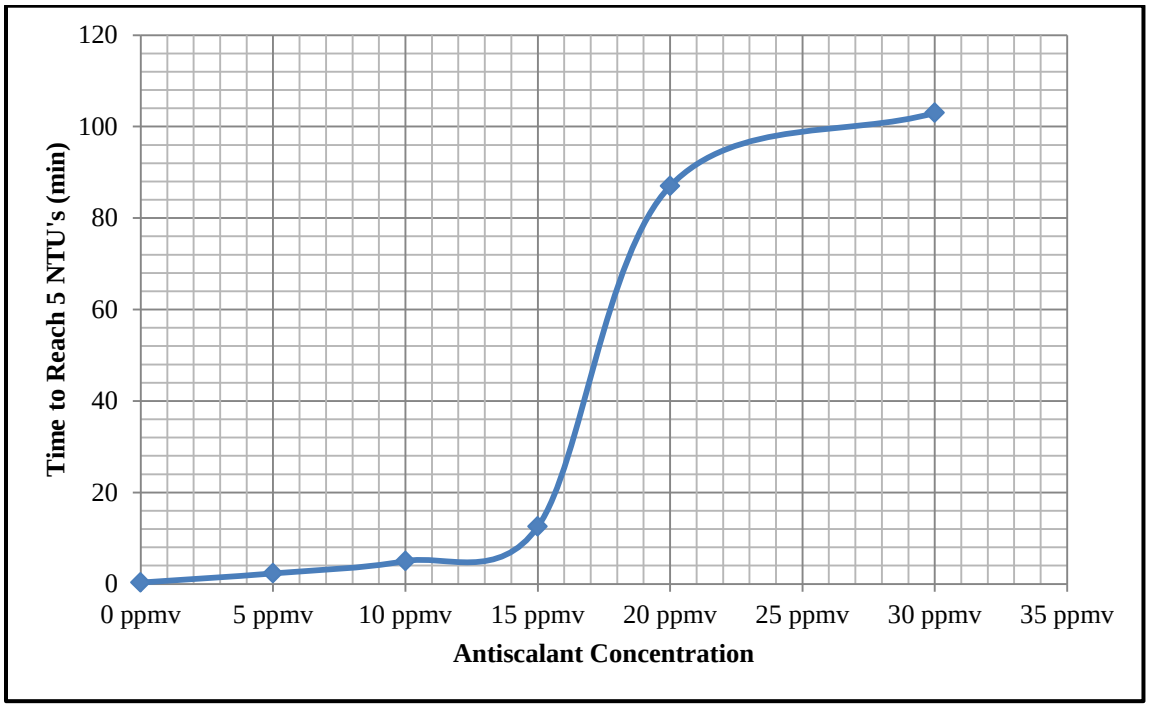

Figure 4.22: AS Performance at 0.1 M $CaSO_4$ Concentration

This experiment was performed with a calcium sulfate concentration of 0.1 M. It can be seen that below 20 ppmv, the antiscalant did not improve the induction time. It was at 20 ppmv where a significant change can be observed. However, there was no improvement in the test with 30 ppmv. For that reason, it was concluded that a concentration above 20 ppmv of antiscalants was not more effective than lower dosages. Considering the concentration factor in the CERRO process and the performance of the antiscalants, it was found that the optimal concentration of antiscalants is between 3 and 5 ppmv. Additionally, it was found that this test

turned out to be a low-cost and effective method to evaluate the performance of different antiscalants.

4.5. Parameter of Operation: Temperature

As mentioned before, the CERRO process recirculates the concentrate flow back to the feed tank. In order to do this, the concentrate passes through a high pressure valve that releases the pressure back to atmospheric conditions. The energy released in the concentrate valve and re-pumping of the concentrate increases the temperature of the water in the system. In fact, heat exchangers had to be placed in the feed tanks of the CERRO units to avoid overheating of the membranes. Figure.23 shows the temperature increase of one batch done using the CERRO SME unit with a heat exchanger.

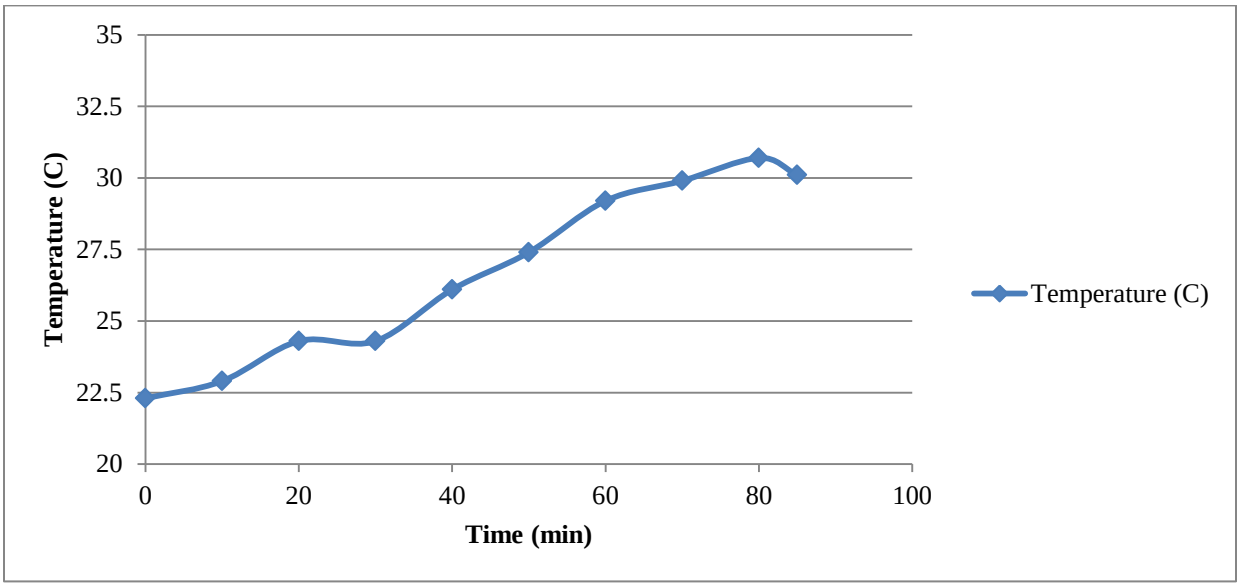

Figure 4.23: Temperature Change over Time

The necessity of heat exchangers to control the temperature of the unit represents an increment in the operating cost of the process. This problem can be solved by the addition of energy recovery devices into the system or by reducing the number of cycles through the system. The evaluation of energy recovery devices was not performed in this study because of the lack of

resources and time, but mostly for the lack of resources. However, energy recovery devices are well known technologies and can be added into the system relatively easy. It is recommended that future projects approach the feasibility of the implementation of these technologies.

4.6. Parameters of Operation: Pressure

The CERRO process is operated at constant pressure. This parameter of operation affects other parameters such as treatment time, crossflow velocity, and permeate flow rate. In the same way, pressure directly affects the cost of operation of the system. As in any RO desalination system, the operating pressure in the CERRO process has to be greater than the osmotic pressure of the water. The osmotic pressure can be calculated by using equation 4.15 (Sawyer et al. 2003)

$$\Pi = cRT$$

Equation 4.15

Where:

Π = Osmotic Pressure of the solution

c = Molar concentration of the solutes

R = Ideal Gas Constant (0.08206 L atm/mol K)

T = Temperature of the solution (K)

The studies made in the CERRO process showed no significant impact at different operating pressures. However, it was determine that the permeate production is limited by the membrane area and discharge pipe line. In some experiments, it was found that the permeate production did not improve at certain pressure increments. This happened because the system reached the maximum permeate flow. It was found that operating pressure should not be higher

than the necessary pressure to operate at maximum permeate flow for a given piping system. Higher pressures will increase the operating cost of the system and will not improve the permeate flow.

4.7. Parameters of Operation: Membrane Flushing

During the studies of the CERRO process, the flushing of the membrane elements with permeate water after each batch was a standard procedure for the preservation of the membranes. After some observation, it was considered that flushing the membranes was part of the parameters of operation of the system. The standard procedure followed after every batch was to flush the membrane elements with permeate water to remove any saturated solutions from the membranes to avoid precipitation inside the system. After every flush, a small batch experiment was performed with permeate water as feed to measure the permeate flow rate at 300 psi. The constant production of permeate at 300 psi was the principal indicator that the system was not getting fouled or scaled after the batch was treated.

As part of the operation procedure of the system, the flush of the unit was evaluated in order to find the minimum amount of water required to restore the membranes to its original condition. This parameter is crucial for the improvement of the system because the water used during the flush reduced the recovery of the system significantly. Several experiments conducted in the CERRO SME unit showed that the optimal time for flushing was about one minute. One experiment was done where 5 gallons of permeate were recirculated into the system after a batch treatment of KBH concentrate. The conductivity of the permeate was monitored over time until the conductivity remained the same. It was found that after one minute, the conductivity of the rinse started to stabilized to the same value (19,500 μS/cm). However, it was determined that there was some mixing in the pretreatment cartridge filter located ahead of the

membrane elements in the CERRO SME unit. Figure 4.17 shows the change in the conductivity in the test mentioned above.

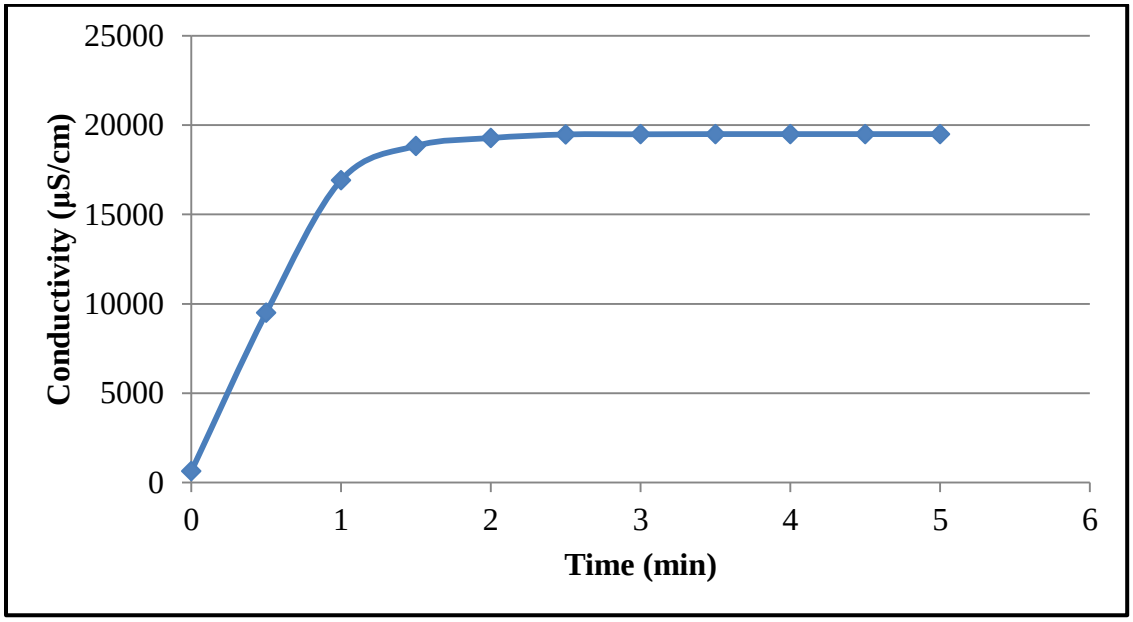

Figure 4.24: Results from the Flush Test with Recirculation of 5 gallons of Rinse Solution.

It was found that the mixing in the pretreatment cartridge filter was showing some interference in the analysis of the flush. This flaw in the design of the system was identified only in the CERRO SME unit. The CERRO TME unit and the CERRO MME unit were designed to flush the membrane elements exclusively without the necessity of passing the water through the pretreatment system. Some studies using the CERRO TME unit suggest that the flush time could be reduced to 15 seconds per flush (Davis and Ortega-Corral 2013). This represents less than 2% of the volume for a 30 gallon batch.

Further analysis is required to improve the flushing procedure in the CERRO process. This parameter of operation is a key factor for the system in order to avoid precipitation of crystals on the membrane surface. In future projects, it is necessary to identify if feed water could be used for the flushing process instead of permeate, and if the flush waste could be diluted

with feed water and treated in the system. These two approaches are fundamental for the improvement of the system.

4.8. Parameters of Operation: Water Chemistry

The chemistry of the water that will be treated in the CERRO process is not a factor that can be modified, but the ionic composition of the water plays an important role in the applicability of the CERRO process to a particular RO concentrate. Mickley et al, 2013 mentioned that there is no perfect desalination system. In other words, the chemical composition of the water plays an important factor in the success of any desalination process. In the case of the CERRO process, the main limitation detected during this study was the precipitation of gypsum during treatment. The flushing procedure proved to be highly efficient preventing scaling of the membranes, even in those experiments where precipitation occurred. However, the decay in the permeate flow rate did not allow the process to continue the treatment after precipitation. Several experiments showed that gypsum precipitation did not scale the SWRO membranes, but the system had to be stopped due to a serious reduction in the permeate flow rate. The same performance was detected with three different sources of feed water: KBH concentrate, Alamogordo brackish water, and Alto brackish water.

4.8.1. CERRO Process Limitations due to Gypsum Precipitation

During study, it was noticed that precipitation of calcium sulfate was an issue in the CERRO unit. Several experiments in the CERRO SME unit using KBH concentrate as feed had to be stopped due to calcium sulfate precipitation. In some cases, precipitation occurred right after the end of the batch. Water samples of the final concentrate showed precipitation during the time that they were taken from the plant to the lab for analysis. This phenomenon gave the

idea that the CERRO unit operated in conditions of supersaturation and that the treatment time of the batch was lower than the induction time for gypsum precipitation.

The software Visual MINTEQ (Gustafsson 2011) was used to calculate the speciation of the ions in the CERRO concentrate. This software has the capacity to calculate the saturation index of all the compounds that can be formed in the water based on its chemical composition. The software calculates the SI using Equation 4.15.

$$SI = \log\frac{IAP}{K_{sp}}$$

Equation 4.15

Where:

IAP = Ion Activity Product

Some authors often use this equation to calculate the SI (Zhu and Anderson 2002). When this equation is used, the scale of the SI changes from the one described in section 2.3.1. The analysis of the SI calculations using Equation 4.3 should be as follows:

- If the SI is lower than zero, the mineral will remain in solution.
- If the SI is equal to zero, the mineral is in equilibrium.
- If the SI is greater than zero, the mineral will precipitate.

Table 4-17 shows the saturation index and IAP values of gypsum in the CERRO concentrate calculated using Visual MINTEQ.

Table 4-17: Saturation Index for Gypsum in the CERRO Concentrate

Mineral	log IAP	Sat. index	Stoichiometry	
Brucite	2.076	-15.024	1	Mg^{+2}
Epsomite	-3.993	-1.867	1	Mg^{+2}
Gypsum	-4.609	0.001	1	Ca^{+2}
Halite	-2.902	-4.452	1	Na^{+1}

The chemical composition of the CERRO concentrate was measured using IC analysis (see appendix A-2). It is important to note that the sample had precipitation at the time of analysis (2 hours after it was taken). The sample was filtered and diluted to be analyzed in the IC. The results obtained in the IC were uploaded into the VMINTEQ software. The results showed that gypsum was in equilibrium, but because the sample precipitated before analysis, it was assumed that the CERRO unit operated in conditions of supersaturation. One mathematical simulation using the software Matlab was done to support this assumption.

4.8.1.1. Mathematical Modeling for Ionic Composition

A simple mathematical model was built in Matlab to calculate the possible concentration of different ions in the CERRO concentrate at a determined recovery rate. This was a simple simulation because the activity corrections were not included in the model. The model was built to calculate the concentrations of the ions at a determined recovery using Equation 4.4.

$$C_{Rec} = C_0 * \frac{1}{1-r}$$

Equation 4.15

Where:

C_{Rec} = Concentration of the ion at a determined recovery

C_o = Initial concentration of the ion

r = Recovery of the system

Different ions were included into the model to calculate their concentrations. Table 4-18 shows the list of the ions included in the model.

Table 4-18: List of Ions included in the Model

Ion	Calcium	Magnesium	Sodium	Chlorides	Sulfates	Silica
Symbol	Ca^{+2}	Mg^{+2}	Na^{+1}	Cl^{-1}	SO_4^{-2}	SiO_2

The composition of the initial feed was uploaded in the model and the results were compared with the results obtained in the IC. Figure 4.25 compares the values of C_{Rec} calculated by Equation 4.3 of the ions concentration at a 92% recovery and the values measured by IC.

The analysis of the results showed that the sodium, magnesium and chloride concentrations are very close to the IC results and the model results, but the calcium and sulfate concentrations obtained in the IC are much lower than the concentrations projected by the model. The precipitation of gypsum before the IC analysis explains this difference.

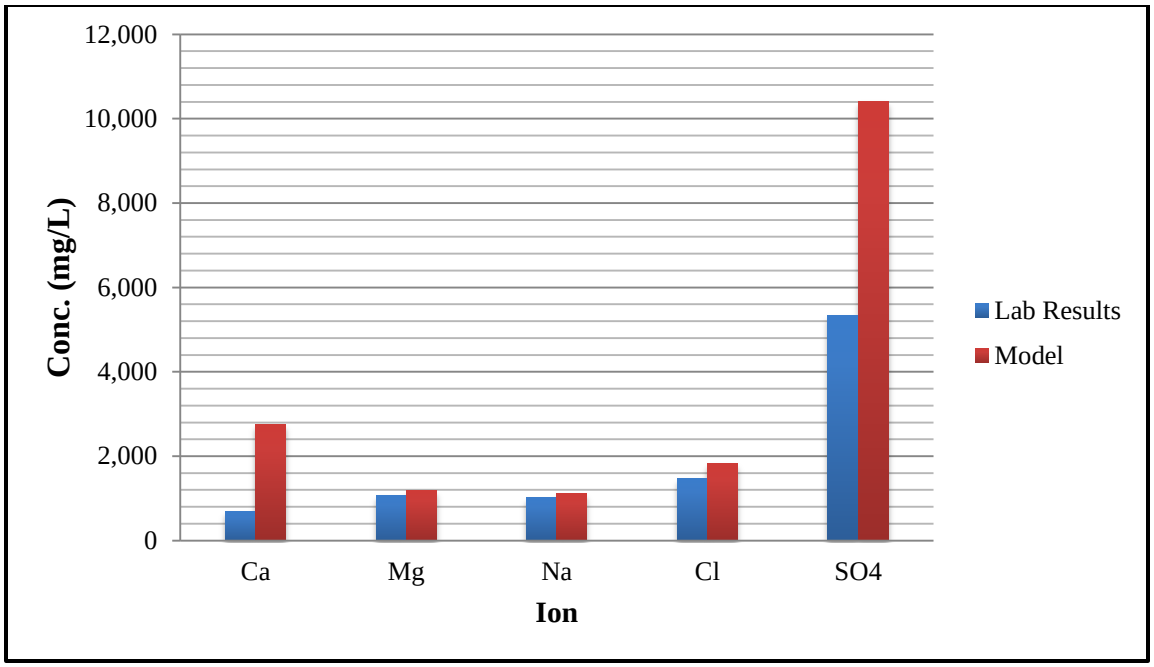

Figure 4.25: Ion Concentrations Comparison between IC analysis and the Matlab Model

The capacity of the CERRO process to operate under conditions of supersaturation is due to the treatment time of the process. It appears that the treatment time can be shorter than the induction time of gypsum precipitation. The use of antiscalants improves the performance of the system as well. The same characteristic was observed for silica supersaturation.

4.8.1.2. Treatment Approach in Gypsum Saturated Water

The precipitation of gypsum was a recurrent problem in the CERRO process. In 2010, the CERRO TME unit was taken to the BGNDRF located in Alamogordo, New Mexico. This facility operates wells rich in calcium and sulfate ions (60% of the TDS). The unit was tested to evaluate the performance of the CERRO unit in conditions of supersaturation of gypsum. Figure 4.26 shows the chemical composition of the brackish water in the BGNDRF (Well #3).

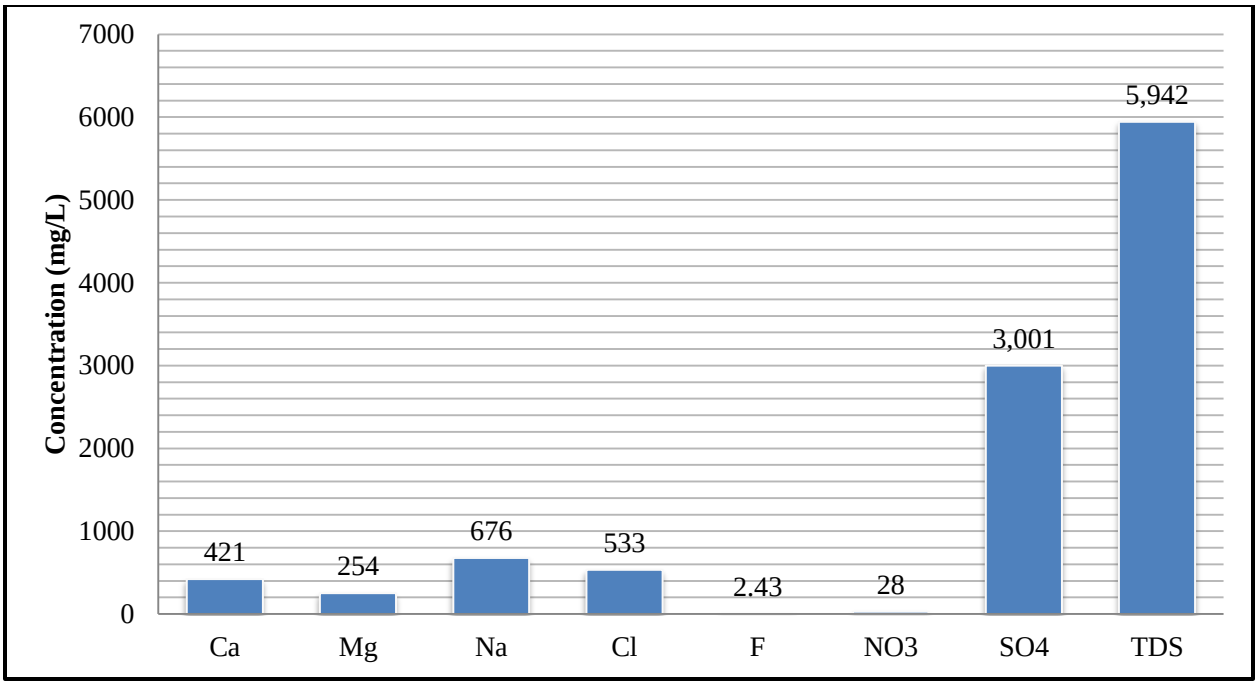

Figure 4.26: Brackish Water Composition in the BGNDRF

The preliminary results of treatment of BGNDRF water with the CERRO TME unit indicated that the maximum recovery of the system was 68%. This experiment was performed without the addition of antiscalants. The intention of the experiment was to identify the capacity of the water to be concentrated without modifying its chemistry. The experiment was performed with a first stage RO pilot unit with a 50% recovery. The concentrate of the RO unit was then sent to the CERRO TME unit for further treatment. It was found that only 36% recovery of concentrate could be reached in the CERRO unit before gypsum precipitated. Table 4-25 shows the analytical data of this experiment.

Table 4-19: IC and TDS Data

	Cations (mg/L)			Anions (mg/L)				TDS (mg/L)
Sample ID	**Ca**	**Mg**	**Na**	**Cl**	**F**	**NO3**	**SO4**	
RO Concentrate	1,020	563	1,320	1,209	2.76	53.55	6,053	10,950
CERRO Final Feed	530	846	1,994	1,817	1.93	77.59	7,599	13,531
CERRO Permeate	5.26	2.89	10.98	35.68	0.33	5.21	26.05	<100

The analysis of the samples was performed after gypsum precipitation occurred. It can be seen that the calcium concentration is lower in the CERRO concentrate than in the RO concentrate. This happened because the samples with gypsum precipitation were filtered and the supernatant of the sample was analyzed.

The addition of antiscalants did not improve the recovery of the unit with this type of water. As mentioned before (section 4.4.), antiscalants tend to stop working at high gypsum concentrations. It was found that the recovery of the CERRO TME unit reached a maximum value of 72% if antiscalants were added to the brackish water. However, even high dosages of antiscalants (20 ppmv) did not improve the recovery significantly.

It was later found an article describing the fact that gypsum solubility increases as the concentration of sodium chloride increases (Messinger and Anna Hahn 1921). Figure 4.27 shows the solubility of calcium sulfate as a function of sodium chloride concentration.

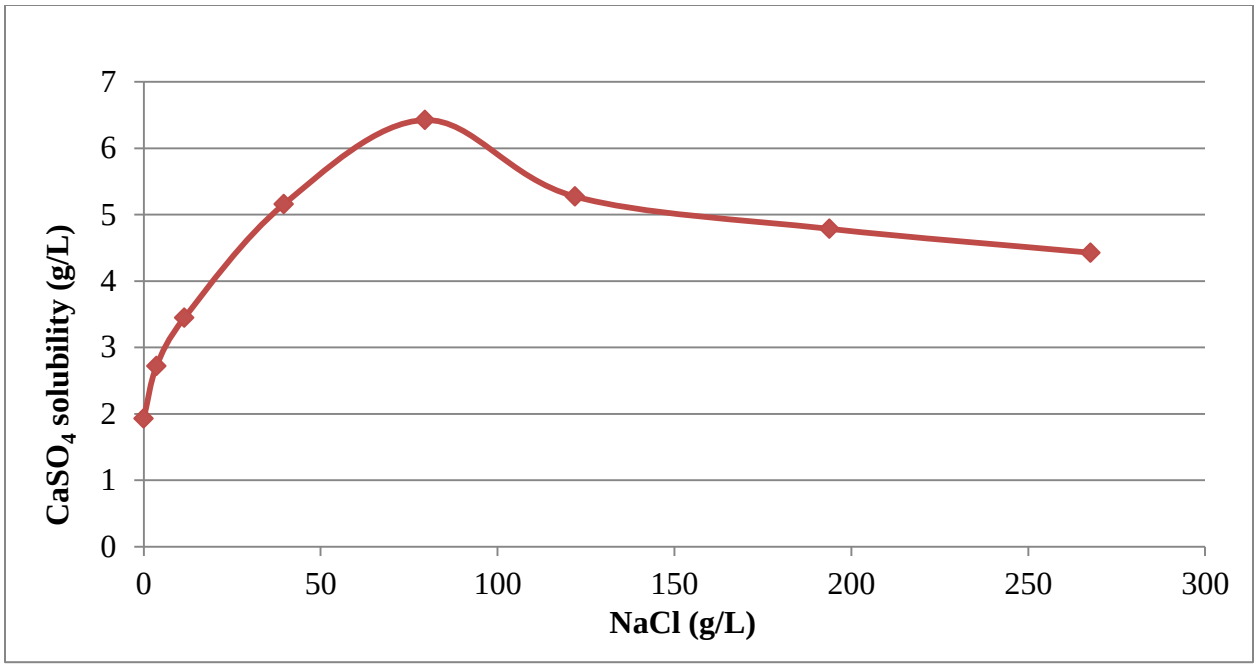

Figure 4.27: $CaSO_4$ Solubility as a Function of NaCl Concentration (Cameron and Seidell 1901)

This particular characteristic of gypsum was tested in the CERRO TME unit by adding a brine solution prepared with a sodium chloride concentration of 300,000 mg/L. This brine was added into the feed tank of the CERRO TME unit and mixed with the brackish water. This mixture was intended to raise the sodium chloride concentration to 10,000 mg/L. It was calculated that this concentration was the optimal to start the batch. According to Figure 4.11, the solubility of gypsum will increase as the sodium chloride concentration increases during treatment. The results of this experiment showed that 87% recovery could be achieved before gypsum precipitated. A batch without antiscalants or brine solution was run as a control. Precipitation of gypsum occurred at 65% in the control batch. Figure 4.28 shows how the addition of NaCl affected the turbidity and permeated flow during the experiment.

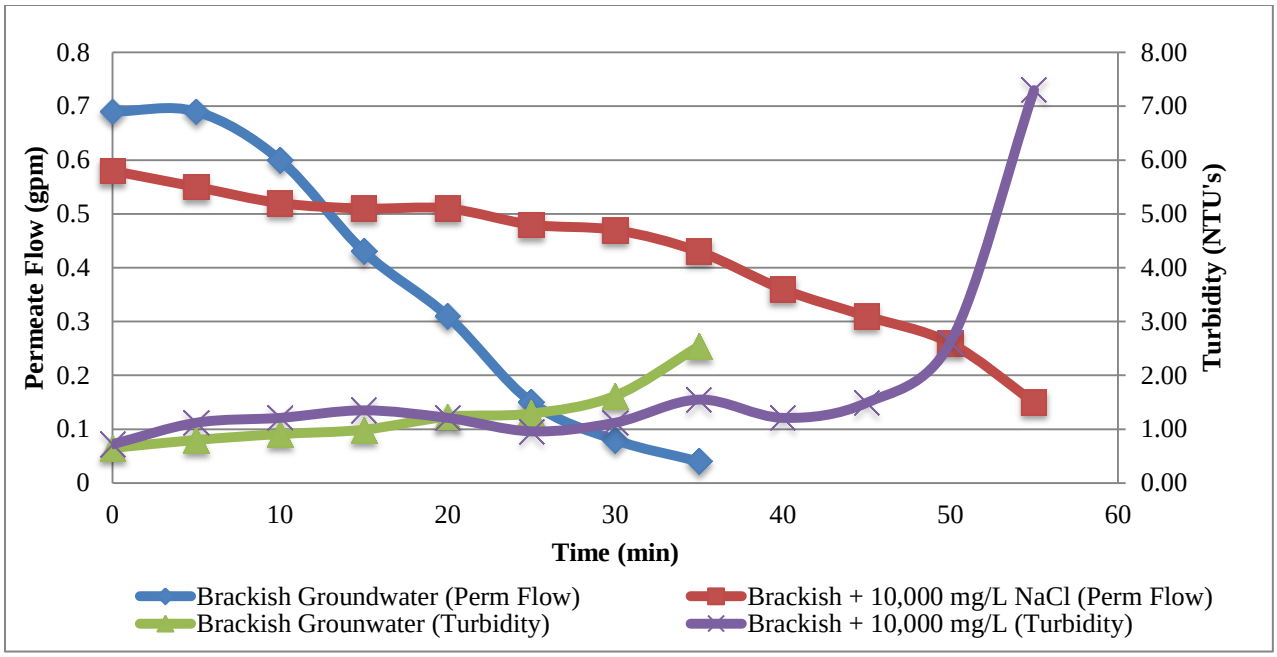

Figure 4.28: Permeate Flow and Turbidity from the Brine Experiment and the Control

The economic considerations of the addition of sodium chloride to the brackish water were not evaluated. However, it is unlikely that salt addition would be cost effective. What can be inferred from the observations of these experiments is that the ionic composition of the water will affect the recovery of the CERRO process by decreasing or increasing the solubility of calcium sulfate.

4.8.1.3. Recovery Improvement by Precipitation of $CaSO_4$

The CERRO SME unit was tested to treat brackish water from Alto, New Mexico. The TDS concentration of the brackish water was relatively low and the preliminary tests showed that 96% recovery could be achieved before gypsum precipitation. However, the feasibility of the project was restricted to a recovery of 98% or higher. This restriction was due to the limitation in the capabilities to manage the concentrate produced by the process. The approach to improve the recovery of the system was by precipitating the gypsum from the CERRO concentrate by the addition of lime (CaO). The excess in calcium forces the gypsum to precipitate and stay in

equilibrium with the water. After the gypsum precipitated, it was removed from the CERRO concentrate, and the concentrate was the mixed with feed water and treated in a new batch to increase the recovery of the system. Table 4-20 shows the ionic composition of the Alto brackish water.

Table 4-20: Ionic Composition of Alto Brackish Water

	Concentration (mg/L)					
	Ca	**Na**	**Cl**	**PO_4**	**SO_4**	**TDS**
Alto Brackish Water	237	105	165	<1	887	1,779

It was necessary to identify the optimal dosage of lime to precipitate the calcium sulfate. After several tests, the water was shown to have a buffering capacity at a pH of about 10.3. This buffering capacity was not expected, since the alkalinity was removed in the pretreatment process with sulfuric acid. IC analysis showed that the magnesium precipitated at a rate faster than gypsum. After most of the magnesium was depleted, the gypsum precipitation occurred faster. Table 4-21 shows the IC, conductivity and TDS analysis (see appendix A-6) of the CERRO concentrate with different amounts of lime.

Table 4-21: IC, Conductivity, and TDS Analysis of CERRO Concentrate and Lime

			Cations and Anions Concentration (mg/L)						
Sample ID	**conductivity (microS/cm)**	**pH**	**Cl**	**SO_4**	**Ca**	**Mg**	**K**	**Na**	**TDS (mg/L)**
CERRO Conc. (92%)	11,030	3.2	1,127	6,157	1,437	1,209	78	791	10,723
500 mg/L (CaO)	10,490	10.22	1,070	6,106	1,706	952	20	750	10,684
1000 mg/L (CaO)	10,670	10.54	1,089	3,746	934	615	21	755	7,349
2000 mg/L (CaO)	7,400	11.02	1,098	2,131	742	45	27	764	5,134
4000 mg/L (CaO)	13,040	12.22	1,097	1,663	1,294	0.0	26	765	5,888

After the analysis, an article was found that describes the fact that magnesium chloride increases the solubility of gypsum (Ostroff and Metler 1966). Actually, magnesium chloride increases the solubility of gypsum more significantly than sodium chloride. In this analysis, it was found that calcium sulfate can be removed with the addition of lime, but the presence of magnesium will be an interference in the process. Further study of the concentrate showed that the magnesium precipitates with lime addition because the increment in the pH will form $Mg(OH)_2$, which has a very low solubility in water. A titration of the CERRO concentrate with NaOH showed the buffering capacity of magnesium at a pH of 10.3. Figure 4.29 shows the conductivity and pH of the titration. It was found that the end of the titration occurred when 100 mEq/L of NaOH were added to the CERRO concentrate. This value fits perfectly with the magnesium concentration obtained in the IC analysis (Table 4-21) since 100 mEq/L of magnesium are equal to 1,215 mg/L.

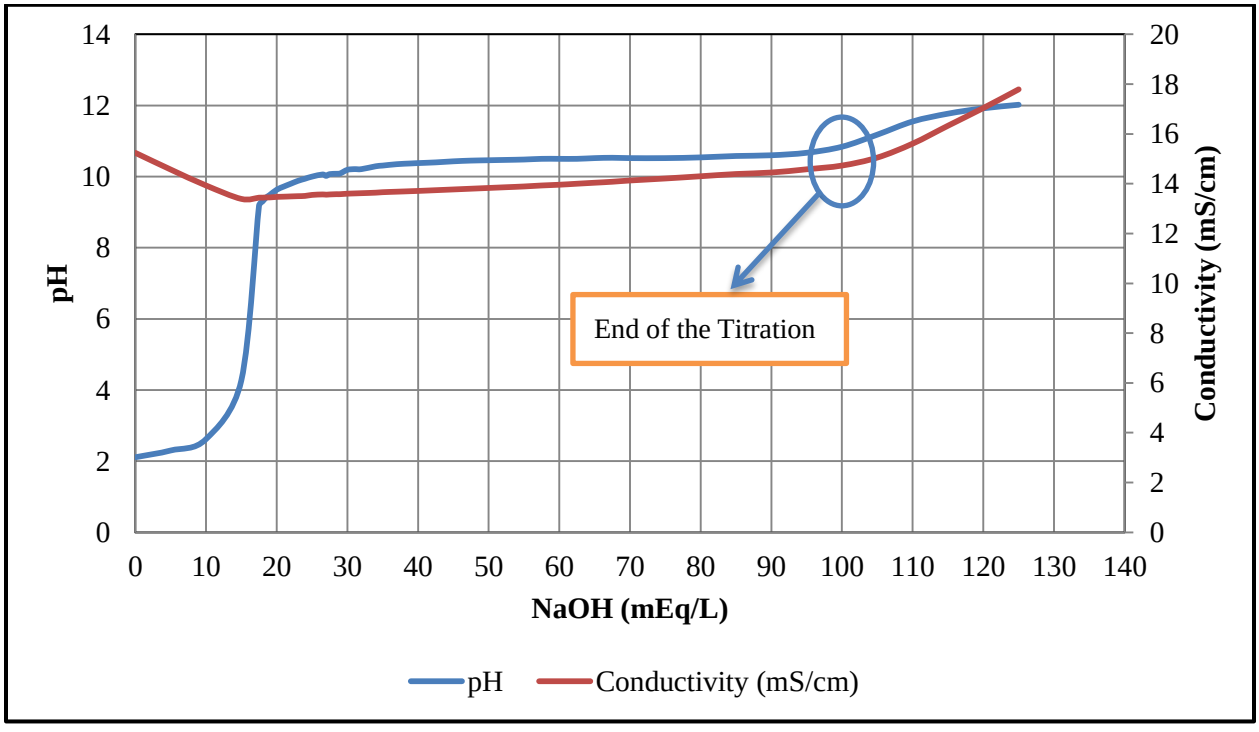

Figure 4.29: CERRO Concentrate Titration with NaOH

The experience gained from this experiment led the author to conclude that the concentrate can be mixed with feed water and again treated in the CERRO process, increasing the recovery of the system to 99%. However, it was found that the sodium and chloride concentrations increased after every batch. This continuous increment in the concentration of sodium and chloride will, eventually, produce a volume of concentrate that cannot be treated further and will have to be disposed. The economic impact of this lime addition was not evaluated. Even though the addition of lime turned out to be an efficient method for the precipitation of gypsum, it is unknown if this process would be cost-effective.

4.8.2. CERRO Process Resistance to Silica Fouling

The most important factor that protects the membranes in the CERRO process from silica fouling is the treatment time. The analysis of the results and a review of current literature indicate that the induction time of silica polymerization inside a membrane element is several hours. It has been shown that the treatment time of the CERRO process could be from 20 to 120 minutes and with the new improvements, the treatment time was made shorter. This characteristic prevents the silica polymers from precipitating in the membrane surface. All the CERRO units have shown the same resistance to silica fouling. The results showed that concentrations above 1,000 mg/L of silica can be achieved by the CERRO process without any kind of pretreatment. Several batches using the CERRO SME unit and the KBH concentrate as feed were performed and the concentration of silica was measured at different recoveries. The silica analysis (see appendix A-1) was performed immediately after the sample was taken. The silica concentration was calculated using equation 4.3. The calculated concentration of silica was compared with the concentration obtained in the analysis. Figure 4.30 shows the comparison between calculated silica and measured silica. It can be seen that there is a

difference between the calculated silica concentration and the measured silica concentration after 50% recovery. The difference between the two concentrations happens because the colorimetric method of analysis for silica only measures monomeric silica. The polymers of silica will not be shown in the results. It can be seen that 18% of the silica is already polymerized at 75% recovery, and 27% of the silica was in the polymer form at the end of the batch with an 84% recovery.

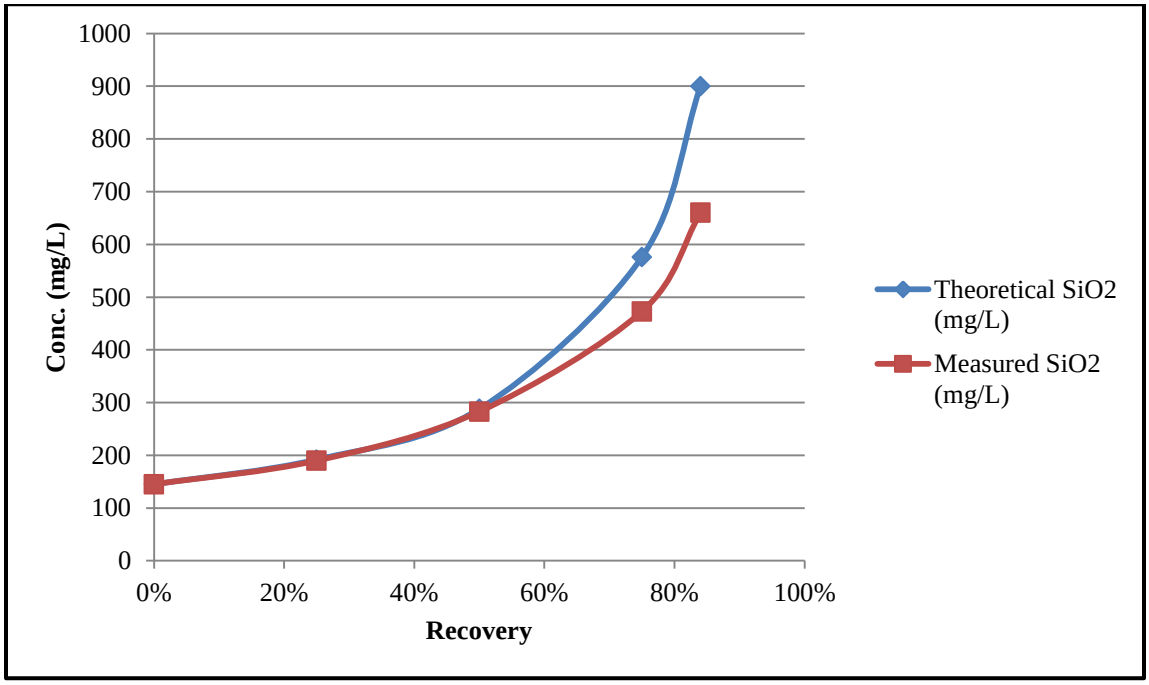

Figure 4.30: Calculated Silica vs Measured Silica

It was found that the treatment time of the batch was fundamental to avoid the polymerization of silica on the surface of the membrane. For this experiment, the treatment time of the batch was 135 minutes. At that time, only 27% of the total silica polymerized before the water was removed from the system. The control test showed that there were no signs of membrane fouling due to silica polymerization. After the analysis, it was concluded that the

treatment time and a fast rinse of the membranes are key factors to operate with silica saturated water. The use of antiscalants can increase the batch treatment time if necessary, but ongoing research projects are showing that the process can handle high concentrations of silica even without the use of antiscalants (Davis and Ortega-Corral 2013).

Another important factor of the CERRO process is the flushing of the membranes modules after every batch treatment. This procedure turned out to be very important for removing the high concentrations of silica from the system, thereby avoiding its polymerization inside the membrane elements.

These two factors combined are the most important elements that allow the system to operate with high concentrations of silica without fouling the membranes.

Chapter 5: Conclusions

After several months of experimentations, the primary objectives of this project were achieved. The most important parameters of operation of the CERRO process were determined, and the system performance was improved. However, this project is just an advance in the understanding of this process. Further evaluation is required for the implementation of the process in the scale of well-known processes such as the HERO process, the SPARRO process, and others. The CERRO process can be considered in the earliest stage of development, but after this evaluation, it can be considered as a serious option in the desalination of RO concentrate and brackish water, especially those that are rich in silica.

5.1. Identification of the Parameters of Operation

5.1.1. Treatment Time

During the evaluation of the process, eight parameters of operation were identified as important factors in the performance of the CERRO process. The treatment time, crossflow velocity, acid dosage, antiscalant dosage, temperature, pressure, membrane flushing and the chemistry of the water were shown to be the most important factors for the system.

The analysis made in the treatment time in the system showed that it is the most important factor for the CERRO process. It was found that the treatment time can be lower than the induction time of precipitation or polymerization (sections 4.1, 4.8.1, and 4.8.2). This characteristic prevented the polymerization of silica on the surface of the membrane. For that reason, the CERRO process is capable of operating in conditions of supersaturation of silica. Additionally, it was found that the addition of membrane elements reduced the treatment time significantly. The number of cycles in the system was reduced from 9 cycles per batch to 2.4

cycles per batch on average. The reduction in the number of cycles per batch in the system resulted in the reduction of energy consumption. It was calculated that the CERRO SME unit used 73% less energy with the addition of the new membrane elements. Additionally, it was calculated that the cost of energy consumption was reduced from $4.84 per 1000 gallons to $1.29 per 1000 gallons on average. The reduction in the number of cycles of the system was one of the best improvements achieved in this project. The primary idea of this approach was to reduce the number of cycles to one per batch. Future projects should evaluate this possibility.

5.1.2. Crossflow Velocity

The analysis performed on the impact of crossflow velocity on the performance of the CERRO process showed that it does not affect the process significantly. One of the hypotheses prior the development of this project was that the crossflow was the key factor for the success of the CERRO process, but the analysis of the results showed that this hypothesis was not true. Contrary to the initial supposition, the crossflow velocity is not a factor that allows the unit to perform satisfactorily under conditions of supersaturation. Several experiments were performed (section 4.2) where the crossflow velocity was reduced. The results of these experiments did not show any indications of the membranes getting fouled or scaled, even in experiments where the crossflow was reduced by 74% of the usual operation. The only time where scaling was noticed was in the experiment conducted in 02/27/2013. In this experiment, the crossflow velocity was reduced to 94% lower than the usual operation. Additionally, the CERRO SME unit was operated in a continuous flow configuration for 35 minutes. After the experiment was finished, it was determined that the membrane lost 27% of its permeability. Several cleaning procedures were performed to the unit with silica and calcium sulfate cleaning agents. However, the fouling scaling factor was irreversible (It was assumed that the membrane was fouled with silica)

5.1.3. Acid Dosage

Before this project, it was believed that calcium carbonate precipitation could be a serious problem in the CERRO process. For that reason, the addition of sulfuric acid to the feed water was implemented as a protocol to protect the membranes from precipitation of calcium carbonate. The dosage of sulfuric acid was the amount required to lower the pH of the feed below 4.5. At this pH, all the alkalinity is in the form of carbonic acid and it does not represent a problem of precipitation. As an example of this procedure, the KBH concentrate required 1 mL of sulfuric acid per gallon of concentrate to reduce the pH to below 4.5. According to the information reported by Tarquin et al in 2010, this dosage of sulfuric acid will produce a cost of $0.63 per 1000 gallons of KBH concentrate. During the development of this project, it was determined that the treatment time of the process was lower than the induction time for silica polymerization and, to some extent, calcium sulfate. Based in that observation, it was supposed that the treatment time could also be lower than the induction time of calcium carbonate. Several tests were performed where the dosage of sulfuric acid was reduced to 50% of the previous dosage (1 ml/gal). The results showed that there was no significant change in the performance of the CERRO process with the reduction in sulfuric acid. Additionally, it was calculated that the cost of the addition of sulfuric acid could be reduced to $0.33 per 1000 gallons. The results of this analysis showed that the CERRO process can operate with at least 50% less acid without the risk of fouling or scaling the membranes with calcium carbonate. Further analysis will be required to evaluate if the CERRO process can operate with lower acid dosages or without any acid in the feed at all.

5.1.4. Antiscalant Dosage

An important contribution from this study was the method developed to evaluate the performance of the antiscalants (section 4.4). This approach showed that the performance of the antiscalants can be tested without the necessity of expensive materials and/or pilot testing. The results obtained during this analysis gave enough information for the selection of the type and dosage of antiscalants required for a given gypsum concentration. Additionally, the cost of the analysis was considerably low. This analysis was shown to be very helpful, and it could be used for the selection of antiscalants for any desalination process, and not the CERRO process only.

The result of this project showed that the optimal amount of antiscalants should be between 3 and 5 ppmv (parts per million by volume). The analysis of this parameter indicates that the antiscalants are concentrated at the same rate as the ions in the water. Additionally, it was found that high dosages of antiscalants do not improve the induction time greatly. The evaluation of antiscalants designed to increase the induction time of calcium sulfate showed that different types of antiscalants will perform differently, and different dosages of antiscalants will increase the induction time of gypsum. However, it was determined that any antiscalants will not be efficient at gypsum concentrations of 0.06 M or higher. For brackish water and RO concentrate with high concentrations of calcium and sulfate ions, the addition of antiscalants will not improve the recovery. A careful evaluation should be made before the addition of antiscalants to the feed water, since they may turn out to be impractical under certain conditions. Another important finding in this evaluation was the method developed to evaluate the performance of the antiscalants (section 4.4). This approach showed that the performance of the antiscalants can be tested without the necessity of expensive materials and/or pilot testing. The results obtained during this analysis gave enough information for the selection of the type and

dosage of antiscalants required for a given gypsum concentration. Additionally, the cost of the analysis was considerably low. This analysis was shown to be very helpful, and it could be used for the selection of antiscalants for any desalination process, and not the CERRO process only.

5.1.5. Temperature

During the operation of the CERRO process, the temperature of the feed water increases over time. The temperature of the feed water gets to the point that heat exchangers have to be used to control the increase in temperature. If heat exchangers are not used in the system, the temperature of the water can get higher than the maximum temperature of operation of the membranes (45^{o} C). It was determined that the water increases its temperature due to the energy loss in the concentrate valve of the CERRO process and the repeated pumping of the feed water. This valve forces the feed water to pass through the membrane and keeps the pressure of the system constant. After the water passes through the concentrate valve, the pressure drops by about 94%. This energy is released in form of heat and heats the water. This problem can be solved if an energy recovery device is added into the CERRO process to recover the energy lost in the concentrate valve. On the other hand, if the CERRO process can be set to one cycle per batch, a heat exchanger will not be required in the system.

5.1.6. Pressure

The CERRO process can be operated at a constant pressure or at a constant permeate flow rate. The operation of the system at a constant pressure reduces the production of permeate over time due to the increase in the osmotic pressure of the feed. Operation at a constant permeate flow will force the pressure to increase over time to keep the permeate flow rate constant. In this analysis, it was found that it is better to operate at a constant pressure. The increase in the pressure of the system does not improve the recovery of the system greatly and

affects the operation cost of the system. An important consideration in the operating pressure of the CERRO process is the maximum flux achievable. The permeate flow rate is a function of the pressure, but it is a function of the membrane area as well. It was found that the system can be operated with maximum flow at different pressures. The minimum pressure to obtain the maximum flow should be identified to avoid the waste of energy for the extra pressure applied in the system.

5.1.7. Membrane Flushing

The flushing with permeate water was a protocol established to preserve the membranes from possible precipitation of calcium sulfate and/or polymerization of silica after each test using the CERRO units. However, it was found that it is an important parameter in the CERRO process. It has been mentioned that the treatment time is the most important factor of the CERRO unit. However, the flushing of the membranes is essential to remove the supersaturated solutions from the membrane elements. In fact, the results showed that the precipitation of calcium sulfate inside the membrane elements can be cleaned if the flush is performed immediately. In this evaluation, the minimum amount of time needed to flush the membranes was determined. According to the results, it was found that 99% of the concentrate is removed from the membranes of the pilot unit after one minute of low pressure flushing. The test was conducted in the CERRO SME unit and it was found that there was some mixing in the cartridge filters ahead of the membrane vessels. That mixing presented a delay in the flushing time. One ongoing project in the CERRO TME unit is showing that the minimum flushing time could be as low as 15 seconds per flush (Davis and Ortega-Corral 2013). The difference between the CERRO SME unit and the TME unit is that the TME unit has a specific line for the flush flow that is directly connected to the membrane elements. This simple change in the design should be

considered in the design of future units. Future projects should address the possibility of operating the flushing procedure with feed water and, the possibility of recirculating some of the flush back into the system to improve the hydraulic recovery of the system.

5.1.8. Water Chemistry

It was mentioned in section 4.8 that the chemical composition of the water is not a parameter that could be modified in the CERRO process. However, it plays a very important role in the performance of the system. During the development of this project, it was determined that the main limitation of the CERRO process was the precipitation of gypsum during the treatment due to supersaturation. Even though the system did not get scaled by the precipitation of gypsum, the system was not capable of treating water with suspended gypsum in it. Different approaches were taken to improve the recovery of the system in gypsum-saturated water. The addition of large dosages of antiscalants did not significantly improve the recovery of the system. The addition of sodium chloride in the water increased the solubility of the gypsum and better recoveries were obtained, but the cost effectiveness of this approach is unlikely. The precipitation of gypsum with lime turned out to be very effective, but the economic impacts of this approach were not studied. It was found that magnesium increases the solubility of gypsum greatly and it presents a large interference in the precipitation of gypsum with lime. Additionally, it was found that the CERRO process can operate under conditions of gypsum supersaturation because the treatment time of the process can be shorter than the induction time of the gypsum. The use of antiscalants can improve the recovery of the unit, but the dosage of the antiscalant should not be higher than 5 ppmv. The same results were obtained in the analysis of silica supersaturation. It was found that the induction time of silica polymerization could be

on the order of hours. As the results showed, the presence of silica polymers is less than 30% at the end of a batch, and it is only in contact with the membrane surface for a brief period of time.

5.2. Final Conclusions

In-depth evaluation of the CERRO process showed that the original design of the system was not optimal. From the results obtained in this project, it was possible to identify the most important parameters of operation and the process was significantly improved. This project resulted in a significant reduction of the energy consumption of the system. Calcium sulfate precipitation was found to be the main limitation of the process. The resistance of the process to silica fouling was demonstrated and the correct use of antiscalants was investigated. As a conclusion to this document, it was found that the most important parameters of operation of the CERRO process are the treatment time and the immediate cleaning of the membranes by the flushing procedure.

Chapter 6: Recommendations

The improvements made in the CERRO process via this project are significant. This does not mean that the improvement of the system is finished. It is necessary to keep improving the system in order to make it a viable option for desalination. It is necessary to reduce the cost of operation more. It is recommended that energy recovery devices be evaluated. The evaluation of the system to operate in one cycle per batch is recommended as well since it is uncertain if the process will be economically attractive to operate in only one cycle per batch. With lower number of cycles, the process will behave more like a continuous flow system or a conventional RO system, and it is well known that conventional systems tend to get fouled or scaled at high concentrations. If the system is operated at one cycle per batch, the flushing procedure will become the most important parameter of operation in the process. Further evaluation of this procedure is required to minimize the amount of water used in the flush. Additionally, it is necessary to evaluate the use of feed water in the flush and avoid the use of permeate water.

The CERRO process can be implemented in a hybrid system to maximize the recovery of water. It could be used as a secondary treatment for a conventional RO system, and the CERRO concentrate could serve as a feed for a process specifically designed to operate in the presence of suspended solids such as VSEP or ZDD.

As a final comment of this section, it is clear that the CERRO process could become a standard process for desalination. It is necessary to continue the efforts to improve the design of the process for the implementation in large scale systems.

References

Alimi, F., Elfil, H., and Gadri, A. (2003). "Kinetics of the precipitation of calcium sulfate dihydrate in a desalination unit." *Desalination*, 158(1–3), 9-16.

Altela Inc. (2013). "ALTELARAIN 750." http://www.altelainc.com/applications/detail/altelarain-600/ (04/16, 2013).

Aquatech Intl. (2011). "HERO TM High Efficiency Reverse Osmosis." http://www.aquatech.com/technologies/HighEfficiencyReverseOsmosis.aspx (04/10, 2013).

ASTM International. (2013). "Standard Practice for Standardizing Reverse Osmosis Performance Data." http://www.astm.org/ (10/10, 2013).

Cohen, Y. (2008). "Membrane desalination of agricultural drainage water: water recovery enhancement and brine minimization." .

Committee on Advancing Desalination Technology, and National Research Council. (2008). *Desalination: A National Perspective.* The National Academies Press, .

Davis, T., and Ortega-Corral, N. (2013). "Ongoing Desalination Project." .

Davis, T., and Rayman, S. (2008). "Pilot Testing of Zero-Discharge Seawater Desalination – Application to Selenium Removal from Irrigation Drainage." *Rep. No. 135*, USBR, Denver, Colorado.

Delgado, G. (2009). "Treatment of RO concentrate using VSEP technology". University of Texas at El Paso, http://digitalcommons.utep.edu/dissertations/AAI1473859.

Delgado, G., and Tarquin, A. J. (2012). "A Detail Analysis of the Performance of Different Antiscalants in Calcium Sulfate Supersaturated Brackish Water." *2012 AICHE Annual Meeting: Recent Advances in Membrane-Based Brine Minimization Technologies*, AICHE, Pittsburgh, PA, 266.

DOW INC. (2012). "DOW Answer Center." http://dowac.custhelp.com/app/answers/detail/a_id/1220/kw/channel%20velocity (10/10, 2013).

Fan, C., Kan, A. T., Fu, G., and Tomson, M. B. (2010). "Quantitative Evaluation of Calcium Sulfate Precipitation Kinetics in the Presence and Absence of Scale Inhibitors." 15(4), 977.

Gabelich, C. J., Williams, M. D., Rahardianto, A., Franklin, J. C., and Cohen, Y. (2007). "High-recovery reverse osmosis desalination using intermediate chemical demineralization." *J.Membr.Sci.*, 301(1), 131-141.

Gilron, J., and Hasson, D. (1987). "Calcium sulphate fouling of reverse osmosis membranes: Flux decline mechanism." *Chemical Engineering Science,* 42(10), 2351-2360.

J. P. Gustafsson. (2011). "Visual MINTEQ." http://www2.lwr.kth.se/English/OurSoftware/vminteq/index.html (08/12, 2012).

Harsa, M. W. (2005). *Water Treatment Principles and Design.* John Wiley & Sons, Inc., Hoboken, New Jersey.

Hater, W., Kolk, C. z., Dupoiron, C., Braun, G., and Harrer, T. (2011). "Silica scaling on reverse osmosis membranes: Investigation and new test methods." 31(1-3), 326.

He, F., Sirkar, K. K., and Gilron, J. (2009). "Effects of antiscalants to mitigate membrane scaling by direct contact membrane distillation." *J.Membr.Sci.,* 345(1–2), 53-58.

Juby, G., and Schutte, C. (2000). "Membrane life in a seeded-slurry reverse osmosis system." *Rep. No. 1171,* WRC, Pretoria.

Karlsruhe Institute of Technology. (2009). "Viscosity and Density of Water Calculator based in Salinity and Temperature." http://www.ifh.uni-karlsruhe.de/_vti_bin/shtml.dll/misc/search.htm (10/10, 2013).

S. Kim. (2012). "Concentration Polarization in Pressure-Driven Crossflow Membrane Filtration." http://www.yale.edu/env/elimelech/Conc-Polarization/sld001.htm (04/11, 2013).

Klepetsanis, P. G., and Koutsoukos, P. G. (1998). "Kinetics of calcium sulfate formation in aqueous media: effect of organophosphorus compounds." *J.Cryst.Growth,* 193(1–2), 156-163.

Koo, T., Lee, Y. J., and Sheikholeslami, R. (2001). "Silica fouling and cleaning of reverse osmosis membranes." *Desalination,* 139(1–3), 43-56.

Kumar, M., Adham, S. S., and Pearce, W. R. (2006). "Investigation of Seawater Reverse Osmosis Fouling and Its Relationship to Pretreatment Type." *Environ.Sci.Technol.,* 40(6), 2037-2044.

Lisitsin, D., Hasson, D., and Semiat, R. (2005). "Critical flux detection in a silica scaling RO system." *Desalination,* 186(1–3), 311-318.

Lyster, E., Kim, M., Au, J., and Cohen, Y. (2010). "A method for evaluating antiscalant retardation of crystal nucleation and growth on RO membranes." *J.Membr.Sci.,* 364(1–2), 122-131.

Messinger, A., and Anna Hahn, D. (1921). "A Dictionary of Chemical Solubilities: Inorganic." 951.

Mickley, M. C. (2009). "Treatment of Concentrate." *Rep. No. 155*, Bureau of Reclamation, Denver, Colorado.

Mickley, M. C., and Jordahl, J. (2013). "Development of a Knowledge Base on Desalination Concentrate and Salt Management." *Rep. No. 07-02-1*, WateReuse Research Foundation, Alexandria, VA.

Ostroff, A., and Metler, A. (1966). "Solubility of Calcium Sulfate Dihydrate in the System NaCl-MgCl2-H2O from 28° to 70° C." *J.Chem.Eng.Data*, 11(3), 346-350.

A. Parker. (2005). "Mining Geothermal Resources." https://www.llnl.gov/str/JanFeb05/Bourcier.html (04/10, 2013).

Prisciandaro, M., Musmarra, D., and Lancia, A. (2003). "The Retarding Effect of Citric Acid on Calcium Sulfate Nucleation Kinetics." *Ind. Eng. Chem. Res.*, (25), 6647.

Rahardianto, A., McCool, B. C., and Cohen, Y. (2010). "Accelerated desupersaturation of reverse osmosis concentrate by chemically-enhanced seeded precipitation." *Desalination*, 264(3), 256-267.

Sahachaiyunta, P., Koo, T., and Sheikholeslami, R. (2002). "Effect of several inorganic species on silica fouling in RO membranes." *Desalination*, 144(1–3), 373-378.

Sawyer, C. N., McCarty, P. L., and Parkin, G. F. (2003). *Chemestry for Environmental Engineering and Science.* McGraw-Hill, New York.

Sheikholeslami, R., and Ong, H. W. K. (2003). "Kinetics and thermodynamics of calcium carbonate and calcium sulfate at salinities up to 1.5 M." *Desalination*, 157(1–3), 217-234.

Shih, W., Albrecht, K., Glater, J., and Cohen, Y. (2004). "A dual-probe approach for evaluation of gypsum crystallization in response to antiscalant treatment." *Desalination*, 169(3), 213-221.

Shih, W., Rahardianto, A., Lee, R., and Cohen, Y. (2005). "Morphometric characterization of calcium sulfate dihydrate (gypsum) scale on reverse osmosis membranes." *J.Membr.Sci.*, 252(1–2), 253-263.

Tarquin, A. J. (2008). "Cost-Effective Volume Reduction of Silica-Saturated RO Concentrate." *Rep. No. 125*, Bureau of Reclamation, Denver, Colorado.

Tarquin, A. J., Fahy, M. P., and Balliew, J. E. (2010). "Concentrate Volume Reduction Research in El Paso, Texas." ASCE, 358.

Tobler, D. J. (2008). "Molecular pathways of silica nanoparticle formation and biosilicification". Dissertation. University of Leeds, Leeds, England.

Uchymiak, M., Lyster, E., Glater, J., and Cohen, Y. (2008). "Kinetics of gypsum crystal growth on a reverse osmosis membrane." *J.Membr.Sci.*, 314(1–2), 163-172.

Weast, R. C. (2005). "Ionic Conductivity and Diffusion at Infinite Dilution." *CRC Handbook of Chemistry and Physics*, D. R. Lide, ed., CRC Press, New York, 5.95-5.96, 5.97.

Zhang, B., Chen, Y., and Li, F. (2011). "Inhibitory effects of poly(adipic acid/amine-terminated polyether D230/diethylenetriamine) on colloidal silica formation." *Colloids Surf.Physicochem.Eng.Aspects*, 385(1–3), 11-19.

Zhu, C., and Anderson, G. (2002). "Environmental applications of geochemical modeling." Cambridge: Cambridge University Press, 45.

Appendix A: Analytical Methods

Appendix A-1: Silica Analysis

The analysis of silica was performed using the Silicomolybdate method. This method is based on the principle that ammonium molybdate reacts with monomeric silica and any phosphates present in the water at low pH to form yields of heteropoly acids which are yellow in color.

Methodology

For this particular analysis, the spectrophotometer HACH DR/4000 was used. The estimated detection limit for the spectrophotometer is 0.3 mg/L with a built-in calibration curve stored in the spectrophotometer data base. The range of the calibration curve is set from 0 mg/L as SiO_2 to 100 mg/L as SiO_2.

Procedure

- The program 3350 was selected in the DR/4000
  - ✓ The program was designed to use a wavelength of 452 nm
- A volume of 10 mL of sample was taken and poured into a cuvette.
- 1 pillow of HACH molybdate reagent was added into the cuvette and mixed with the sample.
- 1 pillow of HACH Acid Reagent Powder was added into the cuvette and mixed with the sample.
- A period of 10 minutes was set for the reaction to occur.
- After the reaction time ended, 1 pillow of HACH Citric Acid was added to the cuvette and mixed with the sample.
- A period of 2 minutes was set for the reaction to occur.

- The cuvettes with the sample were analyzed in the spectrophotometer giving the concentrations in mg/L as Silica.
- A blank of DI water was used to set the value of zero absorbance.
- Samples with silica concentrations above 100 mg/L were diluted. The dilution factor of the samples was done to yield a concentration between 20 mg/L and 80 mg/L.

Interferences

Table A-1 shows the interference substances for the silica analysis

Table A-1: Interfering Substances in Silica Analysis

Interfering Substance	Interference Levels and Treatments
Color	Eliminated by zeroing the instrument with the original sample.
Iron	High levels of Fe2+ and Fe3+ interfere.
Phosphate	Does not interfere below 50 mg/L $PO4^{3-}$. At 60 mg/L $PO4^{3-}$, a negative 2% interference occurs. At 75 mg/L $PO4^{3-}$ the interference is negative 11%.
Sulfides (S^{-2})	High levels interfere.
Turbidity	Eliminated by zeroing the instrument with the original sample.

This method only analyses monomeric silica (reactive silica). Silica polymers do not react with the molybdate. High concentrations of silica will show lower values.

Appendix A-2: Ion Chromatography Analysis

Ion chromatography (IC) analysis was performed to determine the concentrations of the major ions present in the water. The chromatograph used for these analyses was the DIONEX 2100 Ion Chromatograph with capacity to analyze cations and anions. The column used to analyze cations was the DIONEX CS16 (5 x 250 mm) with Methanesulfonic acid (MSA) as eluent. The column used to analyze anions was the DIONEX AS16 (4 x 250 mm) with potassium hydroxide as eluent. The system had a capacity of 50 samples per batch. Calibration curves were made for every new batch. A total of five standards were prepared in order to make a calibration curve. The standard with the highest concentration (STD 5) was prepared with laboratory reagents, and then, standards with lower concentrations were prepared by diluting the STD 5 with DI water. Table A-2 shows the list of cations and anions analyzed, the reagent used to prepare the standard 5, and the concentration of the standard.

Table A-2: List of Cations and Anions

Cation	**Reagent**	**STD 5 Concentration (mg/L)**
Na^{+}	NaCl	300
Ca^{+2}	$CaCl * 2H_2O$	300
Mg^{+2}	$MgCl_2 * 6H_2O$	150
K^{+}	KCl	100
Anions	**Reagent**	**STD 5 Concentration (mg/L)**
SO_4^{-2}	$Na_2SO_4 * 7H_2O$	300
Cl^{-}	NaCl	300
NO_3^{-2}	$NaNO_3$	20
F^{-}	Fluoride STD	5

The calibration curves developed for the analysis where based in a five point calibration curve. Table A-3 shows the concentrations of the different standards used during the calibration of the IC. DI water was used for STD 0. It was assumed that DI water did not contain significant amounts of ions.

Table A-3: List of Standard Concentrations Used in the IC Calibration

	Standard Concentrations (mg/L)					
Cations	**STD 0**	**STD 1**	**STD 2**	**STD 3**	**STD 4**	**STD 5**
Na^{+}	0	18.75	37.5	75	150	300
Ca^{+2}	0	18.75	37.5	75	150	300
Mg^{+2}	0	9.375	18.75	37.5	75	150
K^{+}	0	6.25	12.5	25	50	100
Anions						
SO_4^{-2}	0	18.75	37.5	75	150	300
Cl^{-}	0	18.75	37.5	75	150	300
NO_3^{-2}	0	1.25	2.5	5	10	20
F^{-}	0	0.3125	0.625	1.25	2.5	5

The correlation factor for the calibration curve was set to be 99.50% or higher to be accepted for data analysis. Calibration curves that presented lower values were rejected and a new calibration curve was built instead.

The samples were diluted in order to fit the concentration to the limits of the calibration curves. Dilution factors were made according to the sample's concentration.

Interferences

IC cationic columns tend to displace the elution time of the ions after some time of use, especially magnesium and potassium. It is necessary to run individual check-standards for each ion along with the samples. This has to be done in order to identify the exact elution time of the ion as well to corroborate the accuracy of the calibration curve.

Appendix A-3 Sulfates (SO_4) Analysis

The concentration of sulfates in the water samples was obtained by two methods: IC analysis (Appendix A-2) and spectrophotometric analysis using the HACH procedure 8051.

The spectrophotometer used for the analysis was the HACH DR/4000. The spectrophotometer has a built-in method with the capacity to analyze sulfate concentrations from 0 mg/L to 70 mg/L as sulfates. The wavelength was automatically selected by the program to be 450 nm.

Procedure

- The program 3450 was selected from the HACH DR/4000 database.
- A sample volume of 25 mL was transferred into one cuvette.
- One pillow of HACH reagent for sulfates was added to the cuvette and mixed with the sample.
- A period of 5 minutes was allowed for the reaction to occur.
- A blank with DI water was used as a baseline for zero absorbance.
- The sample was introduced into the spectrophotometer and the results in mg/L as sulfate were displayed.
- Samples with concentrations above the calibration curve were diluted with DI water.
- The dilution was made according with the concentration of the sample to give a concentration between 20mg/L and 60 mg/L as SO_4.

Interferences

Table A-4 shows the components that may produce interferences in the analysis of sulfates by this methodology.

Table A-4: Interfering Substances for SO_4 Analysis

Interfering Substance	Interference Levels
Calcium	Greater than 20,000 mg/L as $CaCO_3$
Chloride	Greater than 40,000 mg/L as Cl
Magnesium	Greater than 10,000 mg/L as $CaCO_3$
Silica	Greater than 500 mg/L as SiO_2

Appendix A-4: Total and Calcium Hardness Analysis

The concentration of calcium and magnesium was obtained by two methods: IC analysis (appendix A-2) and volumetric titration with EDTA.

The titration method consists of the reaction of calcium and other hardness ions with EDTA. Eriochrome Black T was added as an indicator. The end point of the titration was done visually when the color of the solution changed from red to blue.

Procedure

- A sample volume of 10 mL was poured into an Erlenmeyer flask.
- 3 drops of HACH buffer for total hardness were added to the sample for total hardness. For calcium hardness titration, 3 drops of potassium hydroxide 8 N were added to the sample to precipitate magnesium.
- The sample was mixed continuously during the titration.
- 1 pillow of HACH Eriochrome Black T indicator was added to the sample.
- A standard solution of 0.02 N of EDTA was droped into the sample using a 50 mL graduated buret.
- The end of the titration was determined visually by the color change in the solution from red to blue.
- The volume of titrant was then multiplied by 100 to express the concentration in mg/L as $CaCO_3$.
- Samples containing more than 1000 mg/L as $CaCO_3$ of hardness were diluted with DI water.

Interferences

Table A-5 shows the substances that may interfere with this method. Polyvalent ions are not considered interferences; however, they will present the same reaction as calcium and magnesium.

Table A-5: Interfering Substances for Total and Calcium Hardness Analysis

Interfering substance	Interference level
Acidity	The test can tolerate 10,000 mg/L acidity.
Alkalinity	The test can tolerate 10,000 mg/L alkalinity and can be run directly in sea water.
Aluminum	Aluminum interferes above 0.20 mg/L aluminum.
Barium	Barium is included in the results but is seldom found in natural waters in significant amounts.
Cobalt	Interferes at all levels.
Copper	Interferes at 0.1 mg/L copper.
Iron	Interferes above 8 mg/L by causing an orange-red to green end point.
Manganese	Interferes above 5 mg/L.
Nickel	Interferes at 0.5 mg/L nickel.
Orthophosphate	Causes a slow end point but does not interfere if the calcium phosphate that forms is allowed to redissolve during the titration.
Polyphosphates	Interfere directly and must be absent.
Polyvalent metal ions	Although less common than calcium and magnesium, other polyvalent metal ions cause the same hardness effects and will be included in the results.
Sodium chloride	Saturated solutions do not give a distinct end point.
Strontium	Strontium is included in the results but is seldom found in natural waters in significant amounts.
Zinc	Interferes at 5 mg/L zinc.
Extreme sample pH	May exceed the buffering capacity of the reagents.

Appendix A-5: Chlorides Analysis

The chloride concentration in the water samples was calculated using two methods: IC analysis (Appendix A-2) and volumetric titration with mercuric nitrate.

The titration method consists of the reaction of the chlorides present in the water with mercuric nitrate forming mercuric chloride. Diphenylcarbazone is added to the water as an indicator of the end of the titration. After the chlorides are depleted in the sample, the mercuric nitrate reacts with the diphenylcarbazone changing the color of the solution from yellow to pink.

Procedure

- A volume sample of 10 mL was poured into an Erlenmeyer flask.
- 1 pillow of HACH diphenylcarbazone indicator was added to the sample and mixed with the sample.
- The sample was then titrated with a standard solution of 0.0141 N mercuric nitrate ($Hg(NO_3)_2$) until the endpoint of titration was reach.
- The endpoint of the titration was determined visually by the color change of the solution from yellow to pink.
- The volume of titrant was multiplied by 50 to obtain the concentration in mg/L as chlorides.
- Samples with chloride concentrations greater than 1000 mg/L as Cl were diluted with DI water.

Interferences

Table A-6 shows the substances that may interfere in this analysis.

Table A-0-6: Interfering Substances for Chloride Analysis

Interfering substance	Interference level
Bromide	Cyanide, bromide and iodide interfere directly and are titrated as chloride.
Cyanide	Cyanide, bromide and iodide interfere directly and are titrated as chloride.
Iodide	Cyanide, bromide and iodide interfere directly and are titrated as chloride.
Iron	Iron concentrations over 20 mg/L will mask the end point.
Orthophosphate	Orthophosphate concentrations over 25 mg/L will cause a precipitate to form.
Sulfide	To remove interference from sulfide, add one Sulfide Inhibitor Reagent Powder Pillow to approximately 125 mL of the sample, mix for one minute and filter through filter paper.
Sulfite	To remove interference from at least 10 mg/L sulfite, add 3 drops of 30% hydrogen peroxide to 100 mL of sample before starting the test.

Appendix A-6: Total Dissolved Solids (TDS) Analysis

The dissolved solids present in the water were determined via gravimetric method analysis. This method is highly accurate and easy to perform. However, it takes at least 24 hours to be completed and the error increases at low TDS concentrations.

Procedure

- Ceramic dishes were carefully washed and dried in the oven at 105^{o} C.
- The dishes were taken out of the oven and transferred into a glass desiccator with $CaSO_4$ as a desiccant to cool them at room temperature.
- The dishes were weighed using an analytical balance with a minimum range of 0.1 mg.
- A predetermined volume of sample was poured into the ceramic dish as follows:
  - ✓ 50 mL for Concentrate
  - ✓ 50 mL for Feed
  - ✓ 100 mL for Permeate
- The dishes with the sample were dried in the oven for 12 hours at 80^{o} C to avoid violent evaporation. After 12 hours, the temperature in the oven was changed to 105^{o} C for two hours to ensure complete evaporation.
- The dishes were taken out of the oven and transferred into a glass desiccator with $CaSO_4$ as a desiccant to cool at room temperature.
- The dishes were weighed in the analytical balance.
- The difference in weight was used to calculate the TDS concentration of the sample.

Interferences

The TDS analysis is sensitive to errors in the procedure. Grease, dust particles, and moisture are factors that affect the analysis greatly. It is important to handle the samples and the dishes properly. It is necessary to use latex gloves and carefully clean tongs during the analysis. Another factor that affects the procedure is the presence of suspended solids. It is necessary to filter the samples before pouring them into the dishes. Temperature needs to be monitored at all times to avoid losses due to violent evaporation.

Appendix A-7: Turbidity Analysis

The quantification of the turbidity present in the water was done by using the HACH 2100AN turbidimeter. This turbidimeter was designed for turbidity and attenuation measurement according to International Turbidity Measurement Standards ISO 7027, DIN 38404, and NF EN 27027. The 2100AN laboratory turbidimeter also provides direct measurements in units of NTU's (Nephelometric Turbidity Units) with a range from 0 NTU's to 10,000 NTU's.

Procedure

The instrument was calibrated according to the operator manual guidelines.

Turbidimeter Calibration

The instrument contains a built-in program to facilitate the calibration procedure. The calibration consists of the preparation of a 5 point calibration curve. Four formazin standards have to be prepared to calibrate the instrument. Table A-7 shows the concentrations of each standard in the calibration curve.

Table A-7: Standards with Formazin Solutions

Turbidity Standard	Concentration (NTU's)
Standard 0	<0.1
Standard 1	20
Standard 2	200
Standard 3	1000
Standard 4	4000

DI water was used as a baseline for <0.1 NTU's.

The calibration of the instrument was performed every two months. After the calibration was finished, the samples were poured into cuvettes and analyzed in the turbidimeter. The results were given in NTU's.

Interferences

The analysis of turbidity can be affected by the presence of gases and color in the sample. It is recommended to apply vacuum to the sample before analysis to remove any gas inside the water. This procedure can also be done by heating the water sample. The presence of color may represent an interference for the analysis. It is recommended to filter the sample before analysis, measure the turbidity and subtract the value in the rest of the samples.

Appendix A-8: Conductivity and pH analysis

The conductivity and the pH analysis in all experiments were done using the Oakton PC 300 pH/Conductivity meter.

Conductivity Analysis Procedure

- Samples of water were poured into beakers.
- The conductivity probe was introduced into the beaker and the conductivity value was read in μS/cm.
- The conductivity meter has 5 different ranges to measure conductivity. Table A-8 shows the limits of each measuring range.

Table A-8: Conductivity Meter Ranges

Range Indicator	Conductivity Range (μS/cm)	Recommended Calibration Solution Range (μS/cm)
r 1	0.00 - 19.99	6.00 - 17.00
r 2	0.0 - 199.9	60.0 - 170.0
r 3	0 - 1,999	600 - 1,700
r 4	0 - 19,999	6,000 - 17,000
r 5	0 - 199,999	60,000 - 170,000

- The calibration of the conductivity meter consists of one point calibration for each range of the meter.
- Each range has its own calibration. For that reason, all ranges have to be monitored continuously.

pH Analysis Procedure

- Samples of water were poured into beakers.
- The pH probe was introduced into the beaker and the pH was measured in pH units.
- The calibration of the pH meter consists of a three point calibration curve. The points of calibration are 4.01, 7.01, and 10.01.
- The pH probe was maintained in a potassium chloride solution to avoid bacterial growth.

Appendix B: Raw Data from Batch Experiments

Experiment (06/14/2011) spiked with Na_2SO_4

Antiscalant (ml)	H2SO4 (ml)	Salt Added (g)	Flush Flow Rate (ml/s) Initial	Flush Flow Rate (ml/s) Final	Pressure Flush (psi)	Pressure Experiment (psi)	Initial Volume (gal)	Final Vol Measured (gal)	% Recovery
		Na2SO4							
0.6	20	150	820	820	300	700	20	1.63	92
							Calculated		
							Mass BAL		
Time, min	**Perm, ml/min**	**Perm cond**	**conc cond**	**feed cond**	**temp, C**	**pH**	**Turbidity**	**Turbidity Notes**	**Perm Cond for Mass Balance**
0	1040	773	0	21,300	22.3	4.17	0.270		
5	1,040	455	24,000	21,400	22.6		0.027		
10	1,040	459	26,500	22,800	22.9		0.280		
15	1,020	440	28,500	25,300	23.9		0.200		
20	1,020	454	30,900	27,900	24.3		0.240		
25	1,000	478	32,900	30,200	23.9		0.240		
30	980	515	35,400	31,800	24.3		0.220		
35	920	587	38,100	35,200	25.3		0.200		
40	900	630	41,000	38,400	26.1		0.150		
45	840	736	45,000	42,100	26.8		0.190		
50	760	900	49,400	44,900	27.4		0.230		
55	700	1,036	53,200	51,300	28.5		0.170		
60	570	1,349	59,000	56,600	29.2		0.180		
65	500	1,538	63,200	61,300	29.3		0.200		
70	400	2,020	68,000	66,800	29.9		0.230		
75	340	2,650	73,100	72,000	29.9		0.200		
80	260	3,270	77,300	76,300	30.7		0.350		
85	220	4,130	81,400	79,800	30.1		0.580		
90							0.920		0.0
95							1.130	Precipitation	0.0
100							1.630		0.0
105							1.750		0.0
110							2.200		0.0

Experiment (06/23/2010)

Antiscalant (ml)	H2SO4 (ml)	Salt Added (g)	Flush Flow Rate (ml/s) Initial	Flush Flow Rate (ml/s) Final	Pressure Flush (psi)	Pressure Experiment (psi)	Initial Volume (gal)	Final Vol Measured (gal)	% Recovery
		None							
0.6	30		800	780	300	700	30	3.92	87
							Calculated		
							Mass BAL		

Time, min	Perm, ml/min	Perm cond	conc cond	feed cond	temp, C	pH	silica
0				22100	25.6	3.06	
5	1160	1180	25300	22600	25.4	3.14	
10	1130	1140	26500	23600	25.5	3.19	
15	1100	1639	27400	24700	25.6	3.23	
20	1120	1485	28800	26200	25.9	3.28	
25	1100	1413	30100	27500	26	3.34	
30	1060	1313	31400	29300	26	3.41	
35	1040	1270	33200	30600	26.4	3.47	
40	1030	1185	35200	32300	26.4	3.54	
45	1000	840	36800	34100	26.5	3.63	
50	960	830	38800	35000	26.7	3.7	
55	920	790	40600	38100	26.6	3.81	300,290,300
60	880	1020	43700	40600	27	3.93	
65	800	1060	45700	43200	27	4.02	
70	760	1050	48600	45400	27.1	4.13	
75	730	1082	51800	48600	27.2	4.25	
80	680	1221	54500	52200	27.3	4.32	
85	610	1256	57900	55500	27.2	4.37	
90	530	1575	60900	58200	27.7	4.43	
95	480	1210	64100	61700	27	4.47	
100	440	1420	67100	64700	27.2	4.5	
105	320	1800	69600	68200	26.8	4.52	
110	320	1950	72800	71200	26.5	4.52	
115	260	2390	75000	73600	26.9	4.54	
120	220	2610	77600	76500	27.1	4.54	
125	185	3010	80100	79300	27.3	4.52	
130	145	3450	81400	81000	27.2	4.52	
135	120	4430	83100	83500	27.4	4.52	
140	102	5040	83900	84700	27.8	4.52	710,670,690

Experiment (07/06/2010) spiked with NaCl

Antiscalant (ml)	H2SO4 (ml)	Salt Added	Flush Flow Rate (ml/s) Initial	Flush Flow Rate (ml/s) Final	Pressure Flush (psi)	Pressure Experiment (psi)	Initial Volume (gal)	Final Vol Measured (gal)	% Recovery
		NaCl							
0.6	30	5000 mg/L	800	790	300	700	30	7.50	75

Time, min	Perm, ml/min	Perm cond	conc cond	feed cond	temp, C	pH	silica
0				30,000	26.3	2.98	150
5	1,000	1,960	36,000	32,400	26.4	3	
10	1,000	1,940	37,400	33,300	26.6	3.05	
15	940	1,890	39,100	35,400	27.1	3.1	
20	920	1,740	40,400	37,100	27.3	3.15	
25	920	1,660	42,000	38,300	27.5	3.2	
30	900	1,540	43,500	40,000	27.5	3.25	
35	880	1,520	44,700	41,800	27.7	3.25	
40	800	1,490	46,700	43,100	27.8	3.38	
45	800	1,430	48,800	46,100	27.9	3.46	
50	780	1,839	51,100	46,600	2.82	3.55	
55	700	1,895	52,700	49,500	28.5	3.63	
60	680	1,796	53,800	52,200	28.7	3.72	300, 300, 280
65	640	1,430	57,300	54,500	28.8	3.8	
70	610	1,823	58,700	56,200	29.9	3.89	
75	570	1,879	61,000	58,800	29.4	3.97	
80	500	1,530	63,000	60,900	29.4	4.06	
85	480	1,590	65,600	63,200	29.6	4.14	
90	440	1,520	68,000	64,900	30.1	4.2	
95	410	1,830	70,200	67,800	30.2	4.27	
100	336	2,110	78,100	68,900	30.3	4.31	
105	312	2,310	72,700	71,000	30.2	4.33	
110	292	2,910	75,000	73,300	30.5	4.34	
115	260	2,910	76,600	75,300	30.5	4.37	
120	216	3,180	78,700	76,600	30.9	4.38	
125	192	3,700	77,600	77,000	30.9	4.42	
130	164	4,330	80,500	79,800	31.2	4.41	420,420,420

Experiment (07/22/2010) spiked with $CaCl_2$

Antiscalant (ml)	H2SO4 (ml)	Salt Added (g)	Flush Flow Rate (ml/s) Initial	Flush Flow Rate (ml/s) Final	Pressure Flush (psi)	Pressure Experiment (psi)	Initial Volume (gal)
		CaCl2					
0.6	34	340	800	790	300	700	30
							Calculated
							Mass BAL

Time, min	Perm, ml/min	Perm cond	conc cond	feed cond	temp, C	pH	silica
0				26,300	25.6	3.54	160,160,160
5	1,100	1,017	29,700	26,900	25.9	3.6	
10	1,080	1,028	31,000	28,200	26.0	3.66	
15	1,070	943	32,400	29,300	26.2	3.73	
20	1,060	921	34,100	31,000	26.5	3.82	
25	1,030	927	35,200	32,400	26.7	3.87	
30	1,020	880	37,000	33,900	27.2	3.97	
35	980	876	38,700	35,500	27.3	3.99	
40	960	901	40,900	37,700	27.7	4.14	
45	940	789	43,000	39,700	27.6	4.24	
50	900	819	45,200	41,500	28.0	4.33	
55	860	898	47,400	42,200	28.5	4.44	
60	815	921	50,200	46,200	28.8	4.53	
65	755	964	52,300	48,900	29.2	4.62	
70	725	1,389	53,300	51,700	29.1	4.67	
75	680	1,258	57,700	55,100	29.6	4.94	
80	610	1,339	60,100	57,300	29.9	4.84	
85	550	1,438	63,600	60,300	30.4	4.89	
90	500	1,797	65,300	63,700	30.2	4.91	
95	430	1,480	68,800	66,600	30.9	4.95	
100	390	1,820	71,800	69,900	31.0	4.95	
105	330	2,180	74,000	72,500	31.4	4.95	
110	272	2,480	75,800	72,900	31.6	4.95	
115	232	3,030	78,800	76,600	31.6	4.96	
120	204	3,770	80,800	78,000	32	4.98	
125	164	4,220	82,400	80,300	32.2	4.98	
130	140	4,840	83,500	81,900	32.4	4.98	
135	112	4,490	82,600	83,600	32.2	4.98	
140	96	6,350	86,500	84,900	32.8	4.97	600,600,600

Experiment (08/02/2010) spiked with $CaCl_2$

Antiscalant (ml)	H2SO4 (ml)	Salt Added (g)	Flush Flow Rate (ml/s) Initial	Flush Flow Rate (ml/s) Final	Pressure Flush (psi)	Pressure Experiment (psi)	Initial Volume (gal)	Final Vol Measured (gal)	% Recovery
		CaCl2							
0.6	30	568	800	800	300	700	30	7.50	75

Time, min	Perm, ml/min	Perm cond	conc cond	feed cond	temp, C	pH	silica
0	0				27.0	3.1	130,130,130
5	0	1,870	27,400	1,870	27.5	3.11	
10	0	1,795	28,900	1,795	27.7	3.16	
15	1,160	1,764	30,300	1,764	28.5	3.23	
20	1,150	1,665	31,800	1,665	28.7	3.31	
25	1,140	1,531	33,200	1,531	29.2	3.38	
30	1,120	1,448	35,400	1,448	29.6	3.45	
35	1,110	1,333	37,500	1,333	29.8	3.54	
40	1,050	1,218	40,200	1,218	30.3	3.67	
45	1,030	1,185	42,200	1,185	30.8	3.31	
50	980	1,170	45,000	1,170	31.2	3.95	250,240,240
55	940	1,113	48,400	1,113	31.2	4.12	
60	880	1,102	51,300	1,102	31.3	4.29	
65	800	1,067	54,200	1,067	31.8	4.42	
70	740	1,299	58,500	1,299	32.2	4.57	
75	680	1,365	60,900	1,365	32.1	4.71	
80	560	1,565	65,500	1,565	31.5	4.73	
85	460	1,510	68,400	1,510	30.6	4.8	
90	406	1,530	71,400	1,530	30.5	4.87	
95	376	1,840	74,200	1,840	31.4	4.87	
100	324	2,260	75,900	2,260	32.0	4.99	
105	268	2,760	77,500	2,760	32.8	5.06	
110	224	3,000	78,500	3,000	32.1	5.15	
115	164	3,470	80,600	3,470	32.7	5.17	

Experiment (10/01/2010) at 800 psi

Antiscalant (ml)	H2SO4 (ml)	Salt Added (g)	Flush Flow Rate (ml/s) Initial	Flush Flor Rate (ml/s) Final	Pressure Flush (psi)	Pressure Experiment (psi)	Initial Volume (gal)	Final Vol Measured (gal)	% Recovery
		None							
0.6	30				300	800	30	3.00	90

Time, min	Perm, ml/min	Perm cond	conc cond	feed cond	temp, C	pH	silica
0				22,800	25.3	3.84	
5	1,360	514	26,600	23,100	24.8	4.06	
10	1,400	467	28,300	29,000	29.9	4.07	
15	1,340	499	29,900	25,600	25.2	4.11	
20	1,340	517	31,400	27,400	25.6	4.18	
25	1,320	494	33,400	29,600	25.7	4.24	
30	1,300	538	35,600	31,800	26.3	4.33	
35	1,240	594	37,800	34,100	26.7	4.41	
40	1,200	584	40,800	36,600	27	4.5	
45	1,180	619	43,200	39,600	27.1	4.59	
50	1,080	669	46,700	42,700	27.1	4.79	
55	1,020	749	50,300	46,700	27.8	4.94	
60	940	904	54,400	50,700	28.1	5.1	
65	860	1,000	58,900	54,000	28.1	5.28	
70	760	1,186	62,600	59,100	28.6	5.56	
75	640	1,423	67,400	64,300	29.2	5.78	
80	560	1,666	71,900	68,800	20.8	6	
85	440	1,660	76,300	73,700	30	6.27	
90	356	2,020	80,000	78,000	30.1	6.34	
95	312	2,342					*
100	232	3,490	86,800	86,400	31	3.73	
105	180	3,880	89,300	88,400	30.7	3.78	
110	132	4,590	91,400	90,000	30.7	3.78	
115	112	6,120	93,300	93,000	30.4	3.81	
120	92	7,030	94,300	93,500	31.7	3.83	690,690,690

Experiment (03/10/2012) El Alto, NM Brackish Water

Antiscalant (ml)	H2SO4 (ml)	Salt Added (g)	Flush Flow Rate (ml/s) Initial	Flush Flow Rate (ml/s) Final	Pressure Flush (psi)	Pressure Experiment (psi)	Initial Volume (gal)	Final Vol Measured (gal)	% Recovery
		None							
0.3	7		800		300	700	15	0.36	98

Time, min	Perm, ml/min	Perm cond	conc cond	feed cond	temp, C	pH
0	900			2690	8.3	2.92
5	870			2,770	11.2	2.91
10	920			2,910	12.9	2.94
15	960			3,080	14.7	2.9
20	1,020			3,340	16.6	2.91
25	1,100			3,700	18.3	2.9
30	1,160			4,120	20.3	2.83
35	1,360			4,780	22.5	2.87
40	1,420			6,030	25.5	2.87
44	1,440			7,960	28.2	2.8
46	1,510			9,560	30	2.78
48	1,500			13,140	31.7	2.81

RUN 1 Conc. (mg/L)									
	Ca	Na	Cl	PO4	SO4	TDS	Σions	Missing Mass	%error
Raw Water	237	105	165	n.a.	887	1,779	1,394	385	22%
Run 1 Concentrate	2,055	1,109	1,399	17	9,610	15,900	14,190	1,710	11%
Run 1 Permeate	**3**	**3**	**33**	**n.a.**	**8**	>100	~	~	~

Experiment (03/10/2012) El Alto, NM Brackish Water

Antiscalant (ml)	H2SO4 (ml)	Salt Added (g)	Flush Flow Rate (ml/s) Initial	Flush Flow Rate (ml/s) Final	Pressure Flush (psi)	Pressure Experiment (psi)	Initial Volume (gal)	Final Vol Measured (gal)	% Recovery
		None							
0.6	12		840		300	700	30	1.06	96

Time, min	Perm, ml/min	Perm cond	conc cond	feed cond	temp, C	pH	Turbidity
0	820			2,560	6.7	3.4	0.30
5	800	209		2,490	8.4	3.28	0.64
10	825	213		3,240	9.3	3.25	0.62
15	845	254		2,620	10.4	3.24	0.64
20	900	230		2,750	11.2	3.27	0.53
25	930	224		2,890	12.1	3.22	0.40
30	970	391		2,970	13.1	3.23	0.30
35	100	248		3,020	14	3.35	0.24
40	1,030	287		3,250	15.2	3.15	0.26
45	1,080	287		3,210	16.2	3.25	0.29
50	1,110	279		3,600	17.3	3.2	0.22
55	1,140	292		3,780	18.7	3.2	
60	1,250	306		4,070	20	3.18	0.22
65	1,280	338		4,490	21.3	3.18	0.21
70	1,340	367		4,820	22.3	3.17	0.20
75	1,380	406		5,550	23.7	3.17	0.25
80	1,470	462		6,360	25	3.16	0.24
83	1,490	494		7,130	25.8	3.15	0.23
86	1,500	539		8,110	26.7	3.14	0.26
89	1,560	596		9,200	27.7	3.14	0.30
92	1,500	676		11,230	29.5	3.14	0.40
94	1,300	755		12,980	30.8	3.15	0.49
96	750	792		14,000	31.6	3.14	1.02
98	190			15,260	33.6	3.16	6.40

Experiment (06/23/2011) Alamogordo Brackish Water

Salt Added (g)	Flush Flow Rate (ml/s) Initial	Flush Flow Rate (ml/s) Final	Pressure Flush (psi)	Initial Volume (gal)	Final Vol Measured (gal)	% Recovery
1148						
NaCl	0.7			30		80

Time, min	Perm Flow Gal/min	Feed Cond	Conc. Cond	pH	Turbidity	Recovery	Pressure
0	0.68	23500	0	3.9	2.9	0%	665
5	0.6	25,800	28,000	4.08	3.7	10%	602
10	0.58	28,000	30,040	4.07	3.5	18%	605
15	0.55	29,900	32,430	4.2	4.1	26%	608
20	0.53	33,100	35,160	4.35	4.2	35%	615
25	0.51	36,000	38,390	4.46	4.2	43%	631
30	0.46	40,100	42,050	4.61	4.2	50%	628
35	0.42	43,800	46,200	4.69	5.1	57%	638
40	0.38	48,600	50,600	4.81	4.5	62%	649
45	0.35	53,200	55,240	4.83	5.0	68%	670
50	0.3	59,300	60,950	4.9	6.6	72%	692
55	0.25	63,900	67,350	4.89	6.0	76%	714
60	0.19	70,000	73,060	4.88	6.1	78%	733
62	0.17				8.7	79%	746

Experiment (05/02/2013) Alamogordo Bracksih

Salt Added (g)	Flush Flow Rate (ml/s) Initial	Flush Flow Rate (ml/s) Final	Pressure Flush (psi)	Initial Volume (gal)	Final Vol Measured (gal)	% Recovery
0						
N/A	0.7			30		71

Time, min	Perm Flow Gal/min	Feed Cond	Conc. Cond	pH	Turbidity	Recovery	Pressure
0	0.7	6670	0	4.12	0.50	0%	606
5	0.7	7,730	9,080	4.22	0.40	13%	580
10	0.7	8,230	1,060	4.12	0.35	20%	588
15	0.7	9,620	11,280	4.17	0.34	30%	593
20	0.7	10,970	12,990	4.23	0.35	40%	592
25	0.7	13,230	15,580	4.28	0.29	50%	598
30	0.7	16,950	19,050	4.37	0.63	60%	617.0
32	n/a	n/a	n/a	n/a	0.75	n/a	n/a
35	0.56	22,100	22,860	4.46	1.24	69%	683.0
37	0.35	n/a	n/a	n/a	1.43	n/a	n/a
38	0.26	n/a	24,400	4.5	1.67	71%	n/a

IC Results from Alamogordo Water Samples

			Cations			Anions	
	Sample ID (Alamogordo)	**Dil. Factor**	**Ca**	**Mg**	**Na**	**Cl**	**SO4**
1	Initial Feed 20 gal	50	444 mg/L	212 mg/L	499 mg/L	689 mg/L	1,971 mg/L
2	Initial Feed 20 gal	100	466 mg/L	245 mg/L	515 mg/L	523 mg/L	2,053 mg/L
3	Initial Feed 20 gal	200	456 mg/L	251 mg/L	491 mg/L	484 mg/L	1,918 mg/L
4	F. Conc. 326 gr (NaCl) 75% rec 20 gal	50	641 mg/L	1,109 mg/L	8,000 mg/L	10,167 mg/L	8,173 mg/L
5	F. Conc. 326 gr (NaCl) 75% rec 20 gal	100	660 mg/L	1,148 mg/L	8,361 mg/L	10,649 mg/L	8,590 mg/L
6	F. Conc. 326 gr (NaCl) 75% rec 20 gal	200	743 mg/L	1,189 mg/L	8,587 mg/L	10,922 mg/L	8,838 mg/L
7	F. Conc. no salt 67% rec 20 gal	50	493 mg/L	1,226 mg/L	2,828 mg/L	2,032 mg/L	8,956 mg/L
8	F. Conc. no salt 67% rec 20 gal	100	444 mg/L	1,266 mg/L	2,905 mg/L	2,078 mg/L	9,265 mg/L
9	F. Conc. no salt 67% rec 20 gal	200	450 mg/L	1,263 mg/L	2,948 mg/L	2,082 mg/L	9,406 mg/L
10	Initial Feed 30 gal	50	541 mg/L	358 mg/L	774 mg/L	567 mg/L	3,146 mg/L
11	Initial Feed 30 gal	100	567 mg/L	379 mg/L	793 mg/L	587 mg/L	3,283 mg/L
12	Initial Feed 30 gal	200	582 mg/L	391 mg/L	791 mg/L	603 mg/L	3,334 mg/L
13	F. C. 1148 gr 80% 30 gal	50	862 mg/L	1,522 mg/L	18,837 mg/L	25,851 mg/L	10,364 mg/L
14	F. C. 1148 gr 80% 30 gal	100	899 mg/L	1,565 mg/L	19,717 mg/L	27,146 mg/L	10,876 mg/L
15	F. C. 1148 gr 80% 30 gal	200	881 mg/L	1,541 mg/L	19,477 mg/L	26,841 mg/L	10,740 mg/L
16	F. C. no salt 71% rec 30 gal	50	702 mg/L	1,787 mg/L	3,871 mg/L	2,980 mg/L	11,711 mg/L
17	F. C. no salt 71% rec 30 gal	100	659 mg/L	1,680 mg/L	3,705 mg/L	2,844 mg/L	11,299 mg/L
18	F. C. no salt 71% rec 30 gal	200	699 mg/L	1,728 mg/L	3,793 mg/L	3,142 mg/L	12,247 mg/L

Experiment (12/14/2012) with New Membranes

Antiscalant (ml)	H2SO4 (ml)	Salt Added (g)	Flush Flow Rate (ml/s) Initial	Flush Flow Rate (ml/s) Final	Pressure Flush (psi)	Pressure Experiment (psi)	Initial Volume (gal)	Final Vol Measured (gal)	% Recovery
		None							
0.3	10		1520	1530	300	700	10	1.45	86
							Calculated		
NOTE: New membranes (2) run in parallel							Mass BAL		
Time, min	**Perm, ml/min**	**Perm cond**	**conc cond**	**feed cond**	**temp, C**	**pH**	**Conc. Flow**	**Total Flow**	
0	2847	74		20,400		3.67	5,880	8,727	
5	2,840	317		23,730			6000	8,840	
10	2,560	303	50,000	39,100		4.31	6360	8,920	
12.5			57,300	47,500					
SECOND RUN									
Antiscalant (ml)	**H2SO4 (ml)**	**Salt Added (g)**	**Flush Flow Rate (ml/s) Initial**	**Flush Flow Rate (ml/s) Final**	**Pressure Flush (psi)**	**Pressure Experiment (psi)**	**Initial Volume (gal)**	**Final Vol Measured (gal)**	**% Recovery**
		None							
0.3	20		1530	1560	300	700	20	3.90	81
							Calculated		
New Membranes run in series							Mass BAL		
Time, min	**Perm, ml/min**	**Perm cond**	**conc cond**	**feed cond**	**temp, C**	**pH**	**Conc. Flow**	**Total Flow**	
0	2480			16,200		3.5	6,600		
5	2,320	403	22,250	17,140			7,200	9,520	
10	2,260	359	25,830	20,310		3.98	7,080	9,340	
15	2,240	321	31,300	24,630		3.95	7,200	9,440	
20	2,000	303	38,700	31,100		4.19	7,440	9,440	
25	1,920	306	47,800	40,300		4.47	7,200	9,120	
30	1,680	380	60,800	51,700		4.71	7,200	8,880	

Experiment (12/18/2012) with New Membranes

Antiscalant (ml)	H2SO4 (ml)	Salt Added (g)	Flush Flow Rate (ml/s) Initial	Flush Flow Rate (ml/s) Final	Pressure Flush (psi)	Pressure Experiment (psi)	Initial Volume (gal)	Final Vol Measured (gal)	% Recovery
		None							
0.4	20		1720	1700	300	700	20	4.81	76
							Calculated		
NOTE: New membranes (2) run in parallel							Mass BAL		
Time, min	**Perm, ml/min**	**Perm cond**	**conc cond**	**feed cond**	**temp, C**	**pH**	**Conc. Flow**	**Total Flow**	
0				20,680		3.5			
5	2,400	392	30,700	22,630		3.71	6675	9,075	
10	2,240	381	35,100	26,890		4.21	6900	9,140	
15	2,160	353	41,700	32,800		4.08	6,980	9,140	
20	2,000	362	51,700	41,700		4.34	7,050	9,050	
25	1,760	420	64,400	53,800		4.55	7,200	8,960	
SECOND RUN									
Antiscalant (ml)	**H2SO4 (ml)**	**Salt Added (g)**	**Flush Flow Rate (ml/s) Initial**	**Flush Flow Rate (ml/s) Final**	**Pressure Flush (psi)**	**Pressure Experiment (psi)**	**Initial Volume (gal)**	**Final Vol Measured (gal)**	**% Recovery**
		None							
0.4	20		1530	1560	300	700	20	3.90	81
Added 0.3 mL of Acid						Mass BAL			
Time, min	**Perm, ml/min**	**Perm cond**	**conc cond**	**feed cond**	**temp, C**	**pH**	**Conc. Flow**	**Total Flow**	
0	2600			21,100		4.2			
5		2,400							
7.5	2,340								
10	2,300			26,920		3.94			
15	2,200								
16	2,120								
20	2,040			41,200		4.34			
25	1,800			55,100		4.63			

THIRD RUN (3 MEMBRANES) (SERIE)										
Antiscalant (ml)	**H2SO4 (ml)**	**Salt Added (g)**	**Flush Flow Rate (ml/s) Initial**	**Flush Flow Rate (ml/s) Final**	**Pressure Flush (psi)**	**Pressure Experiment (psi)**	**Initial Volume (gal)**	**Final Vol Measured (gal)**	**% Recovery**	
		None								
0.3	21		1530	1738	300	700	20	5.05	75	
			800	800			Calculated			
							Mass BAL			
Time, min	**Old membrane**	**2 membranes**	**Perm, ml/min**	**Perm cond**	**conc cond**	**feed cond**	**temp, C**	**pH**	**Conc. Flow**	**Total Flow**
0	1740	3320	5060			21,320		3.94	3,840	8,900
5	990	2400	3390		38,200	24,810		4.13	5,460	8,850
10	915	2240	3155		47,300	43,400		4.34	5,880	9,035
15	750	1880	2630		57,500	45,300		4.54	6,300	8,930
FOURTH RUN (3 MEMBRANES) (SERIE)										
Antiscalant (ml)	**H2SO4 (ml)**	**Salt Added (g)**	**Flush Flow Rate (ml/s) Initial**	**Flush Flow Rate (ml/s) Final**	**Pressure Flush (psi)**	**Pressure Experiment (psi)**	**Initial Volume (gal)**	**Final Vol Measured (gal)**	**% Recovery**	
		None								
0.4										21.5
			800	800			Calculated Mass BAL			
Time, min	**Old membrane**	**2 membranes**	**Perm, ml/min**	**Perm cond**	**conc cond**	**feed cond**	**temp, C**	**pH**	**Conc. Flow**	**Total Flow**
0	1210	2800	4010			21,450		3.86	4,920	8,930
6.5	1000	2400	3400		39,700	26,070		3.98	5,640	9,040
15	900	2200	3100		45,500	30,900		4.14	5,940	9,040
17.5	780	1960	2740		58,500	42,400		4.41	6,240	8,980

Experiment (12/20/2012) New Membranes

FIRST RUN (3 MEMBRANES) (SERIE)									
Antiscalant (ml)	**H2SO4 (ml)**	**Salt Added (g)** None	**Flush Flow Rate (ml/s) Initial**	**Flush Flow Rate (ml/s) Final**	**Pressure Flush (psi)**	**Pressure Experiment (psi)**	**Initial Volume (gal)**	**Final Vol Measured (gal)**	**% Recovery**
0.4	21.5		1720	1700	300	700	19	4.60	76

Time, min	**Old membrane**	**2 membranes**	**Perm, ml/min**	**Perm cond**	**conc cond**	**feed cond**	**temp, C**	**pH**	**Conc. Flow**	**Total Flow**
0	1000	2520	3520			21,080		3.57	5,330	8,850
50	960	2260	3220		36,100	23,530		3.7	5,880	9,100
10	900	2160	3060		43,400	30,900		3.89	6,000	9,060
15	760	1840	2600		54,700	41,700		4.21	6,600	9,200
19	640	1600	2240		64,700	56,700		4.59	6,720	8,960

SECOND RUN (3 MEMBRANES) (SERIE)

Antiscalant (ml)	**H2SO4 (ml)**	**Salt Added (g)** None	**Flush Flow Rate (ml/s) Initial**	**Flush Flow Rate (ml/s) Final**	**Pressure Flush (psi)**	**Pressure Experiment (psi)**	**Initial Volume (gal)**	**Final Vol Measured (gal)**	**% Recovery**
0.4	21.5		1720	1710	300	700	20	4.75	76

Time, min	**Old membrane**	**2 membranes**	**Perm, ml/min**	**conc cond**	**feed cond**	**pH**	**Conc. Flow**	**Total Flow**
0	1200	2600	3800		21,390	3.25	4,320	8,120
50	1000	2320	3320	3,600	23,590	3.37	5,580	8,900
10	920	2200	3120	43,200	29,920	3.45	5,820	8,940
15	760	1860	2620	54,400	39,500	3.84	6,360	8,980
19	600	1560	2160	66,200	52,500	4.1	6,720	8,880

Experiment (02/22/2013) New Membranes

Antiscalant (ml)	H2SO4 (ml)	Salt Added (g)	Flush Flow Rate (ml/s) Initial	Flush Flow Rate (ml/s) Final	Pressure Flush (psi)	Pressure Experiment (psi)	Initial Volume (gal)	Final Vol Measured (gal)	% Recovery
		None							
0.2	10.3		1400	1300	300	700	10	2.00	80
							Calculated		
NOTE: New membrane run							Mass BAL		
Time, min	**Perm, ml/min**	**Perm cond**	**conc cond**	**feed cond**	**temp, C**	**pH**	**Conc. Flow**	**Total Flow**	
0	2190	236		21,760		4.04	6,780		
5	1,560	153	24,940	22,240		4.38	7440	9,000	
10	1,410	157	29,970	27,120		4.63	7450	8,860	
15	1,320	179	37,300	34,400		4.91	7,680	9,000	
20	1,160		49,600	46,600		5.24	7,680	8,840	

Experiment (02/25/2013) New Membranes and Flushing Test

Antiscalant (ml)	H2SO4 (ml)	Salt Added (g)	Flush Flow Rate (ml/s) Initial	Flush Flow Rate (ml/s) Final	Pressure Flush (psi)	Pressure Experiment (psi)	Initial Volume (gal)	Final Vol Measured (gal)	% Recovery
		None							
0.2	11.4		1360	1360	300	700	10.1	3.98	61

Time, min	Perm, ml/min	Perm cond	conc cond	feed cond	temp, C	pH	Conc. Flow	Total Flow	Recovery based in cond
0	1755	135	21920	21,920					0.0%
5	1,605	142	24,810			4.5	7120	8,725	11.6%
10	1,485	155	29,820	26,540		4.75	7280	8,765	26.5%
15	1,410	177	36,700	33,400		5.02	7,280	8,690	40.3%
20			51,400			5.34		0	57.4%
24			67,000			5.52			67.3%

Time, min	pH	Perm Cond
0	6.75	634
0.5	6.21	9500
1	6.08	16920
1.5	6.04	18840
2	6.03	19280
2.5	6.03	19480
3	6.03	19490
3.5	6.04	19500
4	6.04	19500
4.5	6.04	19500
5	6.05	19500

Experiment (03/12/2013) New Membranes

Antiscalant (ml)	H2SO4 (ml)	Salt Added (g)	Flush Flow Rate (ml/s) Initial	Flush Flow Rate (ml/s) Final	Pressure Flush (psi)	Pressure Experiment (psi)	Initial Volume (gal)	Final Vol Measured (gal)	% Recovery
		None							
0.2	10.6		930	850	300	700	10	1.22	70

Time, min	Perm, ml/min	Perm cond	conc cond	feed cond	pH	Conc. Flow	Bypass Flow	Total Flow	Recovery based in cond
0	1720		17000	17,000		3,240	3360	8,320	0.0%
5	1,480		27,200	22,400	4.5	4500	3120	9,100	37.5%
10	1,400		32,200	27,200	4.75	4500	3120	9,020	47.2%
15	1,260		37,100	31,300	5.02	4,800	2700	8,760	54.2%
20	1,080		45,100	39,500	5.34	5,040	2880	9,000	62.3%
23	1,020		52,500	47,100	5.52	5,160		6,180	67.6%

Antiscalant (ml)	H2SO4 (ml)	Salt Added (g)	Flush Flow Rate (ml/s) Initial	Flush Flow Rate (ml/s) Final	Pressure Flush (psi)	Pressure Experiment (psi)	Initial Volume (gal)	Final Vol Measured (gal)	% Recovery
		None							
0.2	10.6		930	850	300	700	10	2.14	61

Time, min	Perm, ml/min	Perm cond	conc cond	feed cond	pH	Conc. Flow	Bypass Flow	Total Flow	Recovery based in cond
0	1460		17440	17,340	3.8	4,440	3240	9,140	2.5%
5	1,400		26,400	22,000	4.15	4500	3000	8,900	35.6%
10	1,360		30,400	24,900	4.37	4800	2880	9,040	44.1%
15	1,320		36,800	31,800	4.67	4,980	2700	9,000	53.8%
20	1,320		46,600	38,400	4.8	5,040	2640	9,000	63.5%

Experiment (03/21/2013)

Antiscalant (ml)	H2SO4 (ml)	Salt Added (g)	Flush Flow Rate (ml/s) Initial	Flush Flow Rate (ml/s) Final	Pressure Flush (psi)	Pressure Experiment (psi)	Initial Volume (gal)	Final Vol Measured (gal)	% Recovery
		None							
0.2	10.6		850	860	300	700	10	2.14	61

Time, min	Perm, ml/min	Perm cond	conc cond	feed cond	temp, C	pH	Conc. Flow	Bypass Flow	Total Flow	Recovery based in cond
0	1050		15000	15,000						0.0%
5	1,050		28,400	16,330		4.5	1116	6900	9,066	47.2%
10	1,060		31,700	17,990		4.75	1080	6800	8,940	52.7%
15	1,080		35,300	21,400		5.02	1,140	6600	8,820	57.5%
20	1,065		40,300	25,400		5.34	1,170	6600	8,835	62.8%
25	1,050		48,200	30,300		5.52	1,170	6480	8,700	68.9%
27				31,700						

Antiscalant (ml)	H2SO4 (ml)	Salt Added (g)	Flush Flow Rate (ml/s) Initial	Flush Flow Rate (ml/s) Final	Pressure Flush (psi)	Pressure Experiment (psi)	Initial Volume (gal)	Final Vol Measured (gal)	% Recovery
		None							
0.2	10.5		930	900	300	700	10	1.16	71

Time, min	Perm, ml/min	Perm cond	conc cond	feed cond	temp, C	pH	Conc. Flow	Bypass Flow	Total Flow	Recovery based in cond
0			15120	15,120	25	2.79		5400	5,400	0.8%
5	1,170		23,400	16,300	26.7	2.86	2340	5400	8,910	35.9%
10	1,230		27,100	18,280	27.6	2.97	2220	5640	9,090	44.6%
15	1,110		29,200	22,000	27.8	3	2,640	5160	8,910	48.6%
20	1,035		34,500	26,200	28.4	3.17	2,700	4920	8,655	56.5%
25	975		40,800	32,500	29.5	3.37	2,730	5160	8,865	63.2%
30	780		49,800	42,000		3.98				69.9%

Experiment (03/28/2013) New Membranes

Antiscalant (ml)	H2SO4 (ml)	Salt Added (g)	Flush Flow Rate (ml/s) Initial	Flush Flow Rate (ml/s) Final	Pressure Flush (psi)	Pressure Experiment (psi)	Initial Volume (gal)	Final Vol Measured (gal)	% Recovery
		None							
0.2	10.8		900	900	300	700	10	1.80	65

Time, min	Perm, ml/min	Perm cond	conc cond	feed cond	temp, C	pH	Conc. Flow	Bypass Flow	Total Flow	Recovery based in cond
0			17070	17,070		3.68				0.0%
5	1,005		32,600	17,840		3.85	1100	6900	9,005	47.6%
10	1,005	1,152	43,200	21,400	29.4	3.91	1100	6900	9,005	60.5%
15	945		44,000	23,500	30.5	4.01	1,400	6700	9,045	61.2%
20	900		40,500	27,300	31.7	4.14	1,380	6500	8,780	57.9%
25	825		44,600	32,000	32	4.26	1,500	6500	8,825	61.7%
30	735	100	48,500	36,900	32.5	4.37	1,740			64.8%
34			53,500	42,000		4.37				68.1%

Antiscalant (ml)	H2SO4 (ml)	Salt Added (g)	Flush Flow Rate (ml/s) Initial	Flush Flow Rate (ml/s) Final	Pressure Flush (psi)	Pressure Experiment (psi)	Initial Volume (gal)	Final Vol Measured (gal)	% Recovery
		None							
0.2	10.8		900	900	300	700	10	1.51	67.5

Time, min	Perm, ml/min	Perm cond	conc cond	feed cond	temp, C	pH	Conc. Flow	Bypass Flow	Total Flow	Recovery based in cond
0			17070	17,340		3.48				0.0%
5	1,020	1,107	32,600	18,150	27	3.58	1300	6800	9,120	47.6%
10	975	1,102	43,200	21,900	28.4	3.67	1450	6500	8,925	60.5%
15	945	1,154	44,000	24,600	29.2	3.83	1,500	6500	8,945	61.2%
20	930	1,266	40,500	28,700	30.8	3.9	1,600	6580	9,110	57.9%
25	825	1,376	44,600	32,900	31.1	4.04	1,880	6800	9,505	61.7%
30	780	1,783	48,500	39,400	31.4	4.19	1,800	6500	9,080	64.8%
35			53,500	49,000		5				68.1%

Experiment (04/25/2013) 50% Acid

Antiscalant (ml)	H2SO4 (ml)	Salt Added (g)	Flush Flow Rate (ml/s) Initial	Flush Flow Rate (ml/s) Final	Pressure Flush (psi)	Pressure Experiment (psi)	Initial Volume (gal)	Final Vol Measured (gal)	% Recovery
		None							
0.2	4.0		870	860	300	700	8	1.3	62

Time, min	Perm, ml/min	Perm cond	conc cond	feed cond	temp, C	pH	Conc. Flow	Bypass Flow	Total Flow	Recovery based in cond
0	1240		25500							0.0%
5	1,260		25,500	18,640	27.6	6.52	3180	4200	8,640	0.0%
10	1,160		29,000	23,300	27.8	6.71	3420	4140	8,720	12.1%
15	1,110		34,800	28,000	28.6	7.13	3,420	4140	8,670	26.7%
20	940		41,000	34,900	29.4	7.4	3,750	3960	8,650	37.8%
25	810		51,300	44,700		7.5				50.3%

Antiscalant (ml)	H2SO4 (ml)	Salt Added (g)	Flush Flow Rate (ml/s) Initial	Flush Flow Rate (ml/s) Final	Pressure Flush (psi)	Pressure Experiment (psi)	Initial Volume (gal)	Final Vol Measured (gal)	% Recovery
		None							
0.2	4.0		870	860	300	700	8	0.8	68

Time, min	Perm, ml/min	Perm cond	conc cond	feed cond	temp, C	pH	Conc. Flow	Bypass Flow	Total Flow
0	1300			16,730		6.22			
5	1,215		25,700	18,420	27.5	6.57	3120	4500	8,835
10	1,170		29,400	22,900	28.2	6.73	3120	4410	8,700
15	1,050		33,900	27,400	28.7	7.09	3,360	4320	8,730
20	990		40,900	33,900	29.5	7.37	3,360	4380	8,730
25	720		48,400	43,000	30.2	7.5			

Vita

Guillermo Delgado earned his Bachelor of Engineering degree in Chemical Engineering from the Parral Institute of Technology in 2005. He received his Master of Science degree in Environmental Science and Engineering in 2009 from the University of Texas at El Paso. In 2010, he joined the doctoral program.

Dr. Delgado was the recipient of the Anita Mochen Loya Innovation Fund in Engineering in 2012. In the same way, Dr. Delgado has participated in numerous projects funded by the Bureau of Reclamation, and El Paso Water Utilities.

While pursuing his degree, Dr. Delgado worked as a research assistant for the department of Civil Engineering. During this time, he had the chance to work in several desalination research centers in Texas and New Mexico. Additionally, Dr. Delgado worked as a teaching assistant for the department of Civil Engineering. As one of his most gratifying experiences, he had the opportunity to help more than 300 Civil Engineering students reach their academic goals.

Dr. Delgado will continue working in the improvement of water treatment systems to ensure that the freshwater supply will meet the demand of current and future generations.

Permanent Address: 1524 Upson Apt. 3

El Paso, Texas, 79902

This Dissertation was typed by Guillermo Delgado